AN ABSTRACT OF THE DISSERTATION OF

Daniel Mauricio Palacios of the degree of Doctor of Philosophy in Oceanography presented on April 29, 2003.

Title: Oceanographic Conditions Around the Galápagos Archipelago and their Influence on Cetacean Community Structure.

Abstract approved: _____

Bruce R. Mate

The objectives of this dissertation were to describe the complex oceanographic conditions around the Galápagos Archipelago (eastern equatorial Pacific), their seasonal variability, and their effects on patterns of cetacean occurrence.

The physical and ecological factors leading to a plume of high phytoplankton biomass in the wake of the Galápagos were investigated with principal component and regression analyses of water-column climatologies and satellite-derived ocean color. The results supported the notion that this "island-mass effect" is fueled by upwelling of the Equatorial Undercurrent (EUC) combined with natural iron enrichment from the island platform.

Seasonal variability in long-term monthly fields of satellite-derived sea-surface temperature and ocean color was studied through harmonic analysis and empirical orthogonal function decomposition. Two annual cycles were identified in both variables. The intensification of the Equatorial Front and the South Equatorial Current in the second part of the year was the dominant signal in the data. A secondary cycle reaching its peak in the first part of the year was associated with the topographically induced upwelling of the EUC on the western side of the

archipelago, and with advection of upwelled Panamá Bight water on the eastern side.

The occurrence of nine cetacean species (including seven small and medium-sized delphinids, the sperm whale, and the Bryde's whale) in relation to environmental variability around the archipelago was described. Seasonally persistent sectors of the archipelago characterized by the presence of distinct species assemblages of stratified, upwelling, and nearshore environments were identified through cluster and indicator species analysis. The dominant pattern in species distribution, as extracted by a nonmetric multidimensional scaling procedure, was well correlated with the main environmental gradient (described by the degree of water-column stratification, chlorophyll-*a* concentration, and distance from the islands).

The collective results of this study indicate that the ocean environment surrounding the Galápagos Archipelago is strongly influenced by equatorial flows. However, the archipelago also introduces a disturbance to these flows, creating localized and persistent conditions that favor the establishment of distinct biological communities around the islands.

Oceanographic Conditions Around the Galápagos Archipelago and their Influence on Cetacean Community Structure

by

Daniel Mauricio Palacios

A DISSERTATION

submitted to

Oregon State University

in partial fulfillment of
the requirements for the
degree of

Doctor of Philosophy

Presented April 29, 2003
Commencement June 2003

Doctor of Philosophy dissertation of Daniel Mauricio Palacios presented on April 29, 2003.

APPROVED:

Major Professor, representing Oceanography

Dean of the College of Oceanic and Atmospheric Sciences

Dean of the Graduate School

I understand that my dissertation will become part of the permanent collection of Oregon State University libraries. My signature below authorizes release of my dissertation to any reader upon request.

Daniel Mauricio Palacios, Author

ACKNOWLEDGEMENTS

I am most indebted to my advisor, Bruce Mate, for his continued and unconditional financial support of my graduate education through the Endowed Marine Mammal Program at Oregon State University. Bruce also gave me the latitude and the opportunities to pursue my wide-ranging intellectual interests during these forming years. I also wish to thank the other members of my Graduate Committee, Charlie Miller, Bill Pearcy, Dan Schafer, and Ted Strub, for their feedback and encouragement through this process.

A significant portion of the marine mammal data was collected during a year-long expedition to the Galápagos by the Ocean Alliance/Whale Conservation Institute in 1993–1994 aboard R/V *Odyssey*. Iain Kerr and Kim Marshall-Tilas invited me to participate in this project and supported my continued work on the data post-expedition. Scientific permits and logistical support for this expedition were provided by the Galápagos National Park Service, the Dirección General de la Marina Mercante y del Litoral of Ecuador, and the Charles Darwin Research Station.

I am most grateful to Pablo Bilbao and Antonio Martínez for introducing me to the power and beauty of scientific computing, and for general advice and discussion on analysis techniques. Mention must also be made of all the people who expedited my work tremendously by contributing useful computer routines (Mark Baumgartner, Emilio Beier, Ken Casey, Chris Chickadel, and Joe Haxel) or by writing useful programs and making them freely available (in particular Rich Pawlowicz for his M_Map program and Rich Signell for maintaining the Sea-Mat Tools website). Bruce McCune patiently answered questions about community ordination and related techniques. His remarkably clear and accessible textbook, as well as his software (PC-ORD), made it possible for me to undertake the chapter on community ecology when time was pressing. Jaime Gómez-Gutiérrez was also helpful with this endeavor.

Several people at COAS made my stay more enjoyable, including Joy Burck, Brent Dalrymple, Brenda Davis, Irma Delson, Robin Hlobeczy, Linda LaFleur, Jodi Smith, and Kay Yates. The staff and fellow students with OSU's Marine Mammal Program, Veryl Barry, Mark Baumgartner, Sallie Beavers, Lisa Bridges, Carol DeLancey, Tomas Follett, Ladd Irvine, Greg Krutzikowsky, Barb Lagerquist, Mary Lou Mate, Kate Stafford, Karen Willard, and Martha Winsor, were always helpful and provided various forms of support and encouragement.

Fellow students whose friendship I would like to recognize include: Scott Bennett, Pablo Bilbao, Guillermo Díaz-Méndez, Lisa Eisner, Robert Emmett, Jaime Gómez-Gutiérrez, Jon Hill, Cidney Howard, Nobuyuki Kawasaki, Sam Laney, Krista Longnecker, Antonio Martínez, Gabriela Montaño, Ann Morey-Ross, Julie Pullen, Crystal Sigmon, Daniel Sigmon, and Malinda Sutor. Finally, I would like to thank Dagmar Fertl and Heidi Snell for their daily dose of e-mail jokes, and Consuelo Carbonell-Moore for keeping the spirit of Colombia alive in Oregon.

TABLE OF CONTENTS

TABLE OF CONTENTS (Continued)

TABLE OF CONTENTS (Continued)

TABLE OF CONTENTS (Continued)

TABLE OF CONTENTS (Continued)

LIST OF FIGURES

LIST OF FIGURES (Continued)

LIST OF FIGURES (Continued)

LIST OF FIGURES (Continued)

LIST OF FIGURES (Continued)

LIST OF FIGURES (Continued)

LIST OF FIGURES (Continued)

LIST OF TABLES

LIST OF TABLES (Continued)

I dedicate this thesis to my wife, Kelly, who shared the day-to-day challenges and more personal aspects of this work over the years. She lovingly endured my long hours at the computer and away from her while making sure I had everything I needed.

Oceanographic Conditions Around the Galápagos Archipelago and their Influence on Cetacean Community Structure

1 GENERAL INTRODUCTION

Oceanic islands are of considerable scientific interest, as they can have profound effects on the environments around them. They may act as obstacles in the path of strong currents and winds, causing instabilities at the lee side (Arístegui et al., 1997; Barton et al., 2000) which are significant to biological processes (e.g., Pakhomov et al., 2000; Hernández-León et al., 2001; Rodríguez et al., 2001). In the case of the Galápagos Archipelago, these effects have no doubt shaped the unique marine life for which it is famous. Biologists have long been interested in this group of islands, as they are a textbook example of endemism and island biogeography.

The primary objective of this dissertation is to describe the dominant patterns of oceanographic variability around the Galápagos Archipelago at the seasonal timescale. Emphasis is on the features and processes associated with the local upwelling of the Equatorial Undercurrent (EUC) on the western side of the islands, since this phenomenon is responsible for sustaining the cold, highly productive conditions characteristic of this sector. Because these conditions create distinctive habitats for oceanic biota, the ultimate objective is to describe their influence on cetaceans (the group of oceanic predators that includes whales and dolphins) in terms of distribution and community structure.

A description of the study area and a review of the physical setting of the islands are provided in the remainder of this chapter. The other chapters are organized in the following manner. In Chapter 2, the "island-mass effect" (i.e., the increase in phytoplankton standing stock as an island mass is approached) of the Galápagos Archipelago is described. The physical and ecological conditions associated with this effect, and their connection to the EUC, are investigated. While

Chapter 2 provides a static view of the average phytoplankton distribution around the islands, Chapter 3 examines the evolution of sea-surface temperature and ocean color fields from a seasonal perspective. The observed patterns are explained in terms of the seasonality of equatorial currents and ocean-atmosphere coupling at regional and local scales. In Chapter 4, the composition of the cetacean community around the archipelago is examined in relation to the environmental seasonality. Finally, a General Conclusion section summarizing the main findings of the dissertation is offered in Chapter 5.

An approach common to chapters 2–4 is the use of multivariate statistical methods, namely principal component analysis (PCA), empirical orthogonal functions (EOFs), and nonmetric multidimensional scaling (NMS), for extracting the principal patterns of variability from gridded data sets. In the interest of clarity, it should be noted here that while the results of NMS are presented in a similar manner to those of PCA and EOFs, the internal mechanics of NMS are entirely different. On the other hand, EOFs can be viewed as a specific application of PCA when the data involve time series of a single variable. Indeed, the decomposition of the data matrix is identical in both applications, *via* either eigenanalysis or singular value decomposition. Therefore, the analysis in Chapter 2 is presented using the terminology of PCA because the emphasis is on decomposing the contribution of five different variables, while Chapter 3 uses the terminology of EOFs because the goal is to decompose the temporal evolution of one variable at a time. Using the terminology of Cattell (1966) and Legendre and Legendre (1998), NMS and PCA are instances of "Q-mode" analysis (among sample units based on all observed variables) while EOFs are an instance of "S-mode" analysis (among sample units based on all observed times).

The reader should be cautioned at this point about the limitations of the analyses presented throughout this dissertation. They are based on the multivariate decomposition of long-term averages and climatological fields, rather than on the

more conventional decomposition of actual time series. A problem with using the smooth "climatological time series" (as in chapters 3 and 4) is that they are dominated by the seasonal cycle, while intraseasonal or interannual variability is de-emphasized or lost. There is little variance left to decompose in such time series in comparison to the original ones used to construct them, and the effect is that the extracted patterns will contain either inflated or underrepresented fractions of it. This is evident in the coefficients of determination (R^2) in the EOF and NMS analyses, with R^2 values above 80% for the first pattern and R^2 values below 10% for the second pattern. Thus, the amount of variance represented by each pattern should not be relied upon to quantify their actual strength, nor should it be used for statistical inference. Nevertheless, these data sets are still useful for descriptive and exploratory purposes, especially when the original fields are gappy or otherwise irregular. The intention is to describe the broad outlines of the extracted patterns and to identify potential areas for further research.

Another important point to keep in mind is that, ultimately, this dissertation seeks to describe the response of the biota to seasonal oceanographic change. That restriction on the timescale was imposed from the beginning by the impossibility of obtaining cetacean data at temporal and spatial resolutions comparable to those of available oceanographic data sets. This is because in most regions of the world's oceans, sampling of cetacean occurrence is too sparse for analysis of species-environment associations beyond the limited scope of a single cruise. The results presented here are possible only because the eastern tropical Pacific has received an extraordinary amount of sampling effort for cetaceans over the last three decades. Yet, as will be seen in Chapter 4, even seasonal composites of cetacean distributions in the study area are not completely gap-free.

It is acknowledged that a number of oceanographic processes with biological impacts, from tidal mixing, equatorial waves, and mesoscale eddies at one end of the spectrum, to El Niño and decadal oscillations at the other end, are

filtered out in the climatological data sets used here. However, it should be recognized that seasonal variability is one of the most relevant scales in cetacean ecology, as can be inferred from the long life span, high trophic level, and annual migratory schedules of these animals (e.g., Gaskin, 1976). Seasonal changes result in major redistribution of food supplies at the regional scale, where they are most likely to affect cetacean populations. Although the patterns extracted from the analysis of such data sets may be unrealistically strong (or weak), they are useful for understanding the general response of cetacean populations to seasonal change. Also, it is argued that what we learn from the role of seasonal change can provide insights into the possible effects of longer-term variability, at least in a qualitative sense.

1.1 STUDY AREA

The Galápagos Archipelago is made up of 13 large islands (> 10 km^2), six smaller islands, and over 100 islets and rocks (Jackson, 1993; Snell et al., 1995). A map of islands is show in Figure 1.1. The area for this study is defined as a 7 × 7-degree latitude-longitude box extending from 3°N–4°S and from 87°–94°W, with the geographic center of the Galápagos (0.5°S, 90.5°W) (Snell et al., 1995) at its center. This delimitation ensures that all oceanographic conditions occurring around the Galápagos are represented. The spatial extent of the area thus defined is about 605×10^3 km^2 or 597×10^3 km^2 once the area of the islands is subtracted.

1.2 PHYSICAL SETTING OF THE GALÁPAGOS ARCHIPELAGO

The Galápagos Archipelago straddles the equator between 1°40’N and 1°25’S latitude and between 89°15’W and 92°00’W longitude. The nearest land, continental Ecuador (to which they belong), is approximately 960 km to the east.

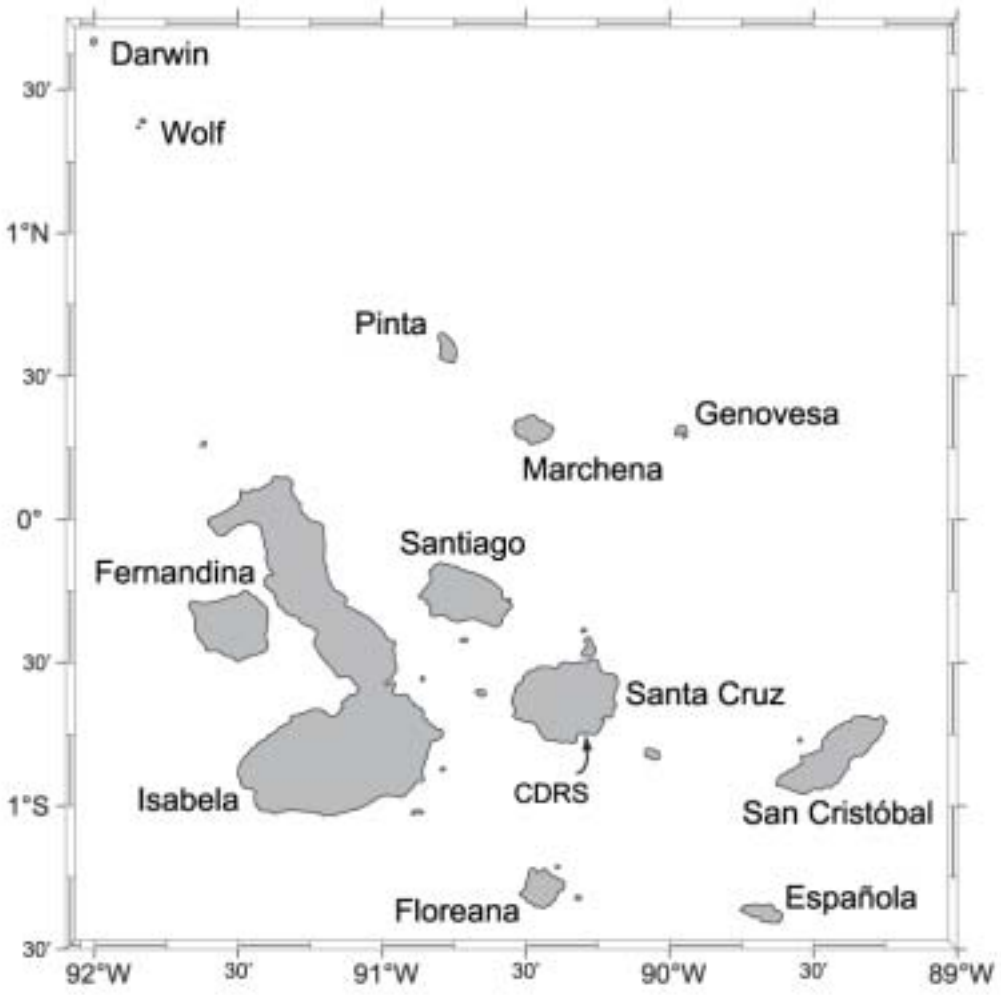

Figure 1.1: Map of the Galápagos Archipelago with the names of the main islands. The arrow indicates the location of the Charles Darwin Research Station (CDRS).

The islands are the product of "hotspot activity" (ocean floor volcanism) and are formed by the emerging tips of submarine volcanoes that rise from the 40000 km^2-wide Galápagos Platform, at a depth of 1300 m (Glynn et al., 1983; Houvenaghel, 1984). Water depth in the study area reaches a maximum of about 3500 m, according to the Smith and Sandwell (1997) global sea-floor topography, version 8.2. A bathymetric map of the study area based on this data set is presented in Figure 1.2.

1.2.1 Climate

Climatic conditions at the Galápagos are determined by the tightly coupled ocean-atmosphere system of the eastern tropical Pacific. This system is driven by the seasonal meridional migration of the northeast and southeast trade wind belts and the associated intertropical convergence zone (ITCZ). The ITCZ is most intensified in August, when it reaches its northernmost position near 10°N, while it weakens and retreats to near 3°N in February [see, for example, Figs. 3 and 6 in Fiedler (2002)]. Thus, the ITCZ is always situated north of the equator in the eastern tropical Pacific (Philander et al., 1996; Wang and Wang, 1999), leaving the Galápagos under the southeast trade wind regime. This confers the islands a subtropical austral character and an unusually dry climate, their equatorial position notwithstanding (Palmer and Pyle, 1966). Consistent with the timing of the north-south migration of the ITCZ, there are two main seasons at the Galápagos: from January to April there is a hot and wet period, and from May to December there is a cool and dry period. During the cold season a low-level atmospheric inversion develops, resulting in the formation of a stratus cloud layer, drizzle (locally known as *garúa*), and heavy fog drip in the highlands of the islands (Palmer and Pyle, 1966). The inversion weakens or disappears during the hot period, and cumulonimbus clouds and heavy rains replace the stratus layer (Palmer and Pyle, 1966).

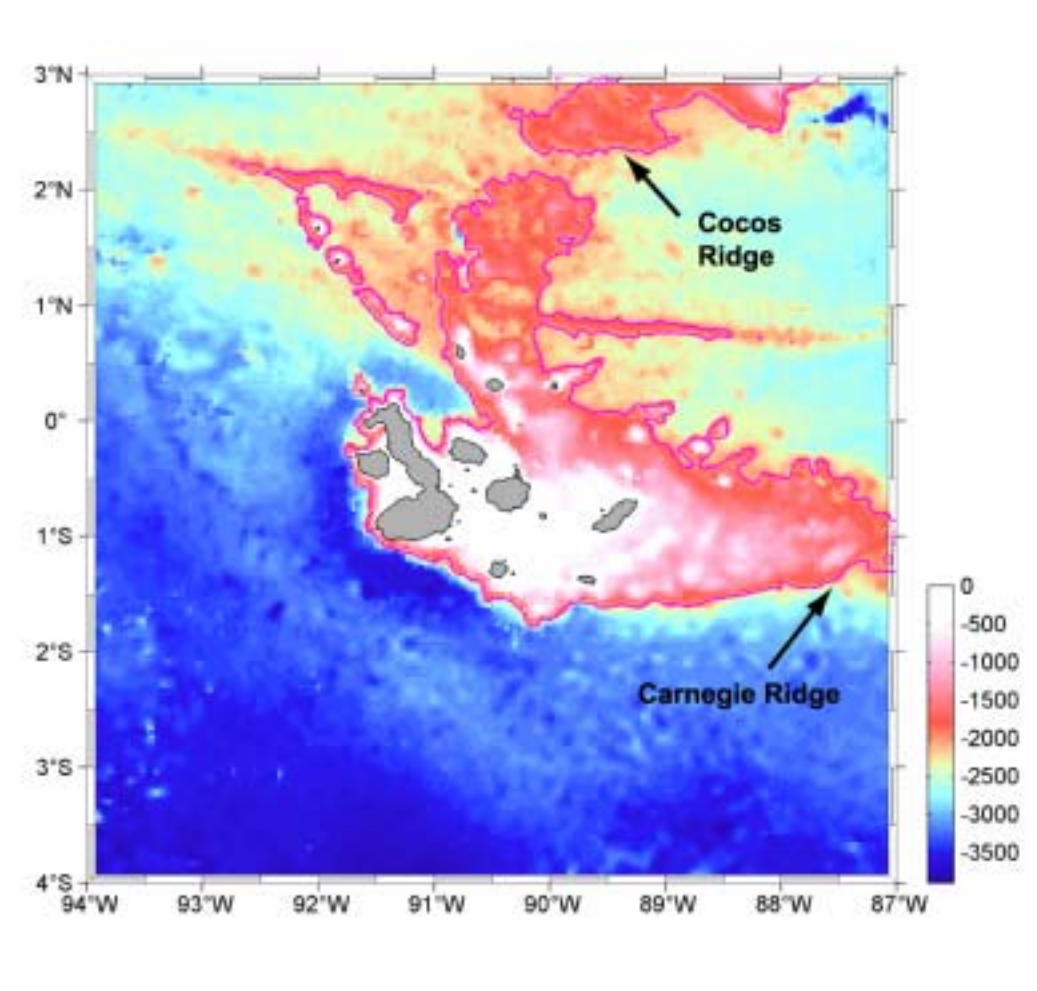

Figure 1.2: Bathymetric map of the study area, based on the Smith and Sandwell (1997) global sea-floor topography. The color scheme emphasizes depths > 1000 m. The 2000-m contour is drawn in magenta. Two submarine mountain ranges meeting at the Galápagos, the Carnegie and Cocos ridges, are indicated.

1.2.2 Oceanographic conditions

Earlier oceanographic reviews of the Galápagos region have been provided by Wooster and Hedgpeth (1966), Houvenaghel (1978, 1984), Glynn et al. (1983), and more recently by Chavez and Brusca (1991). However, significant advances in our understanding of the oceanography of the equatorial Pacific were made during the 1990s, thanks to the implementation of major international programs. The Tropical Ocean-Global Atmosphere (TOGA) Project resulted in the establishment of the Tropical Ocean Atmosphere/Triangle Trans-Ocean Buoy Network (TAO/TRITON), an ocean observing system of instrumented moorings spanning the entire equatorial Pacific for monitoring seasonal-to-interannual climate variability (McPhaden et al., 1998). Intense studies of biogeochemical cycling in the eastern and central part of this basin also took place during the 1990s, as part of the Joint Global Ocean Flux Studies (JGOFS) Equatorial Pacific (EqPac) experiments [see Murray et al. (1995, 1997) and references therein]. In addition, it was in Galápagos waters that the first iron enrichment experiment (IronEx I) was conducted in 1993, to test the hypothesis that low iron concentrations limit phytoplankton production in areas where plant macronutrients are readily available (so-called "high-nitrate, low-chlorophyll" or HNLC conditions), such as the eastern equatorial Pacific (Martin et al., 1994; Coale, 1998).

No attempt is made here to summarize the vast literature that has resulted from these studies (the interested reader is referred to the above-cited sources as a starting point). It is noted, however, that several of the salient results from IronEx I are directly relevant to this dissertation and they are discussed where pertinent. Also, the Galápagos are located near the eastern end of the JGOFS EqPac domain, and it is likely that some of the biogeochemical processes revealed in those studies are pertinent to the waters around the archipelago as well. On the other hand, a revised picture of equatorial circulation as it affects the Galápagos is presented in this section in light of recent observations. In what follows, a description of

currents, fronts, watermasses, upwelling, equatorial waves, and El Niño effects around the Galápagos is given.

1.2.2.1 Currents

Two major trans-Pacific flows affect the Galápagos region (Fig. 1.3), the surface South Equatorial Current (SEC) and the subsurface Equatorial Undercurrent (EUC). The mean fields and the seasonal variations of these flows have been recently estimated from monthly climatologies derived from TAO/TRITON array measurements (Yu and McPhaden, 1999) and associated cruises (Johnson et al., 2002). The westernmost Galápagos islands are located 330 km to the east of the easternmost TAO/TRITON moorings at 95°W. The general picture at the Galápagos should be qualitatively similar (unless otherwise noted), but the currents should be expected to decelerate to some extent.

The SEC is a relatively strong surface current that travels westward from about 10°S to 4°N, driven by the southeast trade winds (Fiedler, 1992). It is fed by the Perú Current and by recirculating flows from the EUC and the Panamá Bight (see below). A near-equatorial minimum in westward surface flow separates a northern and a southern branch [referred to as SEC(N) and SEC(S)] in the vicinity of the Galápagos (Johnson et al., 2002). At 95°W the SEC(N) has a mean zonal velocity of about 40 cm s^{-1} at the surface. In zonal velocity-weighted mean fields this branch appears centered at about 2.5°N at a depth of 35 m. It has a mean zonal transport of 10×10^6 m^3 s^{-1}, and it carries water with a mean temperature of 23.8°C and a mean salinity of 34.1. The SEC(S) also has a mean zonal velocity of about 40 cm s^{-1} at the surface, and in zonal velocity-weighted mean fields it appears centered at 4.2°S at a depth of 35 m. The SEC(S) transports a slightly lower volume (7×10^6

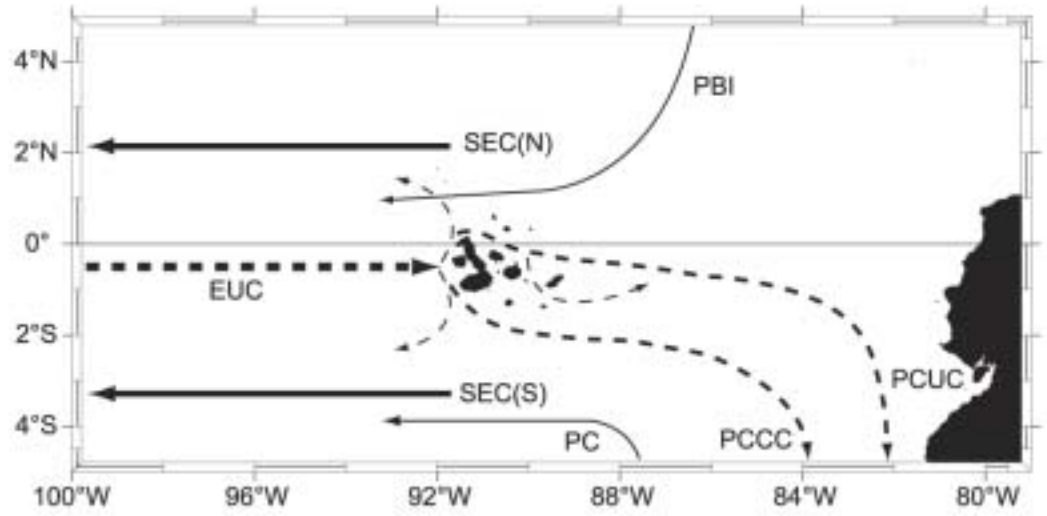

Figure 1.3: Schematic representation of the current systems in the vicinity of the Galápagos Islands. SEC = South Equatorial Current, EUC = Equatorial Undercurrent, PBI = Panamá Bight Influence, PC = Perú Current, PCCC = Perú-Chile Countercurrent, PCUC = Perú-Chile Undercurrent. Dashed arrows represent subsurface flows. Adapted from Pak and Zaneveld (1973), Anderson (1977), Lukas (1986), and Strub et al. (1998).

$m^3 s^{-1}$), with cooler (22.2°C) and saltier (34.9) water than the SEC(N) at the same longitude. The relative warmness and freshness of the SEC(N) with respect to the SEC(S) is due to its proximity to the ITCZ, particularly in January–February, when the ITCZ moves over the SEC(N) (Johnson et al., 2002).

The SEC(N) has minimum westward velocities, low volume transports, warm temperatures and low salinities in January–June, when it also has a shallow core that is shifted to the north. In July–December the current shifts southward and deepens, reaching maximum velocities and transports, cool temperatures, and high salinities. The seasonality of the SEC(S) is roughly in phase with that of the SEC(N), with faster, cooler, saltier, and larger transports in June–January than in February–May. The SEC(S) deepens and shifts southward during the latter period, and it shoals and moves northward during the former. An actual reversal of the normally westward-flowing SEC takes place in April–May, reaching eastward speeds of 30 cm s^{-1} at 110°W (McPhaden et al., 1998; Yu and McPhaden, 1999). This reversal may be associated with the surfacing of the eastward-flowing EUC during that time (e.g., Lukas, 1986; Johnson et al., 2002).

The EUC originates in the western Pacific as the return flow that compensates the westward surface flow of the SEC. This subsurface current travels eastward in the thermocline (as indexed by the depth of the 20°C isotherm) as a narrow jet generally found between 2°N and 2°S. It reaches its full strength between 155°W and 125°W, in the central Pacific, but by 95°W it has weakened considerably (Johnson et al., 2002). In the eastern Pacific the core of the EUC is not on the equator but slightly offset to the south. At 95°W the mean position of the EUC core is at 0.25°S and a depth of 110 m, where its mean zonal velocity is 70 cm s^{-1}. In zonal velocity-weighted mean fields the EUC volume transport is 21 × 10^6 $m^3 s^{-1}$, and it carries water with a mean temperature of 15.6°C and a salinity of 34.9. The core of the EUC is characterized by maxima in oxygen (Anderson, 1977; Lukas, 1986) and dissolved iron (Coale et al., 1996a). Seasonally, the EUC is

shallow, fast, warm, and salty in March–July, and deep, slow, cold, and fresh in August–February.

East of 92°W, the EUC encounters the Galápagos, causing its flow to decelerate and split into two main branches. The southern branch has a shallow but strong velocity core, while the northern branch has a deeper, less intense core (Lukas, 1986; Steger et al., 1998). These branches flow past the southern (most of the flow) and northern margins of the archipelago (Fig. 1.3) and continue toward the South American coast. There they appear to join the Perú-Chile Countercurrent and the Perú-Chile Undercurrent (Lukas, 1986; Strub et al., 1998). Both branches interact with the complex sea-floor topography of the Galápagos Archipelago, causing further branching, return flows (Pak and Zaneveld, 1973; Zaneveld et al., 1973; Anderson, 1977; Lukas, 1986), and topographically induced upwelling at several locations (Houvenaghel, 1978).

In addition to the SEC and the EUC, seasonal influx into the Galápagos region from the Panamá Bight can also be important (Fig. 1.3). The cyclonic gyre that dominates the circulation in the Panamá Bight is enhanced during January–March, and at this time outflow through its western limb reaches mean velocities of order 50 cm s^{-1} (Wooster, 1959; Stevenson, 1970). The northeastern Galápagos region is bathed by this current as it drifts southwest to join the SEC(N) [see Cromwell and Bennett (1959) and Fig. 3 in Fiedler (2002)]. This Panamá Bight Influx (PBI) has been erroneously linked with warm, low salinity water observed every year in the Galápagos around January (Glynn et al., 1983). In fact, PBI water is relatively cool (26–28°C) and salty (34–35), as it is the result of wind-driven upwelling in the Panamá Bight [see review by Wooster (1959), and Figs. A-13 and A-14 in Fiedler (1992)]. Thus, it is more likely that the seasonal warming and freshening reported by Glynn et al. (1983) occur locally in the SEC(N), as the ITCZ moves over the region. Similarly, the North Equatorial Countercurrent (NECC) has been implicated in southeastward flow of warm, low salinity water

reaching the Galápagos during the first months of the year (e.g., Houvenaghel, 1984). This is not likely the case, as the NECC is only present as a weak eastward flow well to the north of the Galápagos (~ 6°N) at this time (Johnson et al., 2002; Kessler, 2002). Rather, the seasonal reversal of the SEC that has been documented farther to the west may also take place at the Galápagos, and this could be a more plausible explanation for this observation.

1.2.2.2 Regional fronts

Two large-scale fronts separate waters with distinct physical and biogeochemical characteristics passing through the Galápagos region at different times of the year. When the SE trade winds are strong, they blow over the shallow equatorial thermocline and induce the "cold tongue", a band of cool water at the surface that extends from the coast of South America to near the international dateline (e.g., McPhaden, 1998). The sharp boundary separating cold tongue waters to the south from the warm waters to the north is known as the Equatorial Front (EF) (Fig. 1.4). The cold tongue persists from about May to January, and at this time the Galápagos are mostly surrounded by it while the EF is just to the north of the islands. The cold tongue retreats toward the South American coast in February–April and the EF disappears. West of the Galápagos, strong oscillations about the mean position of the EF are known as tropical instability waves (TIWs). They are manifestations of shear between the NECC and the SEC. TIWs propagate westward with periods of 20–40 days, wavelengths of 1000–2000 km and phase speeds of about 0.5 m s^{-1} (e.g., McPhaden et al., 1998; Weidman et al., 1999; Chelton et al., 2000a).

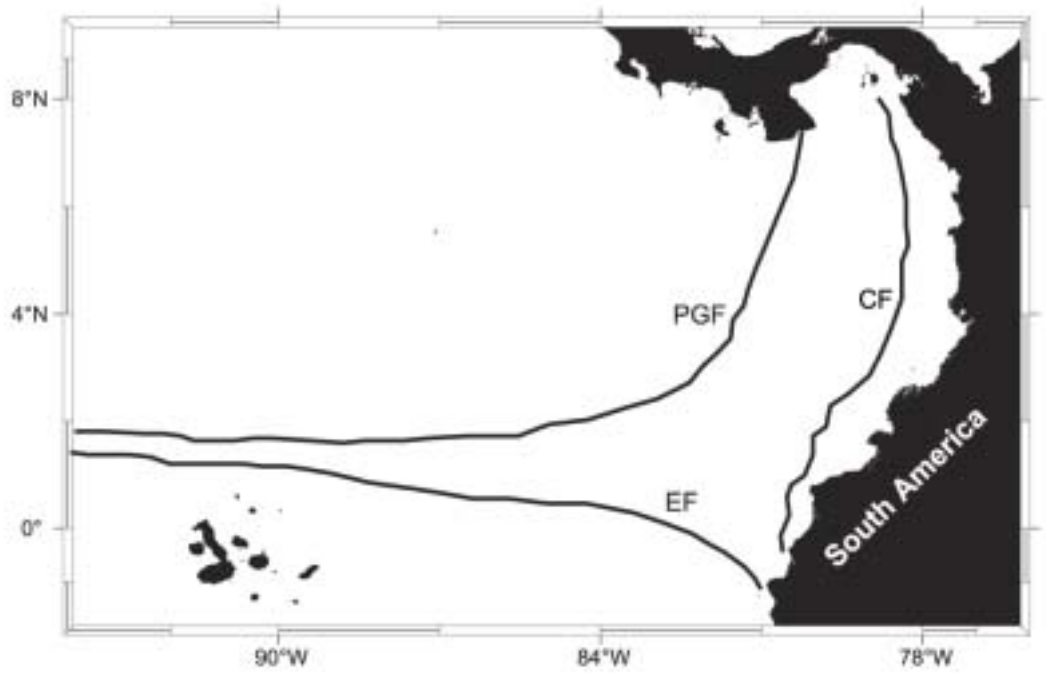

Figure 1.4: Mean front positions in the study area, derived from the satellite SST monthly climatologies described in section 3.3. EF = Equatorial Front, PGF = Panamá-Galápagos Front, CF = Colombia Front (the eastern boundary of the plume of upwelled water in the Panamá Bight).

Another front appears between the Gulf of Panamá and the Galápagos during January–April. This "Panamá-Galápagos Front" (PGF in Fig. 1.4) delineates the western boundary of a meridional plume of cool water extending from the Gulf of Panamá (i.e., the PBI), as it is pushed offshore during upwelling events generated by northeast trade winds crossing the Isthmus of Panamá from the Caribbean Sea (e.g., Wooster, 1959; Legeckis, 1988; Chelton at al., 2000b). Wave-like motions that resemble TIWs modulate the position of the PGF. Based on limited observations, Legeckis (1988) estimated that these waves have periods of about 20 days, wavelengths of 450–750 km and phase speeds of about 0.35 ± 0.12 m s^{-1}.

The mean front positions in Figure 1.4 were derived from the monthly sea-surface temperature (SST) climatologies described in section 3.3. They represent the May–January 24.5°C isotherm for the EF and the January–April 26.5°C isotherm for the PFG. The eastern boundary of the upwelled water in the Panamá Bight, which runs parallel to the South American coast, is termed the "Colombia Front" (CF in Fig. 1.4). Small-scale fronts can also be found in the Galápagos, at the edges of upwelled water, where cold and warm water with different characteristics meet. These are discussed below in the context of local upwellings.

1.2.2.3 Watermasses

A watermass is a body of water with a common formation history (Tomczak and Godfrey, 1994). Watermasses are typically characterized by the unique combination of temperature and salinity conditions at the time of their formation. The major watermass types in the world's oceans can be classified into two main groups: abyssal and surface-layer (i.e. those found in the thermocline and upper 1000 m) watermasses. The abyssal watermasses contain Bottom Water, Deep Water, and Intermediate Water, and the surface-layer watermasses contain Central Water and Surface Water (Tomczak and Godfrey, 1994).

Anderson (1977) used the distribution of watermass properties in the upper 25–400 m of the water column to infer the path of near-surface currents around the archipelago. However, there are no other descriptions of watermass types for the study area, particularly of watermasses in the lower parts of the water column. An effort to fill this gap is presented here by using climatological profiles of temperature and salinity from the World Ocean Atlas 1998 (WOA98) (Conkright et al., 1998) for the study area.

Water-column temperature and salinity values are represented as red dots in the temperature-salinity (T-S) diagram shown in Figure 1.5. Starting with the abyssal waters, it is noted that there is no Antarctic Bottom Water (AABW) in the region because the East Pacific-Chile Rise prevents it from entering the basins off South America (Tomczak and Godfrey, 1994). Pacific Deep Water (PDW) is the deepest watermass in the study area, at depths of 900–3500 m. It has a local salinity maximum near the bottom, a remnant of North Atlantic Deep Water (NADW). This PDW is warmed geothermally by 0.3°C by the Galápagos spreading center (Tomczak and Godfrey, 1994). Antarctic Intermediate Water (AAIW), characterized by $2 < T < 10$°C and $33.8 < S < 34.5$, is "ill-defined" or absent in the region (Tomczak and Godfrey, 1994). The local mid-depth salinity minimum is 34.55 at 900 m. Thus, PDW is the only abyssal water type clearly defined in the study area. The surface-layer watermasses, on the other hand, present a more complex scenario. Salinites ≥ 34.55 at depths ≤ 900 m indicate that Central Water has contact and mixes with PDW (Tomczak and Godfrey, 1994). The nearly linear set of combinations characterizing the T-S relationship between $5 < T < 15$°C and $34.5 < S < 35$ indicates that this Central Water mass corresponds to South Pacific Equatorial Water (SPEW) at its northernmost extent. The salinity maximum (35.1) above 15°C, at a depth of 30 m, is associated with the high-salinity core that

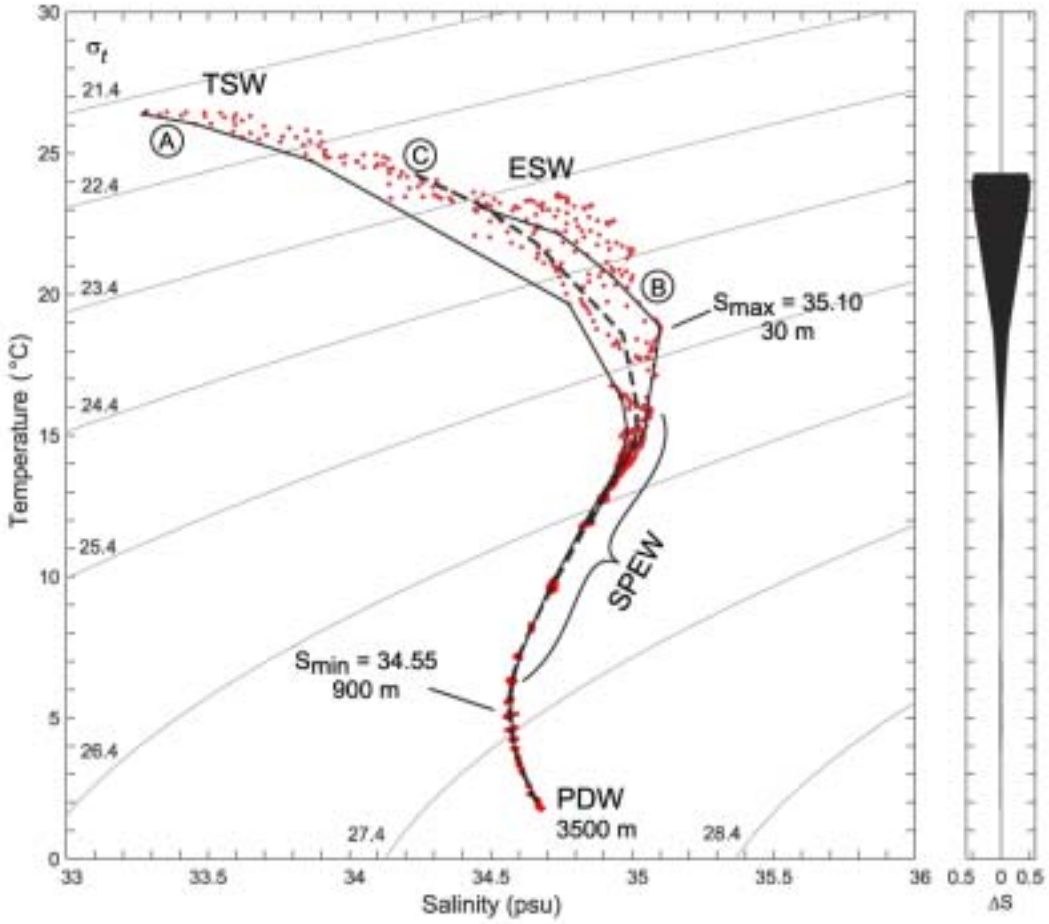

Figure 1.5: Temperature-salinity relationships and T-S curves from WOA98 annual data for the study area. A and B (solid lines) are profiles at locations representing extreme conditions in the study area. A is north of the Equatorial Front and B is in an area influenced by EUC upwelling. C (dashed line) is a mean profile using all the data. The plot on the right represents the standard deviation about that mean.

characterizes the EUC (see Lukas, 1986). Wind-driven and topographic upwelling south of the EF brings SPEW and EUC waters to the surface, where they are modified into Equatorial Surface Water (ESW). North of the EF, under the influence of the ITCZ and the heavy precipitation in the Panamá Bight, SPEW waters are modified into Tropical Surface Water (TSW) (see Wyrtki, 1967; and Fig. 4 in Fiedler, 1992).

1.2.2.4 Upwelling and plumes

Upwelling occurs at the Galápagos throughout the year, with varying intensity owing to topographic and wind-forced mechanisms. Houvenaghel (1978) recognized the topographically forced upwelling of the EUC at several locations in the archipelago as a local, mesoscale phenomenon distinct from the wind-driven equatorial upwelling along the cold tongue that is characteristic of the cold season. These upwellings bring cool, nutrient-rich waters to the surface, creating the conditions for elevated biological production. This is especially evident on the western side of the archipelago, where upwelled water from the EUC is carried westward by the SEC, generating a plume of elevated phytoplankton pigment concentrations that is clearly visible in ocean color satellite imagery (Feldman, 1986). Recent evidence suggests that the extent of and production in the plume are directly dependent on the strength of the EUC, rather than on tidal mixing processes in the islands (Steger et al., 1998). Nevertheless, mixing of the sharp thermal boundaries at the edge of recently upwelled water appears to be an important step in the development of the large pigment patches characteristic of the plume (Hoge et al., 1998). Bio-optical observations further suggest that some of the ocean color seen in the plume actually corresponds to senescent (i.e., inactive) phytoplankton after a biological succession process (Hoge et al., 1998).

1.2.2.5 Equatorial waves

Owing to their geographic position, the Galápagos are subject to remote perturbations traveling in the equatorial waveguide, both at the surface and in the thermocline. These perturbations (or "transients") can be generated by a variety of mechanisms, but they are often the way in which the equatorial ocean responds to variability in wind forcing. Thus, a combination of Rossby and Kelvin waves plays a major role in the westward propagation of seasonal variation in equatorial zonal currents, both for the surface flows and for the EUC (Lukas, 1986; Yu and McPhaden, 1999). Eastward-propagating intraseasonal Kelvin waves with 60–90-day periods are a prominent occurrence in the equatorial Pacific, particularly during El Niño events (see McPhaden et al., 1998; McPhaden, 1999). The vertical motions of the thermocline induced by these waves can bring limiting nutrients into the euphotic zone and stimulate phytoplankton growth (Cipollini et al., 2001; Friedrichs and Hoffman, 2001). At the Galápagos, high-frequency inertia-gravity waves (5-day period), mixed Rossby-gravity waves (10-day period), and intraseasonal Kelvin waves are well documented (Ripa and Hayes, 1981; Hayes, 1985).

1.2.2.6 El Niño/La Niña effects

Interannual variability in the eastern equatorial Pacific associated with El Niño/La Niña oscillations is analogous to seasonal variability of comparable magnitude (e.g., Fiedler, 1992; Johnson et al., 2002). An overview of the El Niño cycle has been provided in McPhaden et al. (1998). In general, La Niña has effects that are similar but opposite in direction to El Niño. Surface temperatures are warmer and salinities are lower than average during El Niño, and cooler and saltier during La Niña. Equatorial currents are weakened during El Niño and enhanced during La Niña, and they also undergo shifts in the latitude of their mean position (Johnson et al., 2002). During El Niño, the cold tongue and the associated EF may

disappear, while it is well developed during La Niña when the EF is sharply demarcated and TIW activity is intense. The EUC has been observed to weaken or disappear at the height of several El Niño events (Johnson et al., 2002). Consequently, the Galápagos plume collapses on the western side of the archipelago, and phytoplankton pigment concentrations around the islands undergo a dramatic redistribution (Feldman et al., 1984). Other physical and biogeochemical effects of El Niño in the Galápagos are well documented (e.g., Boersma, 1978; Robinson and del Pino, 1985; Barber and Chavez, 1983; Hayes et al., 1986; Chavez and Brusca, 1991; Podestá and Glynn, 1997; Valenti et al., 1999).

1.2.3 Inter-island zones

One of the most striking features of the waters around the Galápagos is the existence of distinct zones among the islands. These are undoubtedly a result of the degree of exposure of the different sectors of the archipelago to the equatorial currents and other oceanographic conditions described in the previous sections. Harris (1969) attempted to describe this complexity in terms of differences in SST. He divided the archipelago into five zones, which are shown in Figure 1.6. A south-central zone 1, with intermediate temperatures, extends as a band from southeastern Isabela toward Santa Cruz and neighboring islands. A southern zone 2, with somewhat cooler temperatures, includes the islands of San Cristóbal, Española and Floreana. A northern zone 3 has the warmest temperatures in the archipelago, and comprises the islands of Genovesa, Marchena, Pinta, Wolf and Darwin. A north-central zone 4 comprises the waters around Santiago and eastern Isabela. This zone has a less defined temperature regime, as it has seasonal affinities to both the first and the third zones. Finally, a western zone 5 has the lowest temperatures in the archipelago, and includes the waters around Fernandina and western Isabela (Harris, 1969).

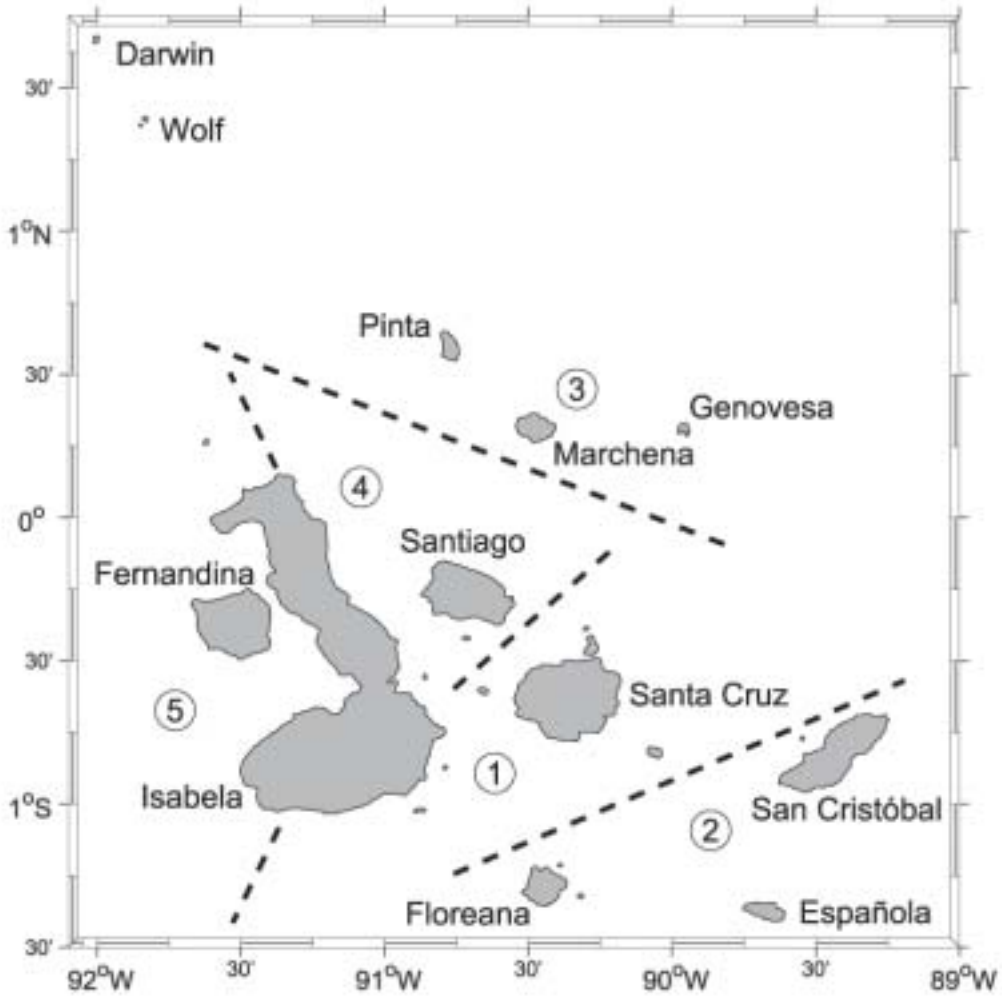

Figure 1.6: The five SST zones in Galápagos waters defined by Harris (1969).

Harris's zonation scheme, which is still widely used (e.g., Glynn et al. 1983; Grove and Lavenberg, 1997), was recently tested by Wellington et al. (2001) using SST time series at six locations in Harris's five zones. Although they found consistent north-south and east-west differences that supported the existence of zones, they concluded that the magnitude of the differences among most locations was much smaller (i.e., statistically non-significant) than those reported by Harris. The validity of these zones is discussed further in section 3.4 in the context of the data sets and analyses of this study.

Feldman (1986) compared the distribution and temporal varibility of phytoplankton pigment concentrations derived from the Coastal Zone Color Scanner among nine regions comprising the main cluster of islands. The regions in the southern and eastern portions of the archipelago had the lowest overall mean concentrations, while the regions to the west contained the highest concentrations. Seasonally, the regions in the western sector underwent a dramatic increase in pigment in the second part of the year (June–December) compared to the first part (February–May). At the same time, pigment concentrations in the regions to the east decreased during the second part of the year. Feldman (1986) explained this seasonal redistribution in terms of a shift in the areas of increased phytoplankton production. A more detailed quantification of the seasonality of phytoplankton distributions around the archipelago is one of the salient results of this study (see Chapter 3).

1.3 REFERENCES

Anderson, J.J. 1977. Identification and tracing of water masses with an application near the Galápagos Islands. Ph.D. Thesis, University of Washington. 144 pp.

Arístegui, J., P. Tett, A. Hernández-Guerra, G. Basterretxea, M.F Montero, K. Wild, P. Sangrá, S. Hernández-León, M. Cantón, J.A. García-Braun, M. Pacheco, and E.D. Barton. 1997. The influence of island-generated eddies on

chlorophyll distribution: a study of mesoscale variation around Gran Canaria. Deep-Sea Research I 44(1):71–96.

Barber, R.T., and F.P. Chavez. 1983. Biological consequences of El Niño. Science 222:1203–1210.

Barton, E.D., G. Basterretxea, P. Flament, E.G. Mitchelson-Jacob, B. Jones, J. Arístegui, and F. Herrera. 2000. Lee region of Gran Canaria. Journal of Geophysical Research 105:17173–17193.

Boersma, P.D. 1978. Breeding patterns of Galapagos penguins as an indicator of oceanographic conditions. Science 200:1481–1483.

Cattell, R.B. 1966. The data box: its ordering of total resources in terms of possible relational systems. Pages 67–128 *in* Cattell, R.B., ed. Handbook of Multivariate Experimental Psychology. Rand McNally & Co. Chicago.

Chavez, F.P., and R.C. Brusca. 1991. The Galápagos Islands and their relation to oceanographic processes in the tropical Pacific. Pages 9–33 *in* James, M.J., ed. Galápagos Marine Invertebrates. Taxonomy, Biogeography, and Evolution in Darwin's Islands. Topics in Geobiology, Vol. 8. Plenum Press, New York and London.

Chelton, D.B., F.J. Wentz, C.L. Gentemann, R.A. de Szoeke, and M.G. Schlax. 2000a. Satellite microwave SST observations of transequatorial tropical instability waves. Geophysical Research Letters 27(9):1239–1242.

Chelton, D.B., M.H. Freilich, and S.K. Esbensen. 2000b. Satellite observations of the wind jets off the Pacific coast of Central America, Part I: Case studies and statistical characteristics. Monthly Weather Review 128:1993–2018.

Cipollini, P., D. Cromwell, P.G. Challenor, and S. Raffaglio. 2001. Rossby waves detected in ocean colour data. Geophysical Research Letters 28:323–326.

Coale, K.H. (Ed.). 1998. The Galápagos iron experiments: A tribute to John Martin. Deep-Sea Research II 45:915–1150.

Coale, K.H., S.E. Fitzwater, R.M. Gordon, K.S. Johnson, and R.T. Barber. 1996a. Control of community growth and export production by upwelled iron in the equatorial Pacific. Nature 379:621–624.

Conkright, M., S. Levitus, T. O'Brien, T. Boyer, J. Antonov, and C. Stephens. 1998. World Ocean Atlas 1998 CD-ROM Data Set Documentation. Technical Report 15. NODC Internal Report, Silver Spring, MD, 16 pp.

Cromwell, T., and E.B. Bennett. 1959. Surface drift charts for the eastern tropical Pacific Ocean. Inter-American Tropical Tuna Commission Bulletin 3(5):217–237.

Feldman, G.C. 1986. Patterns of phytoplankton production around the Galápagos Islands. Pages 77–106 *in* Bowman, M.J., C.M. Yentsch, and W.T. Peterson, Eds. Tidal mixing and plankton dynamics. Lecture Notes on Coastal and Estuarine Studies 17, Springer-Verlag, Berlin.

Feldman, G., D. Clark, and D. Halpern. 1984. Satellite color observations of the phytoplankton distribution in the eastern equatorial Pacific during the 1982-1983 El Niño. Science 226(4678):1069–1071.

Fiedler, P.C. 1992. Seasonal climatologies and variability of eastern tropical Pacific surface waters. NOAA Technical Report NMFS 109:1–65.

Fiedler, P.C. 2002. The annual cycle and biological effects of the Costa Rica Dome. Deep-Sea Research I 49:321–338.

Friedrichs, M.A.M., and E.E. Hofmann. 2001. Physical control of biological processes in the central equatorial Pacific Ocean. Deep-Sea Research I 48:1023–1069.

Gaskin, D.E. 1976. The evolution, zoogeography and ecology of Cetacea. Oceanography and Marine Biology Annual Review 14:247–346.

Glynn, P.W., G.M. Wellington, and J.W. Wells. 1983. Corals and coral reefs of the Galápagos Islands. University of California Press, Berkeley. 330 pp.

Grove, J.S. and R.J. Lavenberg. 1997. The fishes of the Galápagos Islands. Stanford University Press, Stanford, California. 936 pp.

Harris, M.P. 1969. Breeding seasons of sea-birds in the Galápagos Islands. Journal of Zoology, London 159:145–165.

Hayes, S.P. 1985. Sea level and near surface temperature variability at the Galápagos Islands, 1979–83. Pages 49–81 *in* Robinson, G., and E.M. del Pino, eds. El Niño in the Galápagos Islands: The 1982–1983 Event. Publication of the Charles Darwin Research Foundation for the Galápagos Islands, Quito, Ecuador.

Hayes, S.P., L.J. Magnum, R.T. Barber, A. Huyer, and R.L. Smith. 1986. Hydrographic variability west of the Galápagos Islands during the 1982–83 El Niño. Progress in Oceanography 17:137–162.

Hernández-León, S., C. Almeida, M. Gómez, S. Torres, I. Montero, and A. Portillo-Hannefeld. 2001. Zooplankton biomass and indices of feeding and metabolism in island-generated eddies around Gran Canaria. Journal of Marine Systems 30:51–66.

Hoge, F.E., C.W. Wright, R.N. Swift, J.K. Yungel, R.E. Berry, and R. Mitchell. 1998. Airborne bio-optics survey of the Galápagos Islands margins. Deep-Sea Research II 45:1083–1092.

Houvenaghel, G.T. 1978. Oceanographic conditions in the Galápagos Archipelago and their relationships with life on the islands. Pages 181–200 *in* Boje, R., and M. Tomczak, eds. Upwelling Ecosystems. Springer-Verlag, Berlin.

Houvenaghel, G.T. 1984. Oceanographic setting of the Galápagos Islands. Pages 43–54 *in* Perry, R., ed. Key Environments, Galápagos. Pergamon Press, Oxford.

Jackson, M.H. 1993. Galápagos, a natural history. University of Calgary Press, Calgary, Alberta, Canada. 315 pp.

Johnson, G.C, B.M. Sloyan, W.S. Kessler, and K.E. McTaggart. 2002. Direct measurements of upper ocean currents and water properties across the tropical Pacific during the 1990's. Progress in Oceanography 52(1):31–61.

Kessler, W.S. 2002. Mean three-dimensional circulation in the northeast tropical Pacific. Journal of Physical Oceanography 32:2457–2471.

Legeckis, R. 1988. Upwelling off the Gulfs of Panamá and Papagayo in the tropical Pacific during March 1985. Journal of Geophysical Research 93(C12):15485–15489.

Legendre, P., and L. Legendre. 1998. Numerical ecology. Second English edition. Developments in Environmental Modelling 20. Elsevier. Amsterdam. 853 pp.

Lukas, R. 1986. The termination of the Equatorial Undercurrent in the eastern Pacific. Progress in Oceanography 16:63–90.

Martin, J.H., K.H. Coale, K.S. Johnson, S.E. Fitzwater, R.M. Gordon, S.J. Tanner, C.N. Hunter, V.A. Elrod, J.L. Nowicki, T.L. Coley, R.T. Barber, S. Lindley, A.J. Watson, K. Van Scoy, C.S. Law, M.I. Liddicoat, R. Ling, T. Stanton, J. Stockel, C. Collins, A. Anderson, R. Bidigare, M. Ondrusek, M. Latasa, F.J. Millero, K. Lee, W. Yao, J.Z. Zhang, G. Friederich, C. Sakamoto, F. Chavez, K. Buck, Z. Kolber, R. Greene, P. Falkowski, S.W. Chisholm, F. Hoge, R. Swift, J. Yungel, S. Turner, P. Nightingale, A. Hatton, P. Liss, and N.W. Tindale. 1994. Testing the iron hypothesis in ecosystems of the equatorial Pacific Ocean. Nature 371:123–129.

McPhaden, M.J. 1999. Genesis and evolution of the 1997–98 El Niño. Science 283:950–954.

McPhaden, M.J., A.J.Busalacchi, R. Cheney, J.-R. Donguy, K.S. Gage, D. Halpern, M. Ji, P. Julian, G. Meyers, G.T. Mitchum, P.P. Niiler, J. Picaut, R.W. Reynolds, N. Smith, and K. Takeuchi. 1998. The Tropical Ocean Global Atmosphere observing system: A decade of progress. Journal of Geophysical Research 103(C7):14169–14240.

Murray, J.W., E. Johnson, and C. Garside. 1995. A U.S. JGOFS Process Study in the equatorial Pacific (EqPac): Introduction. Deep Sea Research II 42(2–3):275–293.

Murray, J.W., R. Le Borgne, and Y. Dandonneau. 1997. JGOFS studies in the equatorial Pacific. Deep Sea Research II 44(9–10):1759–1763.

Pak, H., and J.R.V. Zaneveld. 1973. The Cromwell Current on the east side of the Galápagos Islands. Journal of Geophysical Research 78(33):7845–7859.

Pakhomov, E.A., P.W. Froneman, I.J. Ansorge, J.R.E. Lutjeharms. 2000. Temporal variability in the physico-biological environment of the Prince Edward Islands (Southern Ocean). Journal of Marine Systems 26:75–95.

Palmer, C.E., and R.L. Pyle. 1966. The climatological setting of the Galápagos. Pages 93–99 *in* Bowman, R.I., ed. The Galápagos: Proceedings of the Symposia of the Galápagos International Scientific Project. University of California Press, Berkeley.

Philander, S.G.H., D. Gu, D. Halpern, G. Lambert, N.-C. Lau, T. Li, and R.C. Pacanowski. 1996. Why the ITCZ is mostly north of the equator. Journal of Climate 9:2958–2972.

Podestá, G.P., and P.W. Glynn. 1997. Sea surface temperature variability in Panamá and Galápagos: Extreme temperatures causing coral bleaching. Journal of Geophysical Research 102(C7):15749–15759.

Ripa, P., and S.P. Hayes. 1981. Evidence of equatorial trapped waves at the Galápagos Islands. Journal of Geophysical Research 86(C7):6509–6516.

Robinson, G., and E.M. del Pino, eds. 1985. El Niño in the Galápagos Islands: the 1982–83 Event. Publication of the Charles Darwin Foundation for the Galápagos Islands (Contribution No. 388). Quito, Ecuador. 534 pp.

Rodríguez, J.M., E.D Barton, L. Eve, and S. Hernández-León. 2001. Mesozoolpankton and ichthyoplankton distribution around Gran Cabaria, and oceanic island in the NE Atlantic. Deep-Sea Research I 48:2161–2183.

Smith, W.H.F., and D.T. Sandwell. 1997. Global seafloor topography from satellite altimetry and ship depth soundings. Science 277:1957–1962.

Snell, H.M., P.A. Stone, P.A., and H.L. Snell. 1995. Geographical characteristics of the Galápagos Islands. Noticias de Galápagos 55:18–24.

Steger, J.M., C.A. Collins, and P.C. Chu. 1998. Circulation in the Archipiélago de Colón (Galápagos Islands), November, 1993. Deep-Sea Research II 45(6):1093–1114.

Stevenson, M. 1970. Circulation in the Panama Bight. Journal of Geophysical Research 75(3):659–672.

Strub, P.T., J.M. Mesías, V. Montecino, J. Rutllant, and S. Salinas. 1998. Coastal ocean circulation off western South America. Pages 273–313 *in* Robinson, A.R., and K.H. Brink, eds. The Sea, Ideas and Observations on Progress in the Study of the Seas, Vol. 11, Global Coastal Ocean Regional Studies and Syntheses. John Wiley & Sons, Inc., New York.

Tomczak, M., and J.S. Godfrey. 1994. Regional oceanography: an introduction. Pergamon, London. 422 pp.

Valenti, G., C. McClain, G. Feldman, G., and R. Bustamante. 1999. SeaWiFS captures El Niño/La Niña transition. Backscatter 10(2):31–33.

Wang, B., and Y. Wang. 1999. Dynamics of the ITCZ–Equatorial Cold Tongue complex and causes of the latitudinal climate asymmetry. Journal of Climate 12:1830–1847.

Weidman, P.D., D.L. Mickler, B. Dayyani, and G.H. Born. 1999. Analysis of Legeckis eddies in the near-equatorial Pacific. Journal of Geophysical Research 104(C4):7865–7887.

Wellington, G.M., A.E. Strong, and G. Merlen. 2001. Sea surface temperature variation in the Galápagos Archipelago: A comparison between AVHRR night-

time satellite data and in-situ instrumentation (1982-1998). Bulletin of Marine Science 69:27–42.

Wooster, W.S. 1959. Oceanographic observations in the Panama Bight, "Askoy" Expedition, 1941. Bulletin of the American Museum of Natural History 118:113–152.

Wooster, W.S., and J.W. Hedgpeth. 1966. The oceanographic setting of the Galápagos. Pages 100–107 *in* Bowman, R.I., ed. The Galápagos: Proceedings of the Symposia of the Galápagos International Scientific Project. University of California Press, Berkeley.

Wyrtki, K. 1967. Circulation and water masses in the eastern equatorial Pacific Ocean. International Journal of Oceanology and Limnology 1(2):117–147.

Yu, X., and M.J. McPhaden. 1999. Seasonal variability in the equatorial Pacific. Journal of Physical Oceanography 29:925–947.

Zaneveld, J.R.V., H. Pak, and W.S. Plank. 1973. Optical and hydrographic observations of the Cromwell Current between 92°00'W and the Galápagos Islands. Journal of Geophysical Research 78(15):2708–2714.

FACTORS INFLUENCING THE ISLAND-MASS EFFECT OF THE GALÁPAGOS ARCHIPELAGO

Daniel M. Palacios

Geophysical Research Letters
2000 Florida Avenue N.W., Washington, DC
Volume 29, Number 23, 2134, doi:10.1029/2002GL016232, 2002

2 FACTORS INFLUENCING THE ISLAND-MASS EFFECT OF THE GALÁPAGOS ARCHIPELAGO

2.1 ABSTRACT

Enhanced phytoplankton biomass in the wake of the Galápagos Islands is thought to result from an island-mass effect (IME) fueled by upwelling of the Equatorial Undercurrent (EUC) and by natural iron enrichment from the island platform. Annual means of five variables describing the thermocline, the pycnocline, and the availability of nitrate at the surface were derived from the World Ocean Atlas 1998 (WOA98). The first principal component of these variables explained 55.8% of the variance, corroborating that the Galápagos IME is associated with features of the EUC, mainly a shallow thermocline/pycnocline and its vertical spreading in the vicinity of the Galápagos. Regression analysis of SeaWiFS-derived chlorophyll-*a* (chl) on the WOA98 variables indicated that the depth of the thermocline and nitrate availability explain 91.9% of the chl variance. A secondary IME of enhanced chl levels associated with the wind-sheltered area north of Isabela Island was evident in the residual variability.

2.2 INTRODUCTION

Biological enhancement in the vicinity of oceanic islands is a well-documented phenomenon. This "island-mass effect" (after Doty and Oguri, 1956) can contribute to the productivity and potential fisheries near islands (Heywood et al., 1990; Signorini et al., 1999), and may be significant to the global CO_2 budget (Heywood et al., 1996). Several non-exclusive, causal mechanisms have been described: lee eddies formed by flow disturbance or by Ekman pumping (e.g., Coutis and Middleton, 1999; Barton et al., 2000); nutrient input from island runoff (e.g., Bucciarelli et al., 2001; Perissinotto et al., 2000); drainage from an internal

lagoon (Sander, 1981); and contributions from benthic processes (Doty and Oguri, 1956; Dandonneau and Charpy, 1985).

The topographically forced upwelling of the eastward-flowing Equatorial Undercurrent (EUC) as it collides with the western side of the Galápagos Archipelago (0.5°S, 90.5°W) (Houvenaghel, 1978) has been linked to enhanced production of phytoplankton (Jimenez, 1981; Feldman, 1986; Chavez, 1989) and zooplankton (Arcos, 1981). Once at the surface, the upwelled waters are carried westward by the South Equatorial Current (SEC), the prevailing surface flow in the region, creating a productive habitat that sometimes extends offshore for several hundred kilometers (Feldman, 1986). Phytoplankton blooming in the wake of the Galápagos contrasts with the high-nutrient, low-chlorophyll (HNLC) conditions that persist throughout the rest of the eastern and central equatorial Pacific. It has been recently shown that while EUC upwelling is responsible for the high levels of macronutrients in the area of enhancement, input of high levels of iron derived from the island platform is necessary to support the observed bloom (Gordon et al., 1998; Lindley and Barber, 1998).

The Galápagos are located in a hydrographically complex region due to their proximity to the Equatorial Front (located between 1°N and 2°N at the Galápagos). South of the front, equatorial upwelling brings cool and salty water to the surface. North of the front warm, low-salinity, and stratified waters result from rainfall in the intertropical convergence zone, particularly in the Gulf of Panamá (Fiedler, 1992). The purpose of this paper is to identify the oceanographic conditions conducive to the island-mass effect of the Galápagos Archipelago. Climatological water-column data are used to explain phytoplankton distributions, as measured by long-term ocean color observations from NASA's Sea-viewing Wide Field-of-view Sensor (SeaWiFS).

2.3 METHODS

Annual climatologies of water-column properties describing the thermocline, the pycnocline, and the availability of nitrate for primary production were derived from the on-line version of the World Ocean Atlas 1998 (WOA98) at one-degree resolution (Conkright et al., 1998). At each grid cell, 1-m vertical resolution profiles of temperature, salinity, and nitrate were obtained from the standard depth levels by cubic spline interpolation. The variables derived were: depth of the thermocline (i.e., the depth of the 20°C isotherm, or Z20); thermocline strength (i.e., the vertical distance between the 20°C and 15°C isotherms, or ZTD); maximum Brunt-Väisälä frequency (i.e., the maximum resistance to turbulent mixing in the pycnocline, or MBVF), also known as maximum buoyancy frequency; depth of the MBVF (ZMBVF), also called the depth of the pycnocline; and nitrate concentration at the surface (NO_3). The four physical variables (Z20, ZTD, MBVF and ZMBVF) are necessary to describe the water column because of the effect of the very low-salinity surface layer originating in the Panamá Bight, which results in some uncoupling between thermocline and pycnocline strength (i.e., a weak thermocline is associated with high MBVF).

A cumulative average of satellite-derived chlorophyll-*a* (chl) for the 4.8-yr period 1 September 1997 – 30 June 2002 at 9-km resolution (Fig. 2.1) was obtained from the SeaWiFS Project (distributed as a Level-3 Standard Mapped Image product, reprocessing No. 4, July 2002). The resolution of this product was lowered by averaging pixels to obtain a data set at one-degree resolution, compatible with the WOA98 data.

A principal component analysis (PCA) was performed on the WOA98-derived water-column variables to rank their relative importance and to describe the dominant patterns of spatial variability in the study area. Multiple linear regression

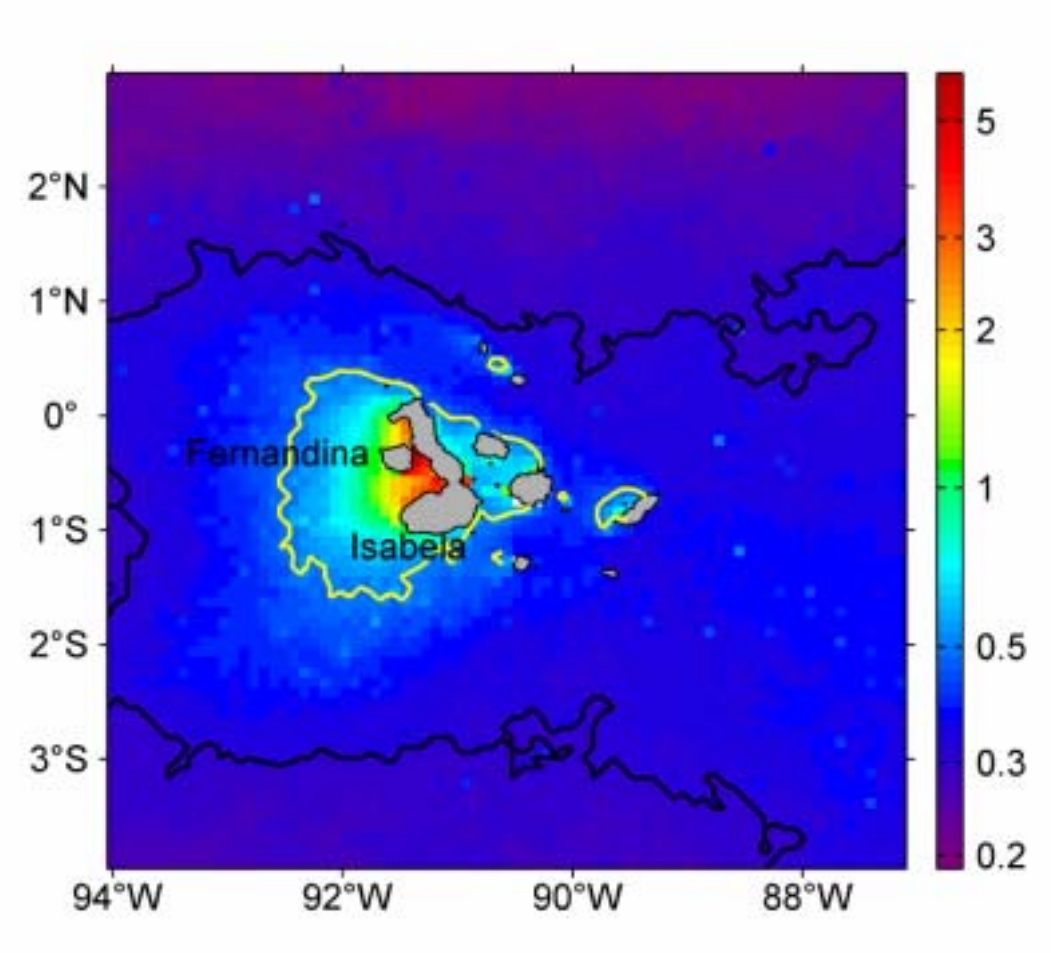

Figure 2.1: Cumulative average of SeaWiFS-derived chlorophyll-*a* (chl) for the 4.8-yr period 1 September 1997 – 30 June 2002. Thick black and yellow lines indicate the 0.3 and 0.5 mg m^{-3} contours, respectively. Thin black lines are island coastlines.

analysis of chl on the WOA98 variables was performed using sequential variable selection procedures to identify the best predictors of chlorophyll abundance. For further details on the implementation of the regression analysis see Appendix A (section 2.8.1).

2.4 RESULTS

The 4.8-yr chl average (Fig. 2.1) indicates that values are above 0.3 mg m^{-3} in an equatorial band between about 3°S and 1°N, while they are lowest north of 2°N, in the oligotrophic waters north of the Equatorial Front. There are areas of elevated chl (> 0.5 mg m^{-3}) associated with most of the major islands. This is most pronounced on the west side of Isabela and Fernandina islands, where the area of enhancement (as defined by the 0.5 mg m^{-3} contour) extends westward for about 120 km and covers about 25000 km^2. Chl reaches a maximum mean value of 6.2 mg m^{-3} at the southern mouth of Canal de Bolívar, the narrow channel separating Isabela and Fernandina.

Component loadings from the PCA are presented in Table 2.1 for the first two principal components (PC), which explain 95.5% of the variability in the data sets. The first PC (55.8%) is characterized by a shallow (deep) thermocline (Z20) and pycnocline (ZMBVF), a weak (strong) thermocline (ZTD), and low (high) pycnocline stability (MBVF), leading to high (low) surface nitrate concentrations (NO_3). The second PC (39.7%) contrasts high (low) pycnocline stability and a weak (strong) thermocline with a shallow (deep) pycnocline and low (high) nitrate concentrations. Depth of the thermocline does not contribute to this component (loading = -0.03). Spatially, the site scores depict an equatorial pattern for the first PC (Fig. 2.2a) and a NE-SW pattern for the second PC (Fig. 2.2b).

Table 2.1: Loadings (eigenvectors) for the first two principal components (PC) of the WOA98 variables.

	PC 1	PC 2
Z20	-0.59	-0.03
ZTD	0.41	0.49
MBVF	-0.34	0.57
ZMBVF	-0.50	-0.34
NO_3	0.34	-0.57

Correlations between chl and the site scores from the PCA are $r = 0.93$ and $r = 0.035$ for the first and second PCs, respectively. Sequential variable selection in the regression analysis of chl on the original WOA98 variables consistently yielded the following model ($R^2 = 0.919$):

$$\log(\text{chl}) = -0.309 - 0.009\,Z20 + 0.115\,NO_3 - 0.019\,(NO_3)^2 + 0.001\,(NO_3)^3$$

2.5 DISCUSSION

From the perspective of long-term ocean color observations from SeaWiFS, the Galápagos IME can be described as a "plume" of elevated chl levels on the west side of Isabela and Fernandina islands that covers an area of about 25000 km^2. While this area has long been identified as the primary upwelling site of the EUC

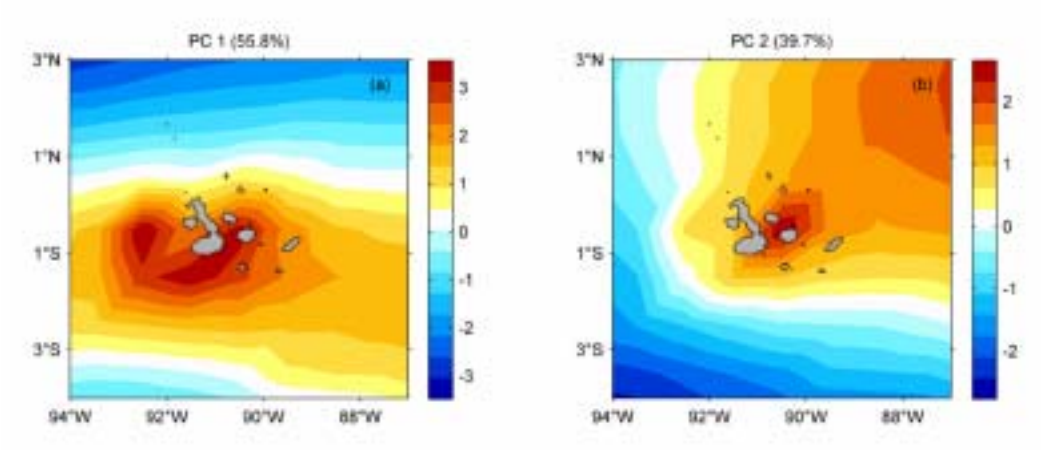

Figure 2.2: Site scores and explained variance for the first (a) and second (b) principal components of the WOA98 variables.

(Houvenaghel, 1978), upwelling alone cannot explain the plume, since nitrate levels in surface waters are already adequate to support phytoplankton production in this HNLC region. Gordon et al. (1998) showed that upwelled waters become significantly enriched with iron by contact with the island platform, particularly at the Canal de Bolívar, where dissolved iron concentrations of up to 3 nM were measured (Martin et al., 1994). Lindley and Barber (1998) provided evidence that this iron input supports nitrate uptake and elevated primary production in the plume. Although the specific source of island-derived iron has not been identified, resuspension of iron-rich sediment caused by interaction of flow with topography and tidal mixing, particularly in the Canal de Bolívar and in the adjacent bays to the north and south, has been suggested (Steger et al., 1998). Hydrothermal fluxes from the interior of western Galápagos volcanoes could also be an important source (cf. Signorini et al., 1999).

The westward extent of the plume of about 120 km in the SeaWiFS average compares favorably with the scale length for dissolved iron transport of 103 km estimated by Bucciarelli et al. (2001) based on the iron measurements of Gordon et al. (1998). Outside the plume, chl values ≥ 0.3 mg m^{-3} in an equatorial band between 3°S and 1°N (Fig. 2.1) are explained in terms of wind-driven equatorial upwelling. The EUC has a relatively iron-rich core (0.35 nM at 200 m, 140°W), and the vertical advection of these waters supports phytoplankton growth throughout the equatorial Pacific (Gordon et al., 1997).

The site scores from the PCA (Fig. 2.2) can be interpreted based on the loadings of the first two principal components (Table 2.1). The equatorial pattern of the first PC represents a shallow, weak thermocline and pycnocline associated with the EUC (Fig. 2.2a). The highest site scores are associated with the islands and represent the vertical spreading of the thermocline and the weakening of stratification as the EUC encounters the Galápagos. The second PC illustrates a regional NE-SW gradient in pycnocline stratification and shoaling independent of

temperature, due to rainfall in the Panamá Bight (Fig. 2.2b). As a result, the distribution of nitrate in surface waters of the study area is closely associated with this stratification regime, as evidenced by the strong inverse relationship with maximum buoyancy frequency (r = -0.94, Fig. 2.3a). However, nitrate concentrations also have a somewhat weaker inverse relationship with the depth of the thermocline (r = -0.52, not shown). These correlations are consistent with the nitrate loadings onto the second and first PCs, respectively (Table 2.1).

Correlations between chl and the site scores only support the existence of a relationship for the first PC, which depicts features of the EUC. This suggests that the contributions of the variables to this PC (Table 2.1) are important for the Galápagos IME. However, while the contribution of nitrate to the first PC is relatively small (loading = 0.34), there is a clear non-linear relationship between chl and nitrate (Fig. 2.3b). This is because the chl-NO_3 relationship adeptly describes the complex response of phytoplankton populations to nitrate and iron availability throughout surface waters of the study area, not only in the plume region (an alternative explanation to this relationship is considered in Appendix B). Chlorophyll concentrations are lowest at nitrate concentrations below about 2 μM, representing the oligotrophic conditions north of the Equatorial Front (nitrate is limiting). The high chl values found at intermediate nitrate concentrations (2–6 μM) represent two processes. The first is equatorial upwelling, which brings both nitrate and EUC iron to the surface and results in enhanced phytoplankton populations and some nitrate removal along the equator (Gordon et al., 1997). The second is the phytoplankton bloom in the plume associated with the topographic upwelling of the EUC and the island-derived iron enrichment (i.e., the Galápagos IME), also resulting in nitrate uptake. Finally, the decrease in chl levels at high nitrate concentrations (NO_3 > 6 μM) corresponds to the transition to HNLC

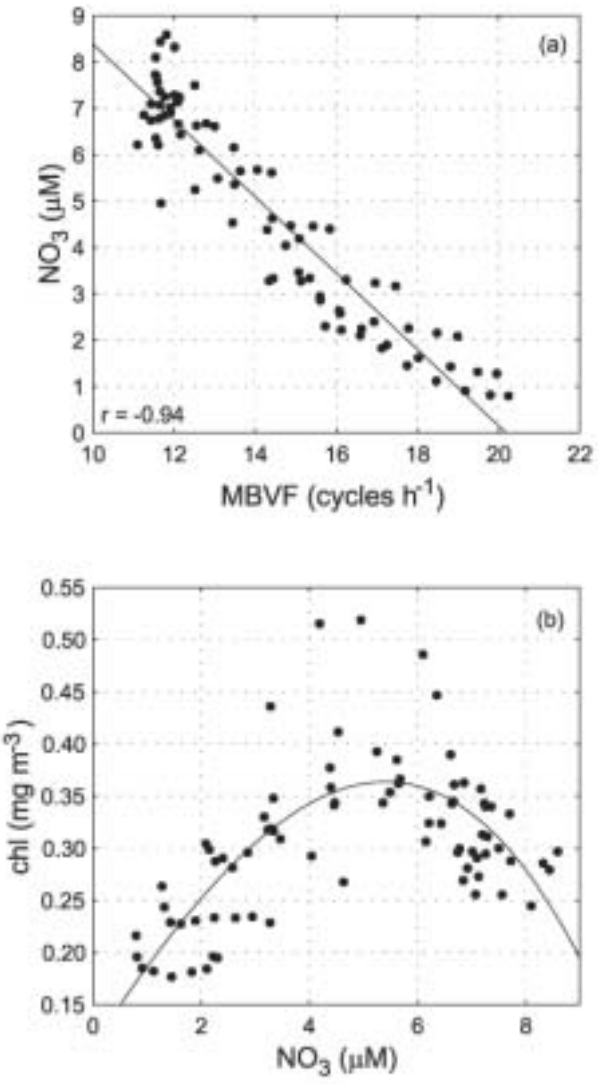

Figure 2.3: Scatterplots of MBVF *vs*. NO_3 (a) and NO_3 *vs*. chl (b). Least-squares fits are shown.

conditions, mainly south of the equator, where excess nitrate is not removed due to iron limitation.

Once the curvature in the chl-NO_3 relationship is accounted for by including a third-order polynomial for nitrate, a multiple linear regression model that includes depth of the thermocline and surface nitrate (the two variables with highest loadings in the first two PCs) appears to most adequately explain chl distributions throughout the study area. It should be noted, however, that if a climatological iron data set were available, its inclusion in the regression along with an interaction term with nitrate (NO_3:Fe) would probably account for the observed curvature without a need for the polynomial terms.

While the regression model explained a large fraction (91.9%) of the chl variance, the residual variability contained coherent spatial structures, including an area centered on the north side of Isabela Island with chl levels up to 0.11 mg m^{-3} above the fitted values (Fig. 2.4). This area lies in the lee of Volcano Wolf, the highest elevation in the Galápagos at 1710 m (Mouginis-Mark et al., 1996). Given that southeast trade winds prevail in the region for most of the year, I suggest that the observed pattern is created by local Ekman pumping (and iron upwelling from beneath the pycnocline) driven by orographically modified wind stress, as has been observed for other mountainous islands in strong wind regimes (e.g., Barton et al., 2000). This pattern represents a secondary wind-induced IME. Although the enhancement appears to be comparatively small, this lee region could be an important area of retention and recruitment for zooplankton and larval fish in Galápagos waters.

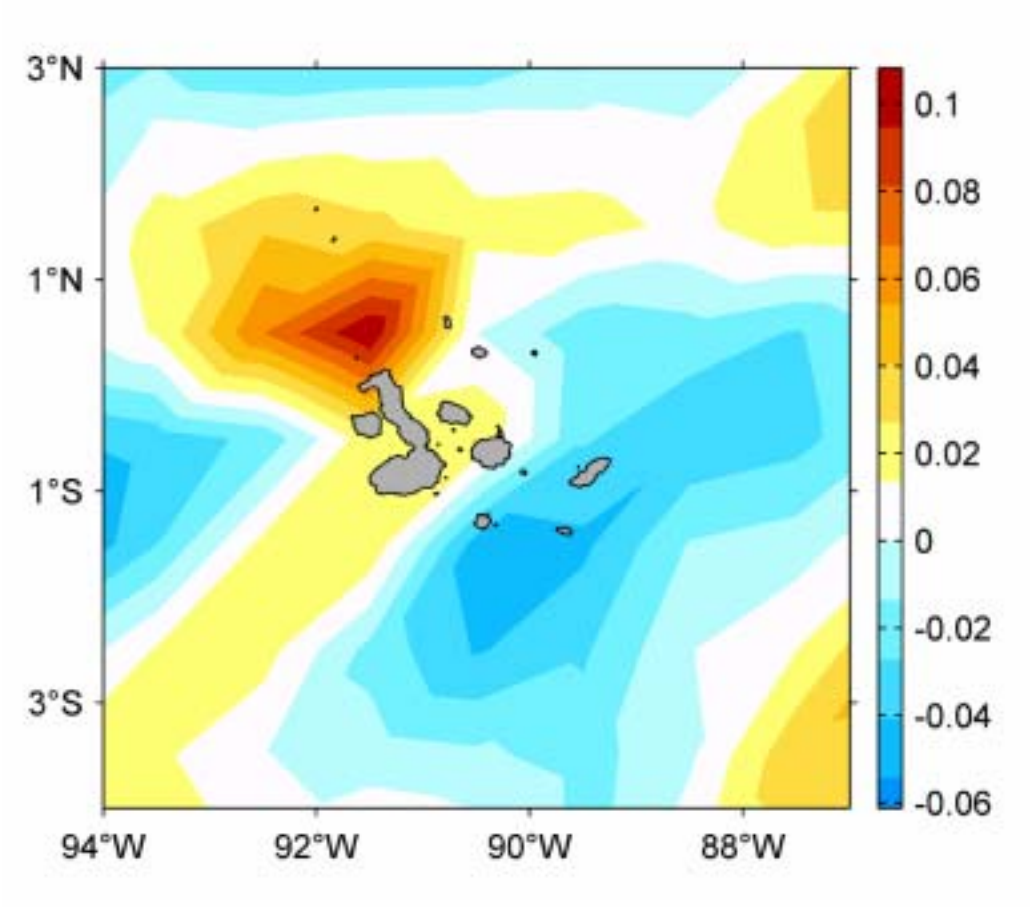

Figure 2.4: Residual or unexplained chl (in mg m^{-3}) from the multiple linear regression of log(chl) on Z20 and NO_3 (with a third-order polynomial).

2.6 ACKNOWLEDGEMENTS

The author would like to thank the SeaWiFS Project (Code 970.2) and the Distributed Active Archive Center (Code 902) at the Goddard Space Flight Center, Greenbelt, MD 20771, for the production and distribution of the ocean color data, respectively. The WOA98 data sets were obtained on line from NOAA's National Oceanographic Data Center at ftp://ftp.nodc.noaa.gov/pub/WOA98/. Funding for this study was provided by the Endowed Marine Mammal Program at Oregon State University. Comments from P. T. Strub, C. B Miller, and two anonymous reviewers greatly improved the clarity of the manuscript.

2.7 REFERENCES

Arcos, F. 1981. A dense patch of *Acartia levequei* (Copepoda, Calanoida) in upwelled Equatorial Undercurrent water around the Galapagos Islands. Pages 427–432 *in* Richards, F.A., ed. Coastal Upwelling. Estuarine Sciences 1, American Geophysical Union, Washington, D.C.

Barton, E.D., G. Basterretxea, P. Flament, E.G. Mitchelson-Jacob, B. Jones, J. Arístegui, and F. Herrera. 2000. Lee region of Gran Canaria. Journal of Geophysical Research 105:17173–17193.

Bucciarelli, E., S. Blain, and P. Tréguer. 2001. Iron and manganese in the wake of the Kerguelen Islands (Southern Ocean). Marine Chemistry 73:21–36.

Chavez, F.P. 1989. Size distribution of phytoplankton in the central and eastern tropical Pacific. Global Biogeochemical Cycles 3:27–35.

Conkright, M., S. Levitus, T. O'Brien, T. Boyer, J. Antonov, and C. Stephens. 1998. World Ocean Atlas 1998 CD-ROM Data Set Documentation. Technical Report 15. NODC Internal Report, Silver Spring, MD, 16 pp.

Coutis, P.F., and J.H. Middleton. 1999. Flow-topography interaction in the vicinity of an isolated, deep ocean island. Deep-Sea Research I 46:1633–1652.

Dandonneau, Y., and L. Charpy. 1985. An empirical approach to the island mass effect in the south tropical Pacific based on sea surface chlorophyll concentrations. Deep-Sea Research 32:707–721.

Doty, M.S., and M. Oguri. 1956. The island mass effect. Journal du Conseil International pour l'Exploration de la Mer 22:33–37.

Feldman, G.C. 1986. Patterns of phytoplankton production around the Galápagos Islands. Pages 77–106 *in* Bowman, M.J., C.M. Yentsch, and W.T. Peterson, eds. Tidal Mixing and Plankton Dynamics. Lecture Notes on Coastal and Estuarine Studies 17, Springer-Verlag, Berlin.

Fiedler, P.C. 1992. Seasonal climatologies and variability of eastern tropical Pacific surface waters. NOAA Technical Report NMFS 109:1–65.

Gargett, A.E. 1997. The optimal stability "window": a mechanism underlying decadal fluctuations in North Pacific salmon stocks? Fisheries Oceanography 6(2):109–117.

Gordon, R.M., K.H. Coale, and K.S. Johnson. 1997. Iron distributions in the equatorial Pacific: implications for new production. Limnology and Oceanography 42:419–431.

Gordon, R.M., K.S. Johnson, and K.H. Coale. 1998. The behaviour of iron and other trace elements during the IronEx-I and PlumEx experiments in the equatorial Pacific. Deep-Sea Research II 45:995–1041.

Heywood, K.J., E.D. Barton, and J.H. Simpson. 1990. The effects of flow disturbance by an oceanic island. Journal of Marine Research 48:55–73.

Heywood, K.J., D.P. Stevens, and G.R. Bigg. 1996. Eddy formation behind the tropical island of Aldabra. Deep-Sea Research I 43:555–578.

Houvenaghel, G.T. 1978. Oceanographic conditions in the Galápagos Archipelago and their relationships with life on the islands. Pages 181–200 *in* Boje, R., and M. Tomczak, eds. Upwelling Ecosystems. Springer-Verlag, Berlin.

Jimenez, R. 1981. Composition and distribution of phytoplankton in the upwelling system of the Galapagos Islands. Pages 327–338 *in* Richards, F.A., ed. Coastal Upwelling. Estuarine Sciences 1, American Geophysical Union, Washington, D. C.

Lindley, S.T., and R.T. Barber. 1998. Phytoplankton response to natural and experimental iron addition. Deep-Sea Research II 45:1135–1150.

Martin, J.H., K.H. Coale, K.S. Johnson, S.E. Fitzwater, R.M. Gordon, S.J. Tanner, C.N. Hunter, V.A. Elrod, J.L. Nowicki, T.L. Coley, R.T. Barber, S. Lindley, A.J. Watson, K. Van Scoy, C.S. Law, M.I. Liddicoat, R. Ling, T. Stanton, J. Stockel, C. Collins, A. Anderson, R. Bidigare, M. Ondrusek, M. Latasa, F.J. Millero, K. Lee, W. Yao, J.Z. Zhang, G. Friederich, C. Sakamoto, F. Chavez, K. Buck, Z. Kolber, R. Greene, P. Falkowski, S.W. Chisholm, F. Hoge, R. Swift, J. Yungel, S. Turner, P. Nightingale, A. Hatton, P. Liss, and N.W. Tindale. 1994. Testing the iron hypothesis in ecosystems of the equatorial Pacific Ocean. Nature 371:123–129.

MathSoft, Inc. 1999. S-PLUS 2000 Guide to Statistics, Volume 1. Data Analysis Products Division, MathSoft, Seattle, WA. 638 pp.

Mouginis-Mark, P.J., S.K. Rowland, and H. Garbeil. 1996. Slopes of western Galapagos volcanoes from airborne interferometric radar. Geophysical Research Letters 23:3767–3770.

Perissinotto, R., J.R.E. Lutjeharms, and R.C. van Ballegooyen. 2000. Biological-physical interactions and pelagic productivity at the Prince Edward Islands, Southern Ocean. Journal of Marine Systems 24:327–341.

Ramsey, F.L., and D.W. Schafer. 1997. The statistical sleuth, a course in methods of data analysis. Duxbury Press, Belmont, CA. 742 pp.

Sakamoto, C.M., F.J. Millero, W. Yao, G.E. Friederich, and F.P. Chavez. 1998. Surface seawater distributions of inorganic carbon and nutrients around the Galápagos Islands: results from the PlumEx experiment using automated chemical mapping. Deep-Sea Research II 45:1055–1071.

Sander, F. 1981. A preliminary assessment of the main causative mechanisms of the “Island Mass Effect” of Barbados. Marine Biology 64:199–205.

Signorini, S.R., C.R. McClain, and Y. Dandonneau. 1999. Mixing and phytoplankton bloom in the wake of the Marquesas Islands. Geophysical Research Letters 26:3121–3124.

Steger, J.M., C.A. Collins, and P.C. Chu. 1998. Circulation in the Archipiélago de Colón (Galapagos Islands), November, 1993. Deep-Sea Research II 45:1093–1114.

2.8 APPENDICES

Due to the length restriction placed by Geophysical Research Letters, details of the regression analysis and a longer discussion on the topic of water-column stability and nutrient limitation were omitted in the published article. They are inlcuded here as appendices A and B.

2.8.1 Appendix A: Searching for associations between the chlorophyll field and water-column variables through multiple linear regression analysis

Although the five WOA98 variables were necessary to describe the water column in the study area, there was also some degree of collinearity among them. Multiple linear regression was applied with the objective of identifying a subset of these variables that adequately explained chlorophyll abundance without redundancies. Two computer-assisted tools in the S-Plus software (MathSoft, 1999) were used for this purpose. First, all possible subsets of models were compared using Mallow's C_p statistic. The C_p criterion focuses on the trade-off between bias due to excluding important explanatory variables and the extra variance due to including too many (Ramsey and Schafer, 1997). Second, regression models were explored using several sequential variable selection procedures: forward selection, backward elimination, and stepwise regression (Ramsey and Schafer, 1997). The model reported in section 2.4 was the one that minimized the C_p criterion, and this

was also the model that consistently emerged from most of the sequential variable selection procedures.

Finding "the important set" of explanatory variables is known as "fishing for explanation" in the regression terminology of Ramsey and Schafer (1997). It should be noted that the chosen model does not necessarily represent a true model or a law of nature, because there could be several equally good models. Further, because of the data snooping involved in the process, it is not possible to interpret the regression coefficients, or to use the *p*-values and confidence intervals for statistical inference (hence, the latter two were not reported).

It should also be emphasized that the use of polynomial terms for nitrate was not for the purpose of curve fitting. There was good reason to suspect that the non-linear response of chl to nitrate was a result of the presence of iron in areas of equatorial and EUC upwelling. Therefore, it was an attempt to account for the presumed effects of a variable that was not available (i.e., iron). The large amount of variance explained by the regression (91.9%) is probably inflated due to the use of climatological data sets (see Chapter 1), and it should not be taken to represent the actual strength of the relationship. Finally, because of the observational nature of this study, it is not possible to arrive at cause-and-effect conclusions. Nevertheless, the regression models extracted in this type of application can be useful for generating hypotheses. The obvious hypothesis that the input of iron fuels elevated phytoplankton production and nitrate removal in the plume region has been widely tested (e.g., Martin et al., 1994; Sakamoto et al., 1998). However, another hypothesis suggested by the residuals of the regression model (Fig. 2.4) is that phytoplankton populations are enhanced in the lee of the tallest volcanoes, an enhancement driven by local wind divergence.

2.8.2 Appendix B: The chl *vs*. NO_3 relationship: Stability- or iron-driven?

The curvature in the chl-NO_3 relationship (Fig. 2.3b) was explained in terms of the complex response of phytoplankton populations to different levels of nitrate and iron. However, considering that nitrate showed a strong inverse relationship with maximum buoyancy frequency (Fig. 2.3a), another possibility is that chl may be in fact responding to the stratification conditions in the region. Gargett (1997) proposed the "optimal stability window" as a mechanistic explanation for the observed correlation between fluctuations in salmon stocks and the strength of atmospheric forcing in the North Pacific. The mechanism is based on the small-scale processes that shape the nutrient and light environment for phytoplankton. Under this concept, the relationship between primary production and water-column stability is depicted by a curve similar to that in Figure 2.3b. Primary production peaks at some intermediate stability range (the optimal stability window) where both light and nutrients are adequate. Production decreases rapidly outside of this window, at one end because stability is extremely weak, resulting in large vertical excursions and low average light for phytoplankton in spite of an adequate nutrient supply, and at the other end because in conditions of very high stability the nutrient supply is scarce in spite of an adequate light field (see Fig. 1 in Gargett, 1997).

To explore this possibility, chl was plotted against MBVF in Figure B2.1. While chl does appear to reach a peak and then decrease with increasing water-column stability, the relationship is much less clear than the chl-NO_3 relationship. Chl increases rapidly between 11 and 13 cycles h^{-1}, peaks at about 14 cycles h^{-1}, and then decreases slowly over the 15–20 cycles h^{-1} range, with a wide scatter (Fig. B2.1). It is concluded that while the stratification regime plays a role in the availability of nitrate in the study area, iron-driven physiological limitation is probably a more important factor in determining phytoplankton stock in the areas where nitrate is otherwise plentiful to support growth. For reference, a map showing the distribution of nitrate in the study area is presented in Figure B2.2.

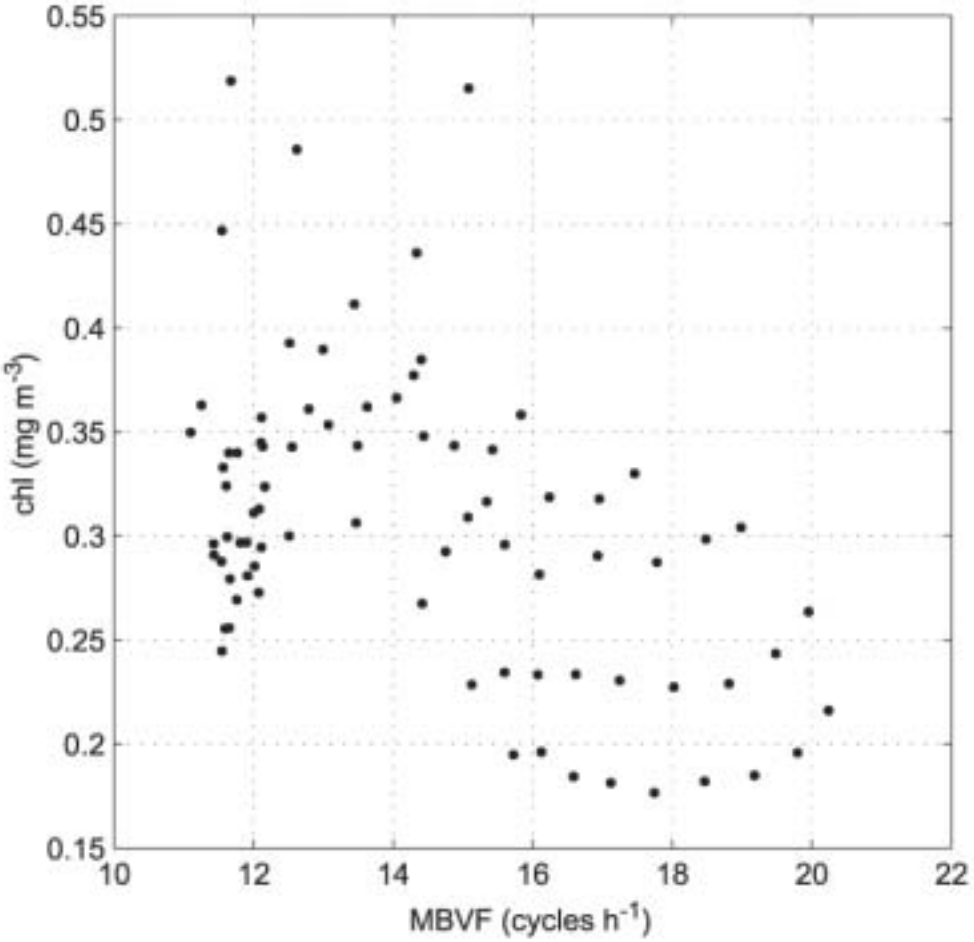

Figure B2.1: Scatterplot illustrating the relationship between water-column stability and chlorophyll concentration.

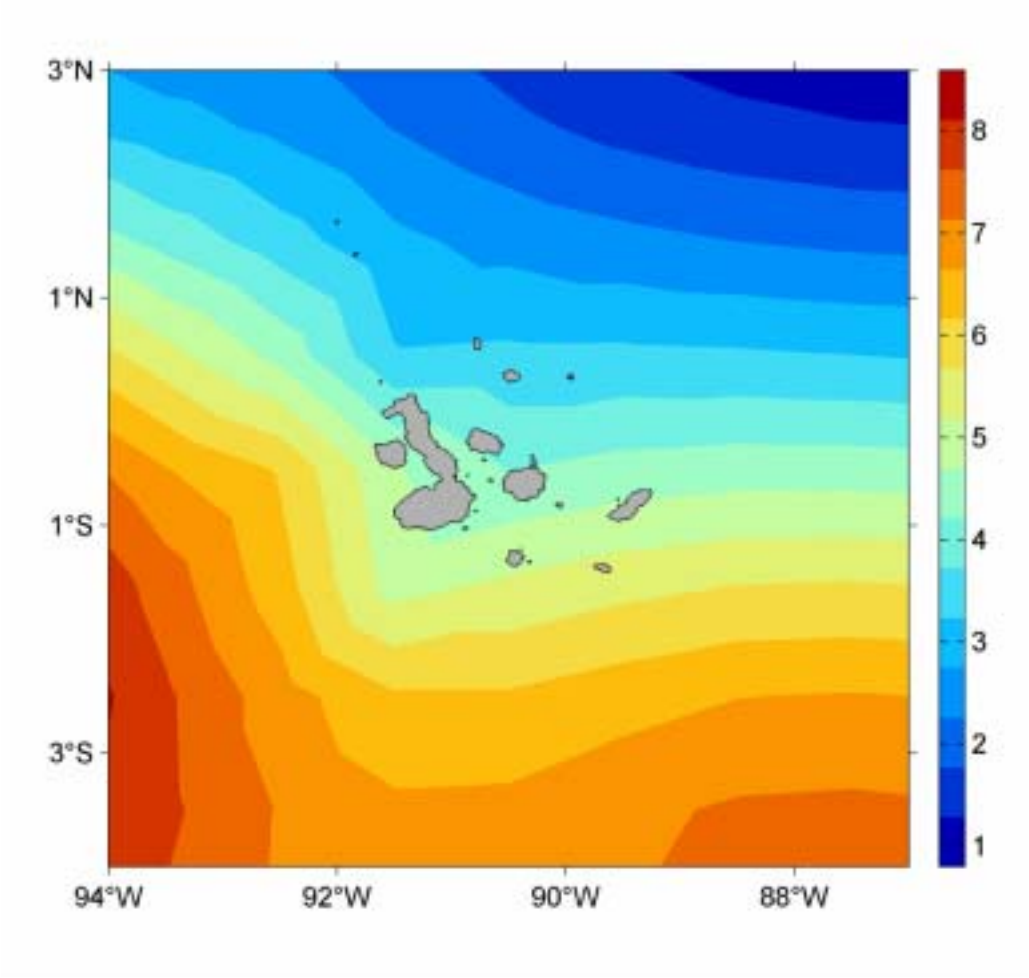

Figure B2.2: The distribution of surface nitrate in the study area from WOA98 data.

3 SEASONAL PATTERNS OF SEA-SURFACE TEMPERATURE AND OCEAN COLOR AROUND THE GALÁPAGOS: REGIONAL AND LOCAL INFLUENCES

3.1 ABSTRACT

Effects of the equatorial circulation around the Galápagos Archipelago are investigated through analyses of the temporal and spatial variability of satellite-derived sea-surface temperature (SST, from AVHRR Pathfinder) and ocean color (from OCTS and SeaWiFS) monthly climatologies. Harmonic analysis of the climatological time series indicates a best fit with annual and semi-annual constituents. The annual amplitude is the dominant signal in SST, corresponding to the basin-wide seasonal cycle of warming and cooling associated with the north-south migration of the intertropical convergence zone. Advection of upwelled water from the Panamá Bight into the northeastern part of the study area is also present in the annual signal. The semi-annual amplitude, most evident in the ocean color signal, is associated with chlorophyll-*a* enhancements at localities where the Equatorial Undercurrent (EUC) upwells. An empirical orthogonal function (EOF) decomposition identifies two main spatial patterns with amplitude time series representing out-of-phase annual cycles. The dominant mode corresponds to the strengthening of the Equatorial Front and the South Equatorial Current during the second part of the year. This mode explains 92.2% of the SST variance and 82.4% of the ocean color variance. The second mode is associated with the topographically induced upwelling of the EUC on the western side of the archipelago, and with advection of upwelled Panamá Bight water on the eastern side, both reaching their peak during the first part of the year. This mode accounts for 6% of the SST variance and 8.4% of the ocean color variance. The seasonal evolution of water-column temperature and nitrate (from World Ocean Atlas 1998 climatologies) is consistent with the satellite-derived patterns. A slight tilt aligned with the east-west axis of the Galápagos Platform (outlined by the 2000-m isobath)

is evident in all property fields, suggesting that the presence of the archipelago introduces a small but noticeable perturbation to the large-scale currents and property gradients of the eastern equatorial Pacific.

3.2 INTRODUCTION

The Galápagos Islands are an oceanic archipelago located on the equator in the eastern tropical Pacific. The islands are renowned for the unique fauna that inhabits their shores, including endemic marine iguanas, seabirds and seals, as well as many other intertidal and subtidal organisms found nowhere else in the world. Indeed, the distinctiveness of the littoral marine biota has led biogeographers to recognize the region as the "Galápagos Province" (Glynn et al., 1983). This biological diversity is supported by the richness of the surrounding marine environments. The islands lie at the confluence of several current systems, and the degree of exposure of the different sectors of the archipelago to the currents, as well as the interaction of these flows with the underwater topography, undoubtedly have important effects. But the question arises as to how do these processes interact to shape the local marine environments? Also, how does the island platform affect the large-scale equatorial circulation?

Multiyear time series of satellite-derived environmental data, with their characteristically refined spatial and temporal sampling resolutions, are particularly attractive for the investigation of recurrent patterns in oceanic environments. Analysis of monthly climatologies of remotely sensed sea-surface temperature (SST) and ocean color (i.e., the concentration of near-surface phytoplankton chlorophyll *a*) are used in this paper to infer the main effects of the equatorial currents around the Galápagos Archipelago. The paper is organized as follows. The satellite data sets used for the study are described in section 3.3. Section 3.4 describes the mean and standard deviation fields. The main analyses are conducted in sections 3.5 and 3.6. The ecological significance of the results is discussed in

section 3.7 from the perspective of water-column thermal structure and nutrient availability, using *in-situ* climatological data. Finally, the conclusions of the study are presented in section 3.8.

3.3 SATELLITE CLIMATOLOGIES

Climatological monthly fields of satellite-derived SST and ocean color (chlorophyll-*a* concentration, or chl) with a spatial resolution of 9.28 km are used here to investigate patterns of spatial and temporal variability around the Galápagos Islands. The SST climatologies are a standard product known as the "Pathfinder + Erosion" monthly climatologies, distributed by the Physical Oceanography Distributed Active Archive Center (PO.DAAC) at the Jet Propulsion Laboratory (JPL) of the California Institute of Technology and the National Aeronautics and Space Administration (NASA). This product was computed from a 13-year period (1985–1997) of Advanced Very High Radiometer (AVHRR) measurements processed with version 4.0 of the Pathfinder Oceans algorithm. Casey and Cornillon (1999) describe the production of these climatologies through 1995. Briefly, daily fields (daytime and nighttime passes) were averaged into monthly time series after applying an erosion filter near cloud-flagged pixels that further reduced the possibility of cloud contamination. For each month of the year, all files corresponding to that month in the 1985–1997 series were averaged, resulting in an initial climatology consisting of 12 monthly means. Subsequently, data gaps were interpolated with two passes of a median filter (Casey and Cornillon, 1999).

Ocean color climatologies were formed for the 5-year period November 1996 – November 2001 by combining chl concentrations derived from two sensors: the Ocean Color and Temperature Scanner (OCTS), which operated between November 1996 and June 1997, and the Sea-viewing Wide-Field-of-view Sensor (SeaWiFS), which has been in operation since September 1997. These data are produced by the SIMBIOS-NASDA-OCTS and the SeaWiFS projects at the NASA

Goddard Space Flight Center (GSFC) and distributed by the GSFC Earth Sciences Data and Information Services Center Distributed Active Archive Center (GES DISC DAAC). The monthly ocean color products at 9.28-km resolution for the OCTS and SeaWiFS sensors were initially combined in an ocean color time series that contained 59 months of data spanning the period November 1996 – November 2001. There was a two-month gap between the two missions in July and August 1997 for which there was no data. A similar procedure to that used by Casey and Cornillon (1999) to compute the monthly SST climatologies was applied to the ocean color time series (except that the fields were not eroded). An average was obtained for each climatological month from all of the available corresponding months in the OCTS/SeaWiFS time series, resulting in an initial climatology consisting of 12 monthly means. Although the global mean fields were essentially complete, small gaps with no data remained in regions with persistent cloud clover. These gaps were filled with the median value of the surrounding chl values from the 7 × 7 pixel box (~ 65 × 65 km) centered on the missing pixel. Only few pixels were missing after the first median filter, and these were interpolated with a second 11 × 11 (~ 102 × 102 km) median filter, effectively removing all remaining gaps, but leaving the non-missing pixels unchanged. Finally, small-scale noise was removed with a 7 × 7 median smoother applied to each entire field.

At the 9.28-km resolution, the gridded monthly fields extracted from the global climatologies for the study area (see section 1.1) contained 80 × 80 pixels. For analysis, the twelve climatological fields were re-arranged into a data matrix $\mathbf{T}_{\mathbf{mn}}$, with M rows representing the spatial points and N columns representing the time points. The SST data matrix contained $M = 6232$ rows by $N = 12$ columns, while the ocean color data matrix contained 6333 rows (out of the 6400 points in each field) owing to differences in the land masks applied in the production of the

data sets. Since chl values spanned three orders of magnitude, the ocean color data were log-transformed prior to analysis in order to homogenize the variance.

3.4 THE MEAN AND STANDARD DEVIATION FIELDS

Figure 3.1 shows the mean and the standard deviation fields for the SST and ocean color monthly climatologies for the study area. It is apparent that the archipelago lies within a region with a strong north-south thermal gradient. The Equatorial Front (EF), a band where the most rapid changes take place (i.e., the 24–26°C interval) is located between 1°–2°N on the western side of the study area and between 0°–1°N on the eastern side (Fig. 3.1a). The island platform stands in the path of the Equatorial Undercurrent (EUC) (see section 1.2.2.1), effectively blocking its eastward flow and forcing some of its waters to upwell and form the pool of cold water on the western side of the archipelago, as seen in Figure 3.1a. Phytoplankton populations in this pool are enhanced, according to the very high chl concentrations observed in Figure 3.1b. A zonal band of cool water (and somewhat elevated chl levels) extends eastward from this pool, mainly along the southern margin of the archipelago, possibly marking the path of the shallow southern branch of the EUC as it continues its journey toward the South American continent (see section 1.2.2.1). The standard deviation fields indicate that waters south of the equator vary the most over the climatological year, while waters to the north vary little (Figs. 3.1c and 3.1d). Areas with the strongest variability are somewhat more localized in the ocean color field (Fig. 3.1d).

Inter-island differences in the mean SST field (Fig. 3.1a) indicate that the waters off western Isabela and around Fernandina are ≤ 23°C, the coldest in the archipelago. Southeastern Isabela, Floreana, Española, San Cristóbal, and Santa Cruz are contained within the 23.5°C isotherm. Santiago, and eastern and northern

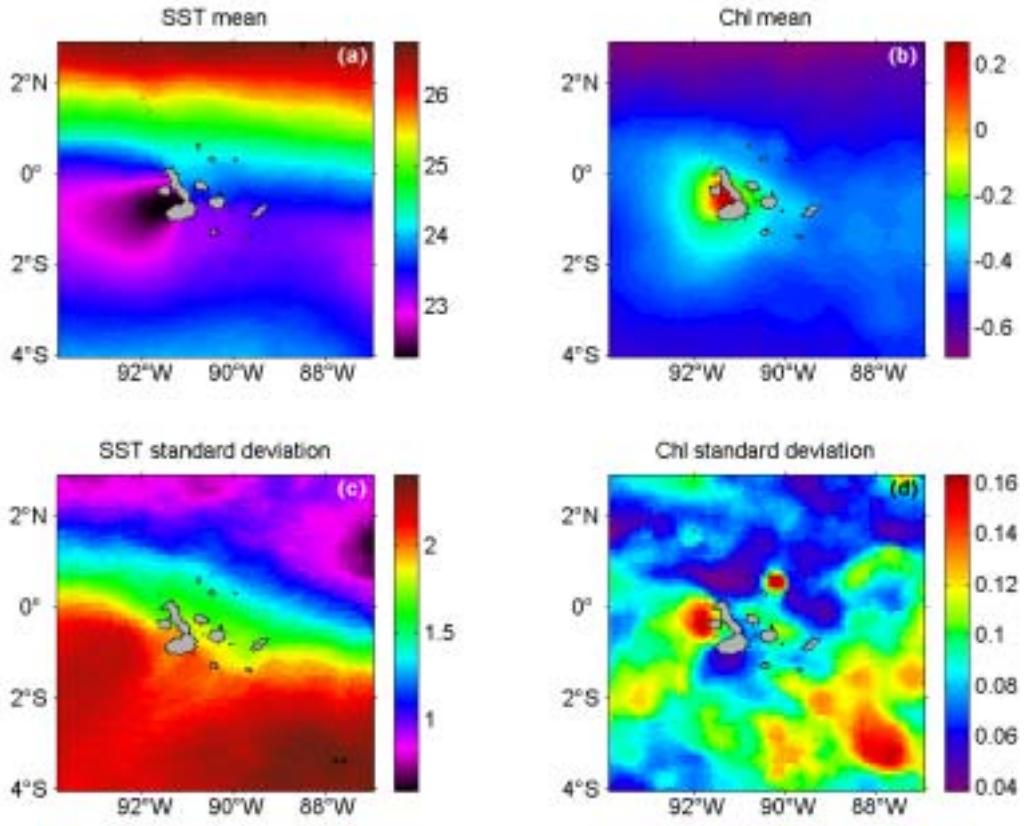

Figure 3.1: Satellite fields. (a) and (b): Temporal mean of "Pathfinder + Erosion" SST (°C) and log-transformed OCTS/SeaWiFS chl (mg m^{-3}) monthly climatologies, respectively. (c) and (d): Standard deviation for the same variables.

Isabela are bounded by the 23.5 and 24°C isotherms. And, finally, the islands of Genovesa, Marchena, Pinta, Wolf and Darwin are surrounded by water ≥ 24°C. A comparison of these differences with the five SST zones defined by Harris (1969) for the archipelago (Fig. 1.6) reveals that areas with mean temperatures ≤ 23°C and ≥ 24°C correspond reasonably well with Harris's zones 5 and 3, respectively. On the other hand, Harris's zones 1 and 2 do not appear to be under different temperature regimes, and the distinctiveness of zone 4 is rather tenuous, at least in a climatological sense. However, considering the spatial heterogeneity of temporal variability in the study area (Fig. 3.1c), it is expected that the different zones will be more or less defined at different times of the year.

3.5 HARMONIC ANALYSIS

Several studies have demonstrated that the seasonal cycle is a major signal in eastern equatorial Pacific data (e.g., Hayes, 1985; Delcroix, 1993; Yu and McPhaden, 1999). Harmonic analysis (Emery and Thomson, 1997) was applied to the SST and ocean color monthly climatologies to investigate their fit to a seasonal cycle composed of an annual and a semi-annual period. The method uses a least-squares approach to solve for the specified annual and semi-annual constituents, yielding the required amplitudes and phase lags (in radians). Phase lags were converted to months relative to 15 January, the first month in the time series.

Figure 3.2 shows the annual and semi-annual amplitudes, together with the percent of the variance explained by the fit. The harmonic fit explains a large percentage of monthly variability for both SST and chl throughout much of the study area (R^2 range: 85.3–99.9% for SST; 12.2–98.5% for chl) (Figs. 3.2e and 3.2f). The SST annual amplitude (Fig. 3.2a) represents a large-scale pattern of warming and cooling that is most evident in the southern half of the study area.

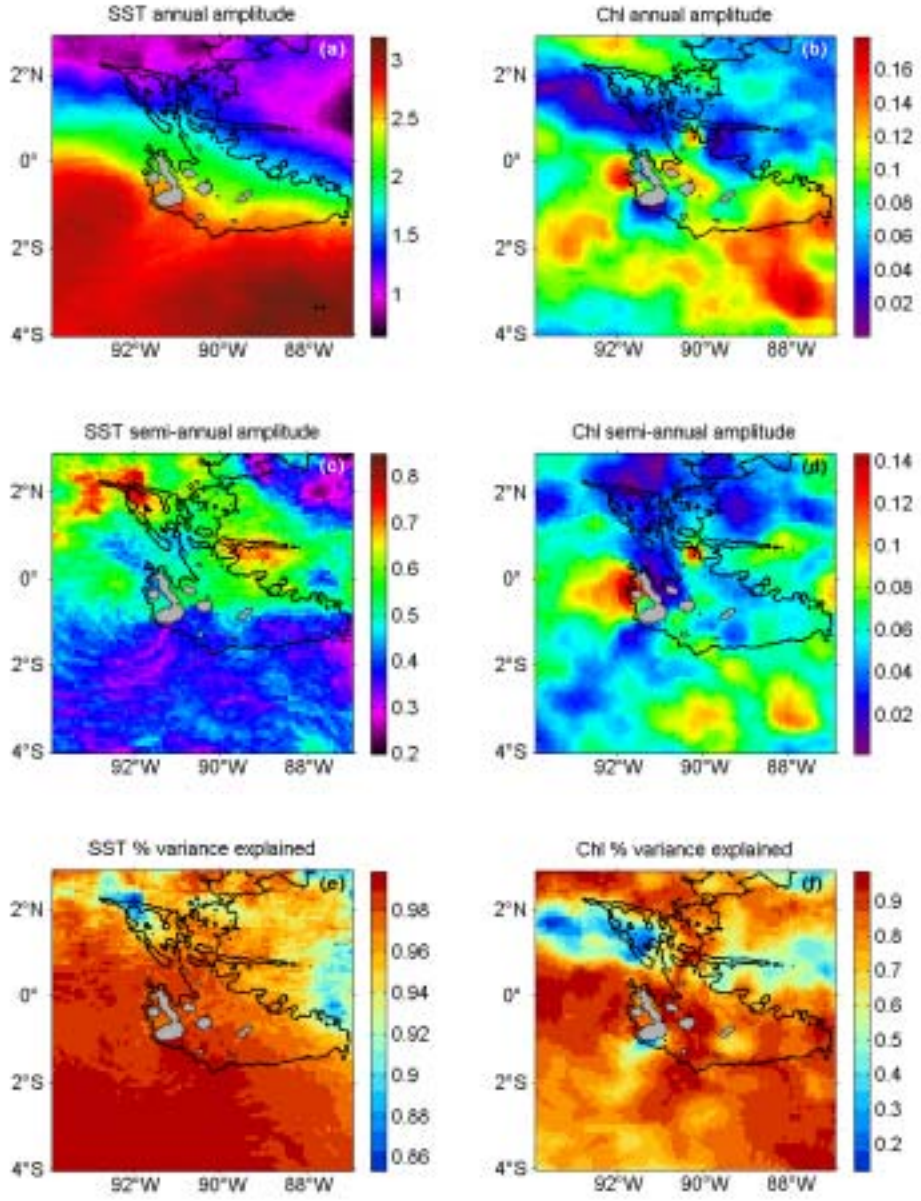

Figure 3.2: Harmonic analysis. (a) and (b): Annual amplitude constituents for SST (°C) and log-transformed chl (mg m^{-3}), respectively. (c) and (d): Semi-annual amplitude constituents for the same variables. (e) and (f): Percent explained variance by the harmonic fit for the same variables. Black contour indicates the 2000-m isobath.

This pattern is very similar to the standard deviation (Fig. 3.1c), indicating that the annual period contains most of the SST variability. Indeed, the semi-annual amplitude (Fig. 3.2c) is small throughout the study area (< 0.9°C), and only becomes important in localized sectors along the northern domain. In contrast, although the chl annual amplitude also represents a regional pattern with large excursions at the southeast corner of study area (Fig. 3.2b), the magnitude of the semi-annual constituent is about as large as that of the annual amplitude. Some of the localities where the SST semi-annual amplitude is important are also evident in the chl semi-annual constituent. This is primarily evident northeast of Marchena and Genovesa islands, and also to some extent in the waters directly to the west of Isabela and Fernandina. There are also areas with increased semi-annual amplitudes for one variable that are not evident in the other (i.e., the northwest sector in SST and the southeast sector in chl).

One particularly interesting feature in the annual amplitude, especially in the SST field, is a southward tilt in the pattern of about 1.5 degrees in latitude from west to east that is aligned with the shape of the archipelago (as indicated by the 2000-m depth contour in Fig. 3.2a). This feature is best explained in terms of the annual phase (Fig. 3.3a), which indicates that much of the study area reaches maximum temperatures around March, when the southeast trade winds that normally cool the region are weakest and the intertropical convergence zone (ITCZ) is at its southernmost position (see section 1.2.1). However, a distinct wedge-shaped area on the eastern sector reaches its maximum temperature about two months earlier. At that time the area begins receiving the influx of upwelled waters from the Panamá Bight, as described in section 1.2.2.1. It appears that the islands act as an obstacle to the penetration of these waters, as the annual phase is locked-in with the shape of the archipelago (indicated by the 2000-m depth contour

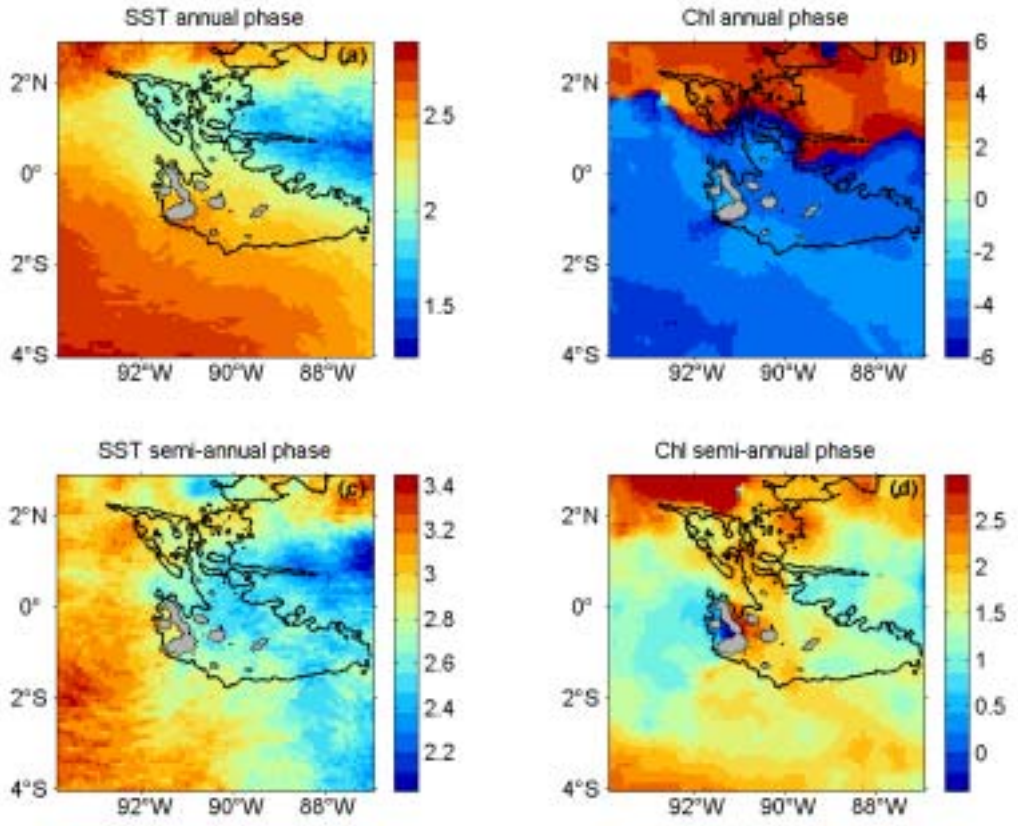

Figure 3.3: Harmonic analysis. (a) and (b): Annual phase constituents for SST and ocean color, respectively (both in months relative to January). (c) and (d): Semi-annual phase constituents for the same variables (both in months relative to January). Black contour indicates the 2000-m isobath.

in Fig. 3.3a) in this sector. This phenomenon also explains the tilt in the amplitude pattern: the influx of cool waters prevents this sector from reaching its maximum temperature during this period.

The chl annual phase (Fig. 3.3b) reveals two distinct annual cycles within the study area, one peaking in the austral fall (around May) in the northern part and the other one peaking in the austral spring (around August) in the southern part. The northern cycle represents the annual advection of waters enriched with phytoplankton (or possibly colored dissolved organic matter) from the Panamá Bight, while the southern cycle represents the increase in phytoplankton biomass resulting from equatorial upwelling during the southeast trade wind season. The phase transition between the two regimes is abrupt and takes place along a meandering band between 1°–2°N that roughly corresponds with the location of the EF.

The SST semi-annual phase (Fig. 3.3c) is very similar to the annual phase, although with a slight temporal offset. The first peak is observed between early March and mid-April, and the first minimum is reached between early June and mid-July. Subsequent maxima and minima are reached six months after the previous ones. As mentioned above, the semi-annual constituents have little explanatory power for SST data in the study area. On the other hand, the chl semi-annual phase appears to be distinctly associated with the EUC (Fig. 3.3d). A chl peak first develops in early December along the equator, mostly outside the island platform (i.e., immediately to the west and to the east). The first minimum occurs around early March, and so on. It is possible that the chl semi-annual constituent is associated with intraseasonal perturbations to the equatorial thermocline (e.g., Kelvin waves) manifested in the near-surface chl field, but the monthly climatologies used here do not adequately resolve them.

3.6 EMPIRICAL ORTHOGONAL FUNCTION ANALYSIS

The harmonic analysis in the preceding section showed that the temporal variability in the monthly satellite climatologies is dominated by a basin-wide seasonal cycle of warming and cooling of surface waters (and its effect on phytoplankton), associated with the north-south migration of the ITCZ. However, the harmonic constituents contained little or no information describing the patterns associated with the topographically driven upwelling of the EUC, evident in the mean fields (Figs. 3.1a and 3.1b). As an alternative, empirical orthogonal function (EOF) analysis can be applied to extract the principal patterns of variability in a data set without specifying *a priori* prescriptions of the underlying processes, as the harmonic fit does. The technique is widely used in oceanography as a method for partitioning the variance of a spatially distributed group of concurrent time series into a few statistical "modes" that are uncorrelated (Emery and Thomson, 1997).

Conventional EOF analysis decomposes the temporal variance of the data matrix after the time-averaged mean (i.e., the row mean) has been removed at each *M* spatial location. Application of this approach yielded the annual and semi-annual components of the seasonal cycle in the first two modes, and it did not provide any new information. Specifically, none of the dominant modes were associated with the local effects of the EUC, which have been described as a quasi-permanent pool of cold water on the western side of Isabela and Fernandina islands, and smaller upwellings at other localities throughout the archipelago (Houvenaghel, 1978).

Alternatively, the EOFs can be computed after removing the spatial (i.e., column) mean from the data matrix at each *N* time step (Lagerloef and Bernstein, 1988). In this case, the EOFs decompose the variability of the spatial property gradients rather than variability of the property itself (Kelly, 1988). These "spatial variance EOFs", also called "gradient EOFs" (Paden et al., 1991), are useful when the purpose is to investigate the variance associated with features that do not vary

strongly over time (Lagerloef and Bernstein, 1988). Ranking of the decomposed modes is based on the amount of spatial variability present in the data.

Following this approach, the SST and chl data matrices were first adjusted by removing the spatial average at each time step. Both averages exhibit a clear seasonality, with a maximum SST in March of 26.9°C and a minimum in August of 22.2°C (Fig. 3.4a). For comparison, the long-term monthly average of a 37-yr (1965–2001) *in situ* SST time series measured daily at the dock of the Charles Darwin Research Station (CDRS in Fig. 1.1), on Santa Cruz Island, is also plotted in Figure 3.4a. The chl maximum is reached in August (0.47 mg m^{-3}) and the minimum in May (0.29 mg m^{-3}), with secondary peaks observed in January and March (Fig. 3.4b). The variance fields of the adjusted data matrices (i.e., that variance which is decomposed by the gradient EOF analysis) are shown in Figure 3.4c and 3.4d for SST and chl, respectively. Because there were no data gaps in the climatological data sets, the computationally efficient method of singular value decomposition was applied to derive the eigenvectors, eigenvalues, and eigenfunctions directly from the adjusted data matrices (Kelly, 1988; Emery and Thomson, 1997).

The dominant mode in the SST EOF decomposition explains 92.24% of the variance of the adjusted monthly climatologies. Its spatial pattern (Fig. 3.5a) is similar to the temporal mean described at the beginning of section 3.4 (Fig. 3.1a). There is a strong north-south temperature gradient with the zero crossing corresponding with the southern boundary of the EF. A large pool of cooler-than-average water extends west of Isabela and Fernandina islands. The first gradient EOF mode for the chl data explains 82.43% of the variance. Although a large-scale north-south gradient is also evident, the main feature is a concentric pattern of

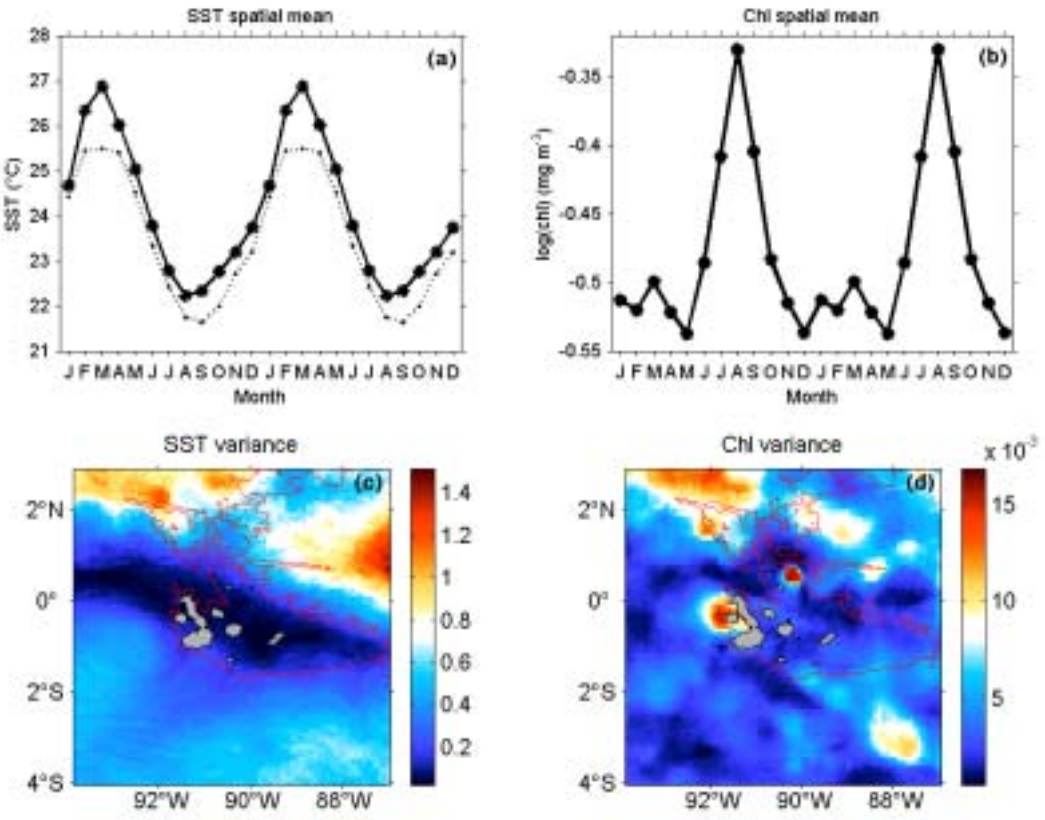

Figure 3.4: EOF analysis. (a) and (b): Monthly spatial means for SST and log-transformed chl, respectively, that were removed from the time series prior to analysis. (c) and (d): Temporal variance decomposed by the analysis for SST ($°C^2$) and log-transformed chl [$(mg\ m^{-3})^2$], respectively. Red contour indicates the 2000-m isobath. Time series are repeated twice for clarity. Dashed line in (a) is the long-term (1965–2001) monthly averaged SST measured at the CDRS dock. The location of the CDRS dock is indicated in Figure 1.1.

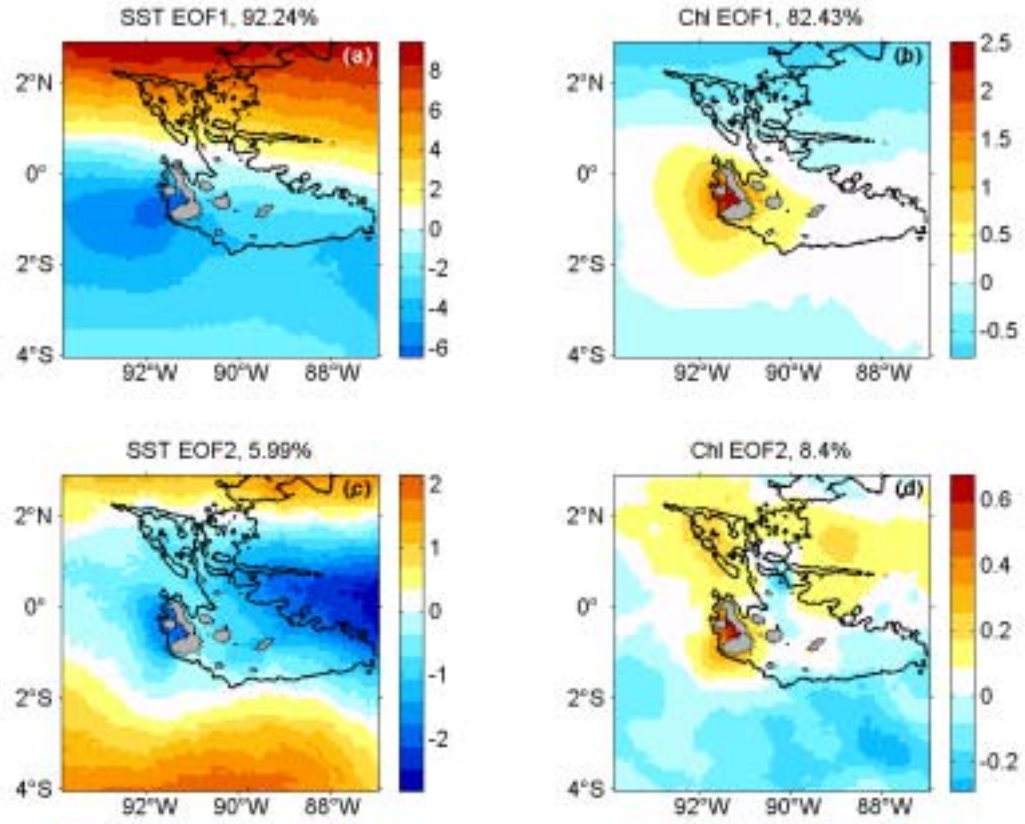

Figure 3.5: EOF analysis. (a) and (b): Mode 1 spatial patterns for SST and log-transformed chl, respectively. (c) and (d): Mode 2 spatial patterns for the same variables. Black contour indicates the 2000-m isobath.

above-average chl centered in Elizabeth Bay, the southern of two bodies of water formed between Isabela and Fernandina islands (Fig. 3.5b).

Gradient mode 2 captures 5.99% of the SST spatial variability. Its spatial pattern exhibits a zonal band of cool water between 2°N and 2°S, with a large pool of cold water on the eastern side of the archipelago and a smaller pool directly west of Isabela and Fernandina islands (Fig. 3.5c). Warmer-than-average waters are found along the northern and southern edges of the study area. For the chl decomposition, the second mode describes 8.4% of the variance. Above-average chl concentrations are found occupying the northern half of the study area, and a distinct center of high chl is again found in Elizabeth Bay (Fig. 3.5d). Below-average chl concentrations are found along the southern sector.

The temporal amplitudes associated with each EOF are presented in Figure 3.6. The mode 1 amplitudes are positive for the SST, and consist of an annual cycle with a minimum in March and a maximum in September (Fig. 3.6a). Thus, the spatial pattern is well developed during the second half of the year, and its timing is consistent with the intensification of generalized wind-driven equatorial upwelling south of the EF (Fig. 3.5a). The linearity of the spatial pattern along east-west bands suggests persistent zonal flows most likely associated the South Equatorial Current (SEC), which is strong between July and December (Johnson et al., 2002). The extent and axis of orientation of the cold pool off Isabela and Fernandina also suggest westward advection of upwelled EUC waters by the SEC. Mode 1 temporal amplitudes for chl also consist of a positive annual cycle with increased chl values between July and January (peaks are in September and in January), and low values between February and June (the minimum is reached in April) (Fig. 3.6b). The spatial pattern associated with this mode (Fig. 3.5b) indicates that the local response by phytoplankton to the annual cold tongue cycle is only strong in the

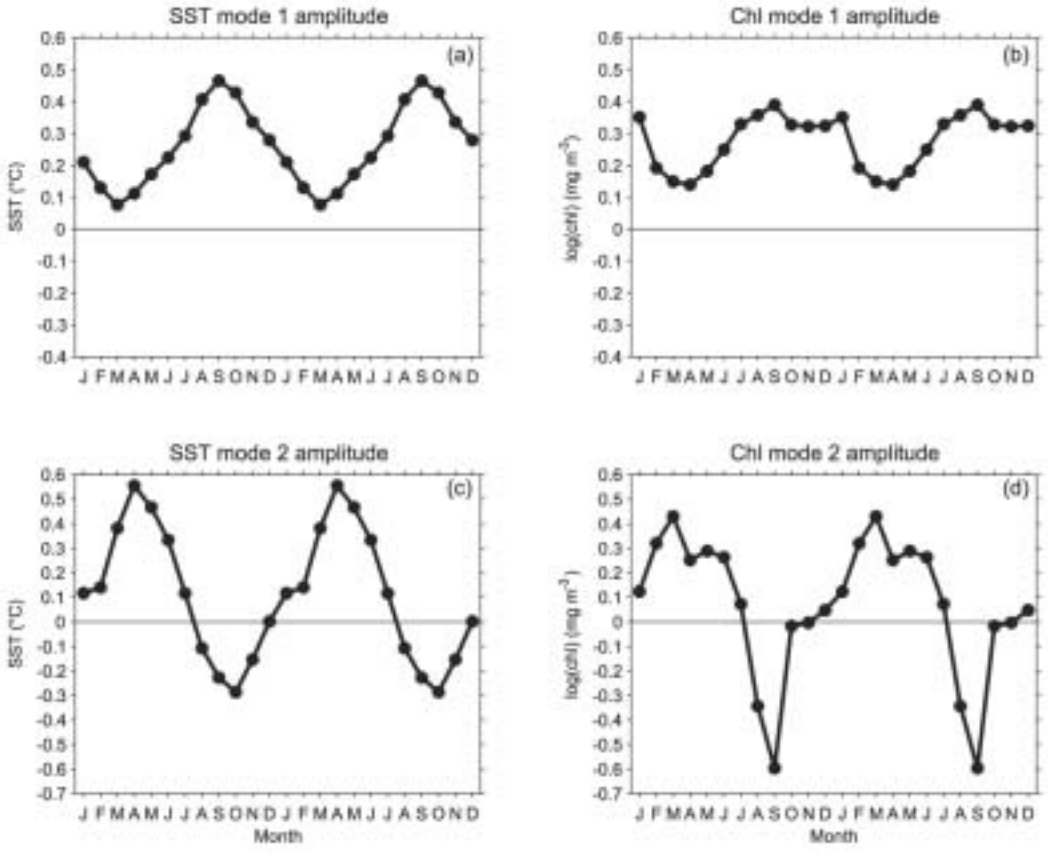

Figure 3.6: EOF analysis. (a) and (b): Mode 1 temporal amplitudes for SST and log-transformed chl, respectively. (c) and (d): Mode 2 temporal amplitudes for the same variables.

waters surrounding the western group of islands, and to a lesser degree in a zonal band extending roughly between 1°N and 3°S. These waters are probably under the enriching influence of the EUC, as will be discussed in the next section.

The temporal amplitudes of the SST mode 2 depict an annual cycle with positive values between December and July (peaking in April) and negative values between August and November (minimum in October) (Fig. 3.6c). The corresponding spatial pattern (Fig. 3.5c) is thus most intensified in April and its timing is consistent with the strengthening and shoaling of the EUC in the eastern Pacific (Lukas, 1986; Johnson et al., 2002). The small pool of cold water on the western side of Fernandina and Isabela during this time represents EUC waters forced to surface by the steep slopes of these islands. Colder-than-average waters also surround the central and northern group of islands, and small cold foci on the western side of Pinta and San Cristóbal are probably additional upwelling locations. The large cold pool impinging on the eastern side of the archipelago may be explained as waters being advected westward from upwelling events in the Panamá Bight, which also occur between December and April. Chl mode 2 temporal amplitudes (Fig. 3.6d) are also positive between December and July (but they peak in March and a secondary peak occurs in May), and negative between August and November (the minimum is in September). As expected, high chl values occupy the same general area where the cool waters are found, although a slight shift to the north is apparent in the chl field in the area affected by the advection of Panamá Bight waters (Fig. 3.5d).

Gradient EOFs picked up patterns consistent with surface manifestations of the EUC as it interacts with the archipelago in the two dominant modes. Because this current is normally present year-round its effects are likely to covary with different processes at particular times of the year, and hence its variability is distributed over several modes. Although gradient mode 2 explains a comparatively small fraction of the total spatial variance (about 6% for SST and 8.4% for chl), the

contribution of the mode to the variability in the data sets is not always small. The reconstructed time series for this mode, obtained by multiplying the values in the spatial pattern at each location by the temporal amplitudes, can at times have greater magnitudes than the reconstructed time series for the dominant mode. This is the case for the SST during March and April, when the reconstructed time series for mode 2 can be greater than the time series for mode 1 by up to 0.85°C in the coldest areas. Therefore, mode 2 or, rather, the SST and chl gradients induced by the processes described above, are important during the fall months.

The long-term monthly average of the 37-yr long SST record from Santa Cruz Island (dashed line in Fig. 3.4a) also serves to illustrate the effects of the EUC at this particular location in the archipelago. Although rapid warming occurs between December and February, the curve flattens out between February and April, revealing the slight cooling influence of an intensified and shallow EUC at a time when the region as a whole reaches maximum temperatures (e.g., solid line in Fig. 3.4a). Podestá and Glynn (1997) have actually documented a dip of a few tenths of a degree in March in an annual cycle estimated from a seasonal-trend decomposition of the daily values in the CDRS time series [see also Fig. 1 in Abbott (1966) for a similar behavior in a time series at Wreck Bay, San Cristóbal Island].

Further insight into the contribution of each EOF mode to the variability of the adjusted data sets can be gained by examining the fraction of variance explained at each M spatial location. For gradient EOFs, this local contribution can be calculated as the ratio of the variance of the reconstructed mode to the variance of the input data matrix, scaled by the total spatial variance. Figure 3.7 shows this ratio (which is essentially an R^2 value) for each mode in the SST and chl data sets. For the two SST modes (Figs. 3.7a and 3.7c), the largest fraction of explained

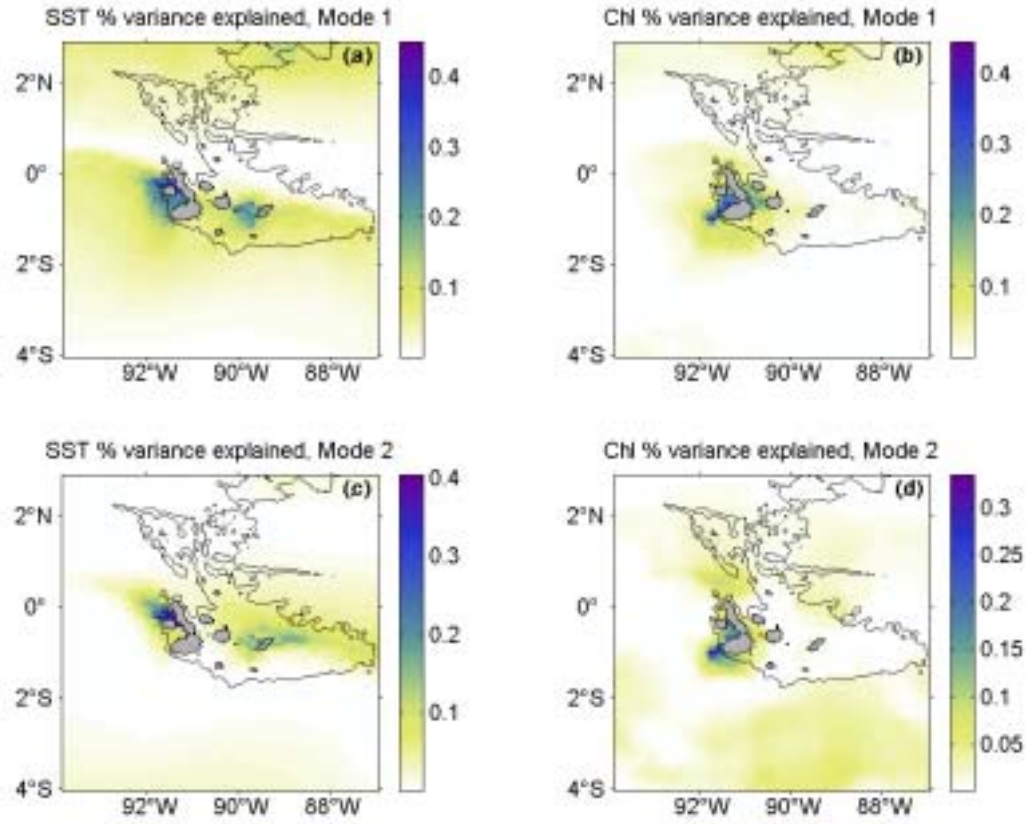

Figure 3.7: EOF analysis. (a) and (b): Local contribution to the variance explained by mode 1 for SST and log-transformed chl, respectively. (c) and (d): Local contribution to the variance explained by mode 2 for the same variables. Black contour indicates the 2000-m isobath.

variance is found in Banks Bay, the northern body of water between Isabela and Fernandina islands, and adjacent waters. The waters surrounding San Cristóbal Island also contribute to the variance. These are areas where interaction between the EUC and the island platform is presumed to be intense. SST mode 1 also contains contributions to the variance in the persistently warm waters to the north of the EF (Fig. 3.7a), and SST mode 2 along the southern boundary of the study area (Fig. 3.7c). The waters off the southwestern tip of Isabela contain the largest contributions to the variance in both chl modes (Figs. 3.7b and 3.7d). The northeast and southeast sectors of the study area also contribute to the variance explained by mode 1 (Fig. 3.7c) and mode 2 (Fig. 3.7d), respectively. In all cases, most of explained variance is found in areas with relatively low variance in Figures 3.4c and 3.4d (i.e., areas where horizontal gradients are strong and persistent), which is expected from the gradient EOF approach.

3.7 WATER-COLUMN TEMPERATURE AND NITRATE

Satellite measurements are restricted to the surface or, at best, to the upper tens of meters of the water column. Additional understanding of processes that drive the observed SST and chl patterns can be gained by considering the vertical distribution of temperature and the role of nutrient availability. For this purpose, the most comprehensive data set available is the World Ocean Atlas 1998 (WOA98) (Conkright et al., 1998) compiled by the National Oceanographic Data Center (NODC) of the National Oceanic and Atmospheric Administration (NOAA). The WOA98 contains objectively analyzed property fields for one-degree squares and standard depth levels. Monthly values of water-column temperature and quarterly values of nitrate concentration at 20 m were used in this study.

Meridional sections of temperature in the upper 150 m along 92.5°W (west of the Galápagos Platform) and 87.5°W (east of the Galápagos Platform) for March and September (Fig. 3.8) were chosen to represent conditions at the seasonal

extremes of the annual cycles identified in the previous sections. The main feature in the western sections is the upward sloping of the isotherms caused by the local upwelling of the EUC between 0° and 1°S, as it impinges against the island platform and is deflected upward. In the eastern sections, past the influence of the archipelago, the presence of a shallow EUC is evident by the upward and downward bulging of the isotherms roughly between 10 m and 100 m. Seasonally, maximum SSTs are reached in March and the water column is strongly stratified during this month (Figs. 3.8a and 3.8b). By September the southern part of the study area has been dramatically changed. The warm upper layer (~ 30 m) has been eroded by the southeast trade winds and these waters have been replaced by cool, upwelled water from the top of the thermocline (Figs. 3.8c and 3.8d). The EF, indicated by the 25°C isotherm at the surface just south of 2°N (the dashed line in Figs. 3.8c and 3.8d), separates warm and stratified waters to the north from mixed waters to the south. The surface divergence created by the wind stress at this time is also conducive to enhanced upwelling of the EUC (Fig. 3.8c), as evidenced by the steep sloping of the isotherms all the way down to the bottom of the thermocline (~ 100 m).

Horizontal distributions of WOA98 nitrate concentration at 20 m (Fig. 3.9) for the four quarterly periods illustrate the seasonal progression of macronutrients reaching the upper layer. During the January–March period (Fig. 3.9a), and away from the area of influence of the EUC (i.e., in the stratified regime), nitrate concentrations are relatively low (≤ 6 μM), implying a mesotrophic to oligotrophic character. Elevated nitrate concentrations expand and propagate along the southern half of the study area from east to west during the rest of the year (Figs. 3.9b–3.9d), as the southeast trade winds and the equatorial upwelling intensify. An opposite trend is evident along the northern half, such that oligotrophic and “high-nutrient,

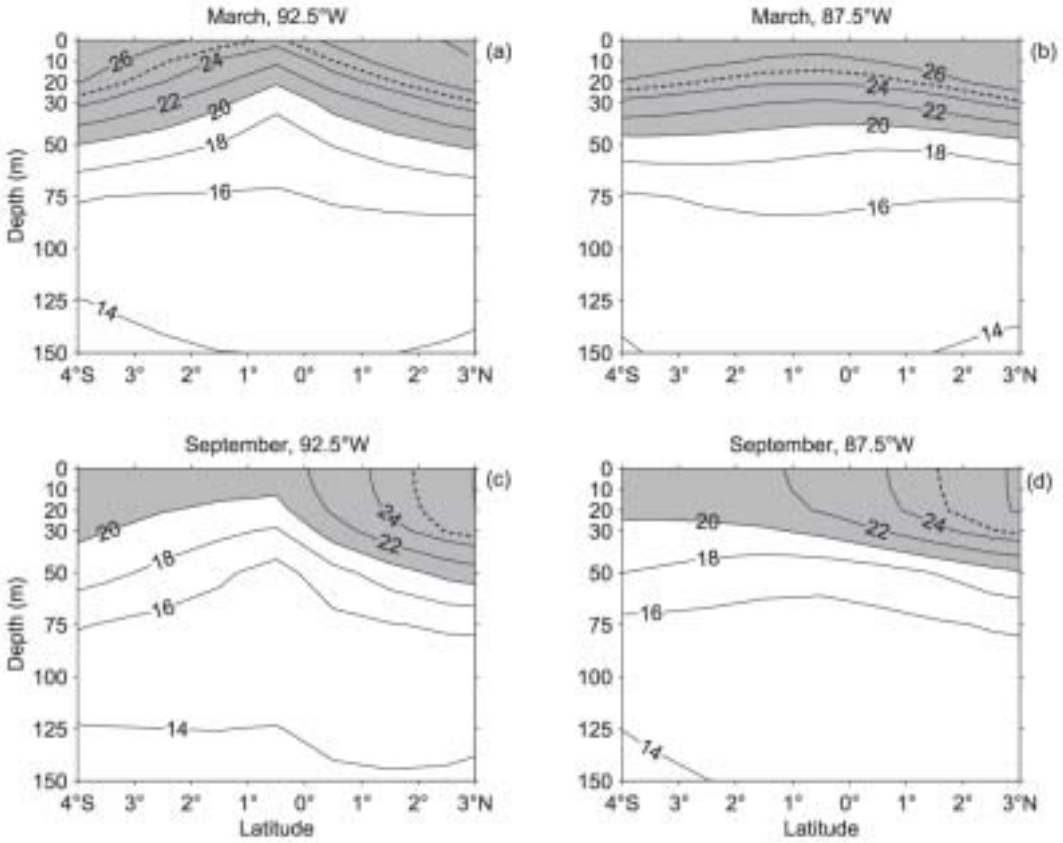

Figure 3.8: WOA98 meridional temperature (°C) sections. (a) and (b): For March along 92.5°W (west of the archipelago) and 87.5°W (east of the archipelago), respectively. (c) and (d): For September. Temperatures ≥ 20°C are shaded, and the 25°C isotherm is dashed.

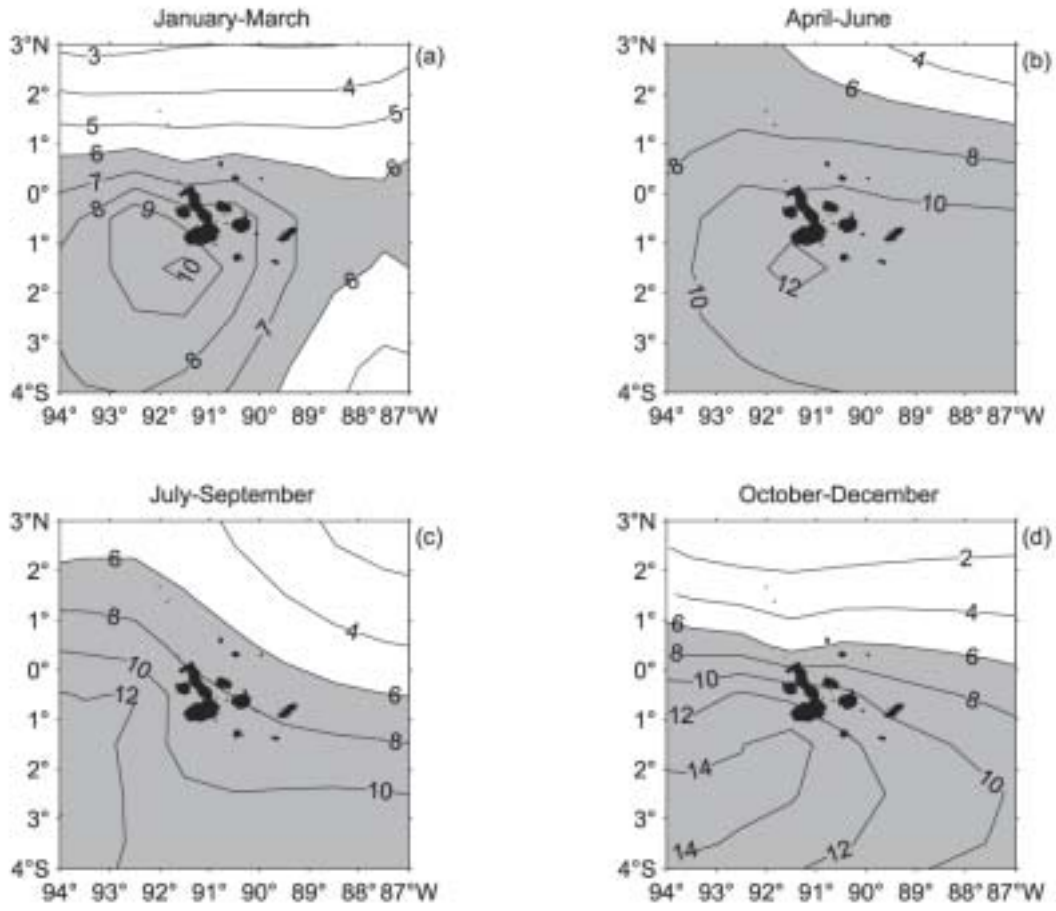

Figure 3.9: WOA98 nitrate concentrations (μM) at 20 m. (a): For January–March. (b): For April–June. (c): For July–September. (d): For October–December. $[NO_3] \geq 6$ μM are shaded.

low-chlorophyll" regimes coexist in the study area during the second part of the year. Minimum 20-m nitrate concentrations can be as low as 0.2 μM north of the EF while maximum concentrations can reach 15 μM in the southwest sector of the study area in the October–December period (Fig. 3.9d).

The difference between nitrate concentration at 20 m and at 0 m (not shown) gives a general indication of the amount of nitrate that is removed by phytoplankton uptake during each period. This difference is most marked in the January–March and October–December periods, when nitrate removal at the location where the EUC upwells is about 4–8 μM. Strong nitrate removal in the October–December period, however, is not restricted to the area of direct EUC influence but expands along the southern part of the study area. These periods of strong nitrate removal, as well as their spatial extent, are consistent with the timing (Figs. 3.6b and 3.6d) and the areas of enhanced phytoplankton biomass (Figs. 3.5b and 3.5d) identified in the EOF analysis. The exception is the sector of elevated chl along the northern part of the study area in Figure 3.5d, which is likely the result of advection from the Panamá Bight and is not associated with local nutrient enhancement.

South of the EF, nitrate levels are adequate to support large phytoplankton populations year-round. Yet, elevated chl levels are primarily observed in association with the pool of cold water on the western side of Isabela and Fernandina islands, where the EUC upwells. The IronEx I and II experiments (Martin et al., 1994; Coale et al., 1996b; Coale, 1998) demonstrated that low ambient iron concentrations limit the ability of phytoplankton populations to fully utilize available nitrate and achieve maximal growth in this region. While the EUC contains somewhat enhanced concentrations of iron (up to 0.35 nM at 140°W) (Coale et al., 1996a), water from the EUC alone cannot explain the high chl levels observed at the upwelling site. A dramatic enrichment of this water takes place by contact with the island platform, accounting for iron concentrations > 1 nM (up to 3

nM were measured in Bolivar Channel between Isabela and Fernandina during IronEx I) (Martin et al., 1994; Gordon et al., 1998). Resuspension of continental-shelf sediments during upwelling events has been documented as the primary source of iron for phytoplankton in a coastal upwelling system (Johnson et al., 1999), and it is probably the mechanism for enrichment in Galápagos waters as well. As the iron limitation is relieved in the Bolivar Channel and Elizabeth Bay, phytoplankton production increases by several fold (Lindley and Barber, 1998) while nitrate levels are locally depleted (Chavez and Brusca, 1991; Sakamoto et al., 1998).

3.8 CONCLUDING REMARKS

Satellite climatologies of SST and ocean color, with their uniform coverage and high spatial resolution, provided a useful representation of long-term ocean conditions around the Galápagos not previously achieved with shipboard sampling. Comparative analyses of the SST and ocean color data sets contributed insightful information to the understanding of the physical forcings and biological effects associated with the complicated circulation around the archipelago. The two analysis techniques applied to the data sets complemented each other in the characterization of temporal and spatial variability in the study area. Harmonic analysis showed the variation in magnitude and the propagation of seasonal variability through the study area. The gradient EOF approach presented a different view of this variability. The two annual cycles described by the first two modes were consistent with the seasonalities of the SEC and the EUC, respectively, suggesting that these modes captured the effects of these currents as they interact with the archipelago. The influx of Panamá Bight waters in the eastern side of the archipelago was also revealed by these analyses.

The satellite data also delineated the long-term behavior of the quasi-permanent pool of cold water and high chl formed by the upwelling of the EUC on

the western side of the archipelago. Elizabeth Bay was identified as the area where the phytoplankton response is most dramatic and persistent, possibly due to resuspension of iron-rich sediments, which relieve the limitation for this micronutrient and allow the phytoplankton to fully use the available macronutrients. The productive ecosystem that develops in this area exemplifies the conceptual model advanced by Margalef (1978) of an upwelling area as a "nodal point of stress" that causes a local deformation in the ecological fields. Stress consists of auxiliary energy supplied by the wind in the case of coastal upwelling (Margalef, 1978; Barber and Smith, 1981), or, in this case, by the upward deflection of the EUC by the island platform.

The annual cycle corresponding to the strengthening of the EUC was not present in the harmonic analysis of the SST climatologies because its amplitude is very small compared to that of the annual cycle associated with the basin-wide seasonal warming and cooling. Effects of the EUC annual cycle on chl were not clearly identified in the ocean color annual harmonic either. However, this cycle was captured in the second mode of the EOF analysis, and although it only explained a small percentage (~ 6%) of the spatial SST variance, it was shown that its effects become important during the austral fall. A slightly higher percentage of the spatial variance (8.4%) was explained by the second EOF mode for the ocean color data, implying that chl gradients associated with the intensification of the EUC are also important at this time.

The identification of distinct annual cycles of phytoplankton abundance in both the harmonic and EOF analyses of the ocean color climatologies is in contrast with previous studies, which had failed to demonstrate a clear chl seasonality (Harris, 1969; Houvenaghel, 1978; 1984; Kogelschatz et al., 1985; Feldman, 1986). This is not surprising, however, considering that the two annual cycles identified here have opposing schedules and that intraseasonal perturbations regularly affect the area, making it difficult to discern seasonal patterns in a time series without

more sophisticated analyses. The ocean color semi-annual harmonic appeared to be important in localized areas. Ocean color measurements represent chl concentrations within the first optical attenuation depth (i.e., the upper 5–25 m of the water column), and it is speculated that perhaps this variability may be associated with 60–90-day period intraseasonal Kelvin waves. These waves induce vertical displacements in the thermocline, possibly injecting limiting nutrients and enhancing phytoplankton populations in near-surface waters, where they can be detected by the ocean color sensors.

The presence of the Galápagos Platform introduces perturbations to the predominantly zonal circulation of the eastern equatorial Pacific. Direct modification of the eastward-flowing EUC, mainly by the islands of Fernandina and Isabela, takes place on the western side of the archipelago in the form of topographically induced upwelling and splitting of the current into northern and southern branches. The Galápagos also modify the large-scale fields by partially deflecting westward flows originating from South America (e.g., SEC, Panama Bight Influence). This results in a slight tilt in the patterns (readily observable in the variance fields) that is aligned with the east-west axis of the Galápagos Platform.

It is important to note that the local effects induced by the islands are relatively small compared to other oceanographic phenomena in the eastern tropical Pacific (e.g., tropical instability waves, the Costa Rica Dome, or upwelling along the Central and South American coasts). These effects would be missed or greatly attenuated if the analyses in this study were carried out on a regional scale. However, the complex oceanography of the archipelago clearly has played an important role in the establishment and evolution of the unique biota found in the nearshore environments. From this perspective, the results of this paper provide a descriptive framework relevant to marine ecological and biogeographic studies of the islands. With the newly established 14-million-hectare “Galápagos Marine

Reserve" (Bensted-Smith, 1998), these results may also be useful for purposes of zonation and management, particularly of the offshore waters.

3.9 ACKNOWLEDGEMENTS

On-line data sets were obtained from several sources. The "Pathfinder + Erosion" SST climatologies from PO.DAAC/JPL/NASA (URL: http://podaac.jpl.nasa.gov/order/ order_sstemp.html#Product112). SIMBIOS-NASDA-OCTS and SeaWiFS ocean color from the SeaWiFS project (code 970.2) and the GES DISC DAAC (code 902) at GSFC/ NASA, Greenbelt, MD 20771 (URLs: http://daac.gsfc.nasa.gov/data/dataset/OCTS/ and http://daac.gsfc.nasa.gov/data/dataset/SEAWIFS/). The "Smith and Sandwell" global sea-floor topography v. 8.2 (for Figures 3.2–3.7) from the Institute of Geophysics and Planetary Physics at the Scripps Institution of Oceanography (URL: http://topex.ucsd.edu/marine_topo/ mar_topo.html). WOA98 temperature and nitrate from NODC/NOAA (URL: http://www.nodc.noaa.gov/). The 37-yr (1965–2001) *in-situ* SST record from Academy Bay was graciously provided by S. Rea of the Monitoring Program at the CDRS. K.S. Casey (Department of Oceanography, U.S. Naval Academy), provided computer code useful in generating the ocean color climatologies. Funding for this study was provided by the Endowed Marine Mammal Program at Oregon State University. Insightful discussions with E. Beier, D.B. Chelton, and A.M. Martínez on analysis techniques were helpful. This manuscript benefited from comments from B.R. Mate, C.B. Miller, P.T. Strub, and the anonymous reviewers.

3.10 REFERENCES

Abbott, D.P. 1966. Factors influencing the zoogeographic affinities of the Galápagos inshore marine fauna. Pages 108–122 *in* Bowman, R.I., ed. The Galápagos: Proceedings of the Symposia of the Galápagos International Scientific Project. University of California Press, Berkeley.

Barber, R.T., and R.L. Smith. 1981. Coastal upwelling ecosystems. Pages 31–68 *in* Longhurst, A.R., ed. Analysis of Marine Ecosystems. Academic Press, London.

Bensted-Smith, R. 1998. The special law for Galápagos. Noticias de Galápagos 59:6.

Casey, K.S., and P. Cornillon. 1999. A comparison of satellite and *in situ*-based sea surface temperature climatologies. Journal of Climate 12(6):1848–1863.

Chavez, F.P., and R.C. Brusca. 1991. The Galápagos Islands and their relation to oceanographic processes in the tropical Pacific. Pages 9–33 *in* James, M.J., ed. Galápagos Marine Invertebrates. Taxonomy, Biogeography, and Evolution in Darwin's Islands. Topics in Geobiology, Vol. 8. Plenum Press, New York and London.

Coale, K.H. (Ed.). 1998. The Galápagos iron experiments: A tribute to John Martin. Deep-Sea Research II 45:915–1150.

Coale, K.H., S.E. Fitzwater, R.M. Gordon, K.S. Johnson, and R.T. Barber. 1996a. Control of community growth and export production by upwelled iron in the equatorial Pacific. Nature 379:621–624.

Coale, K.H., K.S. Johnson, S.E. Fitzwater, R.M. Gordon, S. Tanner, F.P. Chavez, L. Ferioli, C. Sakamoto, P. Rogers, F. Millero, P. Steinberg, P. Nightingale, D. Cooper, W.P. Cochlan, M.R. Landry, J. Constantinou, G. Rollwagen, A. Trasvina, and R. Kudela. 1996b. A massive phytoplankton bloom induced by an ecosystem-scale iron fertilization experiment in the equatorial Pacific Ocean. Nature 383:495–501.

Conkright, M., S. Levitus, T. O'Brien, T. Boyer, J. Antonov, and C. Stephens. 1998. World Ocean Atlas 1998 CD-ROM Data Set Documentation. Technical Report 15. NODC Internal Report, Silver Spring, MD, 16 pp.

Emery, W.J., and R.E. Thomson. 1997. Data analysis methods in physical oceanography. Pergamon, Exeter, UK.

Delcroix, T. 1993. Seasonal and interannual variability of sea surface temperatures in the tropical Pacific, 1969–1991. Deep-Sea Research I 40(11/12):2217–2228.

Feldman, G.C. 1986. Patterns of phytoplankton production around the Galápagos Islands. Pages 77–106 *in* Bowman, M.J., C.M. Yentsch, and W.T. Peterson, eds. Tidal Mixing and Plankton Dynamics. Lecture Notes on Coastal and Estuarine Studies 17, Springer-Verlag, Berlin.

Gordon, R.M., K.S. Johnson, and K.H. Coale. 1998. The behaviour of iron and other trace elements during the IronEx-I and PlumEx experiments in the equatorial Pacific. Deep-Sea Research II 45:995–1041.

Glynn, P.W., G.M. Wellington, and J.W. Wells. 1983. Corals and coral reefs of the Galápagos Islands. University of California Press, Berkeley.

Harris, M.P. 1969. Breeding seasons of sea-birds in the Galápagos Islands. Journal of Zoology, London 159:145–165.

Hayes, S.P. 1985. Sea level and near surface temperature variability at the Galápagos Islands, 1979–83. Pages 49–81 *in* Robinson, G., and E.M. del Pino, eds. El Niño in the Galápagos Islands: The 1982–1983 Event. Publication of the Charles Darwin Research Foundation for the Galápagos Islands, Quito, Ecuador.

Houvenaghel, G.T. 1978. Oceanographic conditions in the Galápagos Archipelago and their relationships with life on the islands. Pages 181–200 *in* Boje, R., and M. Tomczak, eds. Upwelling Ecosystems. Springer-Verlag, Berlin.

Houvenaghel, G.T. 1984. Oceanographic setting of the Galápagos Islands. Pages 43–54 *in* Perry, R., ed. Key Environments, Galápagos. Pergamon Press, Oxford.

Johnson, G.C, B.M. Sloyan, W.S. Kessler, and K.E. McTaggart. 2002. Direct measurements of upper ocean currents and water properties across the tropical Pacific during the 1990's. Progress in Oceanography 52(1):31–61.

Johnson, K.S., F.P. Chavez, and G.E. Friedrich. 1999. Continental-shelf sediment as a primary source of iron for coastal phytoplankton. Nature 398:697–700.

Kelly, K.A. 1988. Comment on "Empirical Orthogonal Function Analysis of Advanced Very High Resolution Radiometer Surface Temperature Patterns in Santa Barbara Channel" by G.S.E. Lagerloef and R.L. Bernstein. Journal of Geophysical Research 93:15753–15754.

Kogelschatz, J., L. Solorzano, R. Barber, and P. Mendoza. 1985. Oceanographic conditions in the Galápagos Islands during the 1982/1983 El Niño. Pages 91–123 *in* Robinson, G., and E.M. del Pino, eds. El Niño in the Galápagos Islands: The 1982-1983 Event. Publication of the Charles Darwin Research Foundation for the Galápagos Islands, Quito, Ecuador.

Lagerloef, G.S.E., and R.L. Bernstein. 1988. Empirical Orthogonal Function analysis of Advanced Very High Resolution Radiometer surface temperature patterns in Santa Barbara Channel. Journal of Geophysical Research 93(C6):6863–6873.

Lindley, S.T., and R.T. Barber. 1998. Phytoplankton response to natural and experimental iron addition. Deep-Sea Research II 45(6):1135–1150.

Lukas, R. 1986. The termination of the Equatorial Undercurrent in the eastern Pacific. Progress in Oceanography 16:63–90.

Margalef, R. 1978. What is an upwelling ecosystem? Pages 12–14 *in* Boje, R., and M. Tomczak, eds. Upwelling Ecosystems. Springer-Verlag, Berlin.

Martin, J.H., K.H. Coale, K.S. Johnson, S.E. Fitzwater, R.M. Gordon, S.J. Tanner, C.N. Hunter, V.A. Elrod, J.L. Nowicki, T.L. Coley, R.T. Barber, S. Lindley, A.J. Watson, K. Van Scoy, C.S. Law, M.I. Liddicoat, R. Ling, T. Stanton, J. Stockel, C. Collins, A. Anderson, R. Bidigare, M. Ondrusek, M. Latasa, F.J. Millero, K. Lee, W. Yao, J.Z. Zhang, G. Friederich, C. Sakamoto, F. Chavez, K. Buck, Z. Kolber, R. Greene, P. Falkowski, S.W. Chisholm, F. Hoge, R. Swift, J. Yungel, S. Turner, P. Nightingale, A. Hatton, P. Liss, and N.W. Tindale. 1994. Testing the iron hypothesis in ecosystems of the equatorial Pacific Ocean. Nature 371:123–129.

Paden, C.A., M.R. Abbott, and C.D. Winant. 1991. Tidal and atmospheric forcing of the upper ocean in the Gulf of California 1. Sea surface temperature variability. Journal of Geophysical Research 96(C10):18337–18359.

Podestá, G.P., and P.W. Glynn. 1997. Sea surface temperature variability in Panamá and Galápagos: Extreme temperatures causing coral bleaching. Journal of Geophysical Research 102(C7):15749–15759.

Sakamoto, C.M., F.J. Millero, W. Yao, G.E. Friederich, and F.P. Chavez. 1998. Surface seawater distributions of inorganic carbon and nutrients around the Galápagos Islands: results from the PlumEx experiment using automated chemical mapping. Deep-Sea Research II 45:1055–1071.

Yu, X., and M.J. McPhaden. 1999. Seasonal variability in the equatorial Pacific. Journal of Physical Oceanography 29:925–947.

4 CETACEAN COMMUNITY STRUCTURE AROUND THE GALÁPAGOS IN RELATION TO ENVIRONMENTAL HETEROGENEITY AND SEASONAL CHANGE

4.1 ABSTRACT

A cetacean community consisting of seven small and medium-sized delphinids (*Stenella attenuata*, *S. longirostris*, *S. coeruleoalba*, *Delphinus delphis*, *Tursiops truncatus*, *Grampus griseus*, and *Globicephala macrorhynchus*), the sperm whale (*Physeter macrocephalus*), and the Bryde's whale (*Balaenoptera edeni*) was studied in relation to environmental conditions around the Galápagos Archipelago, using a compilation of sighting for the period 1973–2000. Sightings were gridded at a resolution of 0.25 degrees and seasonal composites were formed for analysis. Three major groups of sample units were obtained with cluster and indicator species analyses. The spatial distribution of two of the groups and their species composition showed a good correspondence with the main habitats found around the archipelago in all seasons. Areas of strong water-column stratification were characterized by presence of *S. attenuata* and *S. longirostris*, while upwelling and nearshore areas were characterized by presence *D. delphis*, *T. truncatus*, *B. edeni*, *G. griseus*, and *G. macrorhynchus*. The third group, characterized by presence of *S. coeruleoalba* and *P. macrocephalus*, was spatially incoherent. Ordination of the sample units *via* nonmetric multidimensional scaling yielded two axes, which represented 86% and 4.2%, respectively, of the information in the data set. The dominant environmental gradient in the study area (from cold, upwelling, and phytoplankton-rich conditions close to the islands to warm, stratified, and phytoplankton-poor conditions away from the islands) explained 27–35% of the variance in community structure along the first axis. Structure along the second axis was independent of the environmental variables considered.

4.2 INTRODUCTION

Located in the eastern equatorial Pacific, the Galápagos Archipelago lies in an area of rapid change in oceanographic conditions owing to its proximity to the Equatorial Front (EF). The EF is a regional feature that runs zonally between the South American coast and the international dateline, separating warm waters to the north from cool waters to the south. Biological production across this gradient is strongly influenced by the availability of macronutrients (i.e., nitrate) and micronutrients (i.e., iron). Conditions are generally oligotrophic north of the EF due to a meager nitrate supply across the strong pycnocline. South of the EF, wind-induced equatorial upwelling provides nitrate in adequate concentrations but iron is in limited supply, leading to "high-nutrient, low-chlorophyll" (HNLC) conditions through most of this region. Only at the Galápagos is this condition relieved owing to a localized phenomenon, the topographically forced upwelling of the Equatorial Undercurrent (EUC) on the western side of the archipelago. In this area, phytoplankton populations are able to use the upwelled nitrate in the presence of a local source of iron derived from the island platform. The productive habitat that develops in this area can be seen in ocean color satellite imagery as a plume of elevated phytoplankton pigment concentration extending westward for 100 km or more (Feldman et al., 1984; Feldman, 1986; Palacios, 2002). Thus, within oceanic Galápagos waters it is possible to find warm/oligotrophic, cool/HNLC, and cool/eutrophic conditions in close proximity to each other. In addition, a nearshore environment is found around the perimeter of the islands, and includes the shallow coastal waters and the underwater slopes of the volcanoes.

How does this environmental heterogeneity affect the occurrence patterns of top predators such as cetaceans? At the regional level, the distribution, abundance, and environmental associations of eastern tropical Pacific cetaceans have been the subject of a number of studies (Au and Perryman, 1985; Polacheck, 1987; Reilly, 1990; Reilly and Thayer, 1990; Wade and Gerrodette, 1993; Fiedler and Reilly,

1994; Reilly and Fiedler, 1994). In offshore waters, thermocline topography and watermass type appear to be the primary environmental factors that correlate with species distribution. Among the dolphins, the main patterns can be summarized as follows. Two geographically distinct stocks of spotted dolphins (*Stenella attenuata*) and spinner dolphins (*S. longirostris*) occupy the warmest waters of the region. Northeastern spotted dolphins and eastern spinner dolphins are found in Tropical Surface Water east of 120°W along the countercurrent thermocline ridge at 10°N. Western/southern spotted dolphins and whitebelly spinner dolphins are found in Subtropical Surface Water in the northwest and southwest corners of the region, where the thermocline is deep (Fiedler and Reilly, 1994; Reilly and Fiedler, 1994). Short-beaked common dolphins (*Delphinus delphis*), on the other hand, are found along the equatorial thermocline ridge east of 100°W in Equatorial Surface Water, and in the vicinity of the Costa Rica Dome, both areas of upwelling (Reilly, 1990; Reilly and Fiedler, 1994). Finally, striped dolphins (*S. coeruleoalba*) are widely distributed in the region and have no clear association with particular environmental conditions (Reilly, 1990; Reilly and Fiedler, 1994). In nearshore waters (i.e., off the coasts of Central America and northern South America), bottlenose dolphins (*Tursiops truncatus*), Risso's dolphins (*Grampus griseus*), short-finned pilot whales (*Globicephala macrorhynchus*), and, to a lesser extent, common dolphins are the dominant species, particularly in the Gulf of Panamá (Polacheck, 1987).

Among the large whales, the Bryde's whale (*Balaenoptera edeni*) is widely distributed in the region, but apparent areas of concentration are centered at the thermocline ridges along the equator and along 10°N, as well as in the Gulf of Panamá (Volkov and Moroz, 1977; Berzin, 1978; Wade and Gerrodette, 1993). Blue whales (*B. musculus*), on the other hand, have a clear preference for the upwelling-modified waters of the Costa Rica Dome and the Galápagos (Reilly and Thayer, 1990; Palacios, 1999a). Sperm whales (*Physeter macrocephalus*) are

widespread, although the Gulf of Panamá appears to be a particular area of concentration (Polacheck, 1987; Wade and Gerrodette, 1993).

All of the above species are known to occur in Galápagos waters, at least for part of the year (Palacios and Salazar, 2002), providing a unique opportunity to study the influence of strong environmental gradients on cetacean community structure at a local scale. It should be kept in mind that ocean conditions are not static, as processes acting at various temporal and spatial scales constantly modify them. These processes range from tidal mixing, equatorial waves and mesoscale eddies at one end of the spectrum, to El Niño and decadal oscillations at the other end. However, recognizing the importance of the seasonal cycle in the redistribution of forage at the regional scale (Blackburn et al., 1970; Dessier and Donguy, 1985; Fiedler, 2002), this study focuses on the effects of seasonal variability. The general patterns of species distribution, the relationships between species, and the associations between species and environmental variables around the Galápagos are described in this paper through community classification and ordination techniques.

4.3 METHODS

4.3.1 Cetacean data

The area for this study was defined as a 7 × 7-degree latitude-longitude box extending from 3°N–4°S and from 87°–94°W, with the geographic center of the Galápagos (0.5°S, 90.5°W) (Snell et al., 1995) at its center. The spatial extent of this area is about 605×10^3 km^2 or 597×10^3 km^2 once the area of the islands is subtracted. A database of marine mammal sightings collected by research expeditions and by scientific observers aboard fishing vessels operating in this area over the 28-yr period 1973–2000 was compiled for this study. Of the 4817 sightings in this database, 2879 belonged to 21 identified cetacean species, 165

belonged to two otariid pinnipeds, and 1773 corresponded to eight unidentified categories. The database is described in detail in Appendix A (section 4.10.1).

For analysis, the target community was defined using the number of sightings for each species relative to the total number of identified cetacean sightings (see Table A4.1), as a criterion to identify dominant and rare species. Species with less than 4% of the total were considered rare and eliminated from the analysis. The remaining 2739 sightings involved nine species: *S. attenuata* (n = 519, 18%), *D. delphis* (n = 456, 15.8%), *T. truncatus* (n = 366, 12.7%), *B. edeni* (n = 316, 11%), *S. longirostris* (n = 303, 10.5%), *P. macrocephalus* (n = 284, 9.9%), *S. coeruleoalba* (n = 247, 8.6%), *G. macrorhynchus* (n = 131, 4.6%), and *G. griseus* (n = 117, 4.1%). In order to use the sighting data it was necessary to project them onto a uniform grid. The resolution for this grid was determined by the need to preserve the details of the distribution of each species of interest, but also to avoid a division so fine that the grid would be made up of mostly empty cells. A resolution of 0.25 degrees (27.7 km) was found to be a good compromise. The resulting 28 × 28 grid was projected onto the study area and sighting locations were assigned to the center of the grid cell in which they fell. Of the 784 cells making up the grid, 15 occurred on land and were eliminated, while the remaining 769 were allowed to take values.

This gridding scheme was applied on a seasonal basis by combining sightings made in each season without regard to the year, as a compromise between resolving relevant scales of temporal variability (i.e., seasonal to interannual) and obtaining sufficient spatial coverage of the study area. The four seasons were defined as: January–March (JFM), April–June (AMJ), July–September (JAS), and October–December (OND). The resulting seasonal grids contained 392 (JFM), 297 (AMJ), 196 (JAS), and 330 (OND) cells with marine mammal sightings (including rare and unidentified species). However, a grid cell was considered *valid* only if it had sightings of one or more of the nine species of interest. Accordingly, the final

grids contained 309 (JFM), 232 (AMJ), 140 (JAS), and 223 (OND) valid cells. Hereafter, the valid cells in these seasonal grids are referred to as *sample units*.

Associated with each sample unit was the number of sightings per species and per season, accumulated over the 28-yr period of the compilation. Use of these data as an indication of species "abundance" for community analysis would clearly be inappropriate due to the lack of an adequate measure of effort needed to standardize abundance in each sample unit (see Appendix A). However, for the purposes of this study, abundance was not needed because the important information is contained in the pattern of presences and absences of the different species (Fager, 1957; McCune and Grace, 2002). Therefore, the species data were transformed to presence-absence. This binary transformation is particularly useful in studies in which the heterogeneity of the sample units is large (in terms of the *number of species* present), by enhancing the performance of sociological distance measures (McCune and Grace, 2002), like the Sørensen-based coefficient used in section 4.3.3. In this case, the transformation had the added benefit of greatly reducing the problems associated with spatial differences in effort for a given season. After these manipulations, the sighting data set was more analogous to the climatological data sets described in the next section in that it emphasized the long-term seasonal patterns.

4.3.2 Environmental data

Environmental variables were chosen for the roles they play in structuring pelagic communities and for their potential relevance to cetacean ecology (e.g., Sournia, 1994; van der Spoel, 1994), as follows. Sea-surface temperature (SST) is a useful descriptor of horizontal gradients associated with subsurface processes and air-sea interaction. Thermal fronts, in particular, are effective boundaries for most oceanic biota (e.g., Olson, 2002), including cetaceans (e.g., Gaskin, 1968; Selzer and Payne, 1988; Goold, 1998). The tropical thermocline and pycnocline serve as

physical and ecological barriers in the water column (Longhurst, 1998). The oxygen minimum layer (OML), where oxygen concentrations fall below 1 ml l^{-1} due to bacterial decomposition, can be an effective barrier to many organisms, but it also offers refuge and increased food supply to species adapted to thrive in these conditions (Wishner et al., 1995). Considerable amounts of biota aggregate in these oxygen-deficient zones (Longhurst, 1967; Mullins et al., 1985), with the potential to attract large predators like cetaceans (e.g., Perrin et al., 1976). Finally, phytoplankton chlorophyll-*a* concentrations (chl) provide an indication of the standing stock of primary producers available as food to higher trophic levels, eventually reaching cetaceans *via* links in the food web (e.g., Smith et al., 1986).

Contemporaneous measurements of these environmental conditions at the sighting locations were not available for the vast majority of the observations. Environmental data had to be obtained from standard climatological compilations, and therefore they are neither real-time nor sighting-associated measurements. They should be viewed as indicators of the average ocean conditions for the study area. A description of the climatological products used and the procedures followed to extract the variables of interest are given in Appendix B (section 4.10.2). Eight environmental variables were extracted for each season: (1) depth of the thermocline (Z20), (2) thermocline strength (ZTD), (3) pycnocline strength (MBVF), (4) depth of the pycnocline (ZMBVF), (5) depth of the OML (ZOML), (6) thickness of the OML (ZOD), (7) SST, and (8) log-transformed chl (LCHL). These variables were re-gridded from their original resolution to a common resolution of 0.25 degrees for compatibility with the sighting grid (see Appendix B).

A ninth variable, distance from each cell center to the geographic center of the archipelago in the sigthing grid (or RAD), was derived as an attempt to account explicitly for the spatial dependence of cetacean distribution patterns on physiographic features associated with the presence of the archipelago. Because of

the local nature of these features, this was found to be superior to including latitude and longitude as geographic variables. The latter are more useful in large-scale studies where a regional gradient in species morphology may be present or when several stocks of a particular species are being considered (e.g., Reilly and Fiedler, 1994).

4.3.3 Analytical methods

The goals of the analyses were two: (1) to identify the major groups of sample units in terms of species composition, and (2) to characterize the main patterns of variation in the cetacean data sets and to determine the relationship of these patterns to environmental variability. For these purposes, classification and ordination techniques were applied using the implementations in the software package PC-ORD version 4.25 (McCune and Mefford, 1999). The gridded cetacean data sets were arranged into matrices with sample units in the rows and species in the columns for each season (309 × 9 for JFM, 232 × 9 for AMJ, 140 × 9 for JAS, and 223 × 9 for OND). Consistent with the goals, analyses were conducted in "Q mode" (Legendre and Legendre, 1998), which aims at uncovering relationships among sample units based on the observed species. A distance matrix was computed for each seasonal species matrix using the Sørensen distance (see Appendix C, section 4.10.3.2).

4.3.3.1 Classification: Recognizing the major groups of sample units

The purpose of classification was to delineate the major groups[1] of sample units based on differences in species composition. These differences are presumed to arise primarily in response to environmental variability (Fager, 1957; Legendre and Legendre, 1998; McCune and Grace, 2002). As described in the Introduction,

[1] Throughout this paper, the word *group* is reserved to denote the major groups of sample units identified through cluster analysis and associated techniques.

most of the species in this study are known to have distinct habitat preferences, at least at the regional scale. For example, *S. attenuata* and *S. longirostris* are found in warm, offshore waters; *D. delphis* in upwelling-modified waters (e.g., Reilly, 1990; Reilly and Fiedler, 1994); and *T. truncatus* in nearshore environments (e.g., Polacheck, 1987). Because the study area can be readily divided into stratified *vs*. upwelling zones with regard to water-column structure, and into nearshore (i.e., within the 2000-m depth contour) *vs*. offshore zones with regard to distance from shore, it seemed reasonable to assume that at least three distinct cetacean habitats, stratified, upwelling, and nearshore, are present locally.

Cluster analysis was performed on the distance matrices, using flexible beta as the group linkage method, with $\beta = -0.25$ (McCune and Grace, 2002). The program was instructed to partition the distance matrices into three groups of sample units, which were presumed to represent the three types of habitat described above. The statistical validity of the three groups was assessed with a multi-response permutation procedure (MRPP) (Mielke, 1984; Mielke and Berry, 2001) on the rank-transformed distance matrices. MRPP tested the null hypothesis of no difference in average within-group ranked distance. It also provided an agreement statistic (A) describing average within-group homogeneity compared to random expectation (A increases as distances become more similar, with maximum $A = 1$ when all distances within each group are identical) (McCune and Grace, 2002).

The differences in species composition between the groups was described with indicator species analysis (Dufrêne and Legendre, 1997). Indicator values for a species are formed by combining information about specificity (i.e., the abundance of a species in a group in relation to the mean abundances of that species across groups) and fidelity (i.e, the number of sample units in a group where a species was present in relation to the total number of sample units in that group). Indicator values are expressed as a precentage of perfect indication. A species is an indicator of the group for which it has the largest indicator value. The

collection of indicator species characteristic of a group is referred to here as an *assemblage*. The indicator species provide a useful criterion in the ecological interpretation of groups of sample units that are presumed to describe particular environmental conditions. The significance of the indicator values was assessed with a Monte Carlo procedure by randomly reassigning sample units to groups 1000 times (Legendre and Legendre, 1998; McCune and Grace, 2002).

4.3.3.2 Ordination: Representing sample units and environment in reduced space

The purpose of ordination was to characterize the main patterns of variation among sample units in the species matrices and to establish the influence of environmental variability on those patterns. As a preliminary step, the species data were transformed with the Beals smoothing function (McCune, 1994). This transformation replaces the presence-absence data for a given species in a sample unit with a probability of occurrence (hereafter referred to as *synthetic abundance*) estimated on the basis of observed species co-occurrences in that sample unit, according to the formula given in Appendix C (section 4.10.3.3). Transformation was necessary in order to improve the stability of the solution in the ordination procedure (see below) because the Sørensen distances among sample units obtained from the presence-absence data produced two "populations" with little or no overlap (see Appendix C), leading to unstable solutions. Although the Beals transformation enhances the detection of the main compositional gradient (i.e., the pattern of joint occurrences) in heterogeneous and sparse community matrices, it does so at the expense of weaker patterns (McCune, 1994; Ewald, 2002). By filtering out the noise from the signal, the procedure sacrifices the use of inferential statistics, and therefore, the results of the ordination can only be used for descriptive purposes.

The Beals-transformed seasonal matrices were combined into a single 904 × 9 matrix, and a distance matrix was computed from this array of synthetic

abundances using the Sørensen distance. Community ordination of the distance matrix was sought through nonmetric multidimensional scaling (NMS) (Legendre and Legendre, 1998; McCune and Grace, 2002). Details of the setup and the intermediate steps of the analysis are provided in Appendix C (section 4.10.3.4).

For assessment of the relationship between the ordination axes and the environmental variables, values were extracted from the 0.25-degree gridded environmental data sets for grid cells with valid data in the corresponding species matrices (see section 4.3.2). The extracted environmental/spatial data were re-arranged into a matrix with sample units in the rows and variables (Z20, ZTD, MBVF, ZMBVF, ZOML, ZOD, SST, LCHL, and RAD) in the columns for each season. A principal component analysis was performed on the variables describing direct effects of physical forcing on the system (i.e., Z20, ZTD, MBVF, ZMBVF, ZOML, ZOD, SST) as a data reduction strategy, but also to eliminate the multicollinearity and improve the normality of these variables (see Appendix B for a description of the principal components). The resulting matrix containing the scores of the first three principal components (PC1, PC2, and PC3), was combined with LCHL and RAD. This 904 × 5 matrix contained the "external" variables of interest (environmental and spatial descriptors). Relationships between the external variables and the solution of the NMS ordination were established through rotation, overlays, correlations, and biplots (McCune and Grace, 2002).

4.4 RESULTS

4.4.1 Distribution

The predominant cetacean community was composed of seven small and medium-sized delphinids (*S. attenuata*, *S. longirostris*, *S. coeruleoalba*, *D. delphis*, *T. truncatus*, *G. griseus*, and *G. macrorhynchus*), the sperm whale (*P. macrocephalus*), and the Bryde's whale (*B. edeni*). The quarterly number of sightings for these nine species combined is shown in Figure 4.1. Maps with

sighting locations for each species are shown in Figure 4.2. These maps indicate clear differences in distribution within the study area. Two species were found along the northern and southern margins (*S. attenuata* and *S. longirostris*), three species had scattered distributions (although with some clustering near the islands) (*S. coeruleoalba*, *G. macrorhynchus*, and *P. macrocephalus*), and the remaining four species were primarily concentrated near the islands (*D. delphis*, *T. truncatus*, *G. griseus*, and *B. edeni*), especially around the western islands of Isabela and Fernandina.

4.4.2 Classification

MRPP supported the statistical significance of the three-group partition obtained with cluster analysis for all seasons (p-value < 0.0001) (Table 4.1). The hierarchical structure of the groups is shown in the dendrograms in Figure 4.3. The number in bold type inside each box indicates the number of sample units for that group. Also listed is the species assemblage characteristic of each group from the indicator species analysis, along with the indicator value (i.e., the percentage of perfect indication) for each species, in parenthesis. The spatial distribution of the groups is shown in Figure 4.4.

At this level of partition, within-group homogeneity (quantified by the agreement statistic A in Table 4.1), was fairly high for all seasons (A range: 0.38–0.46). Average within-group Sørensen distances were generally low for groups 1 and 2, and higher for group 3 (Table 4.1). These differences were directly related to the number of species characteristic of that group, as described below. Group sizes were varied, with groups 1 and 3 having the largest number of sample units in all seasons except JAS (Fig. 4.3). The branching in the dendrograms indicated that group 2 was more similar to group 3 in JFM and JAS, and more similar to group 1 in AMJ and OND.

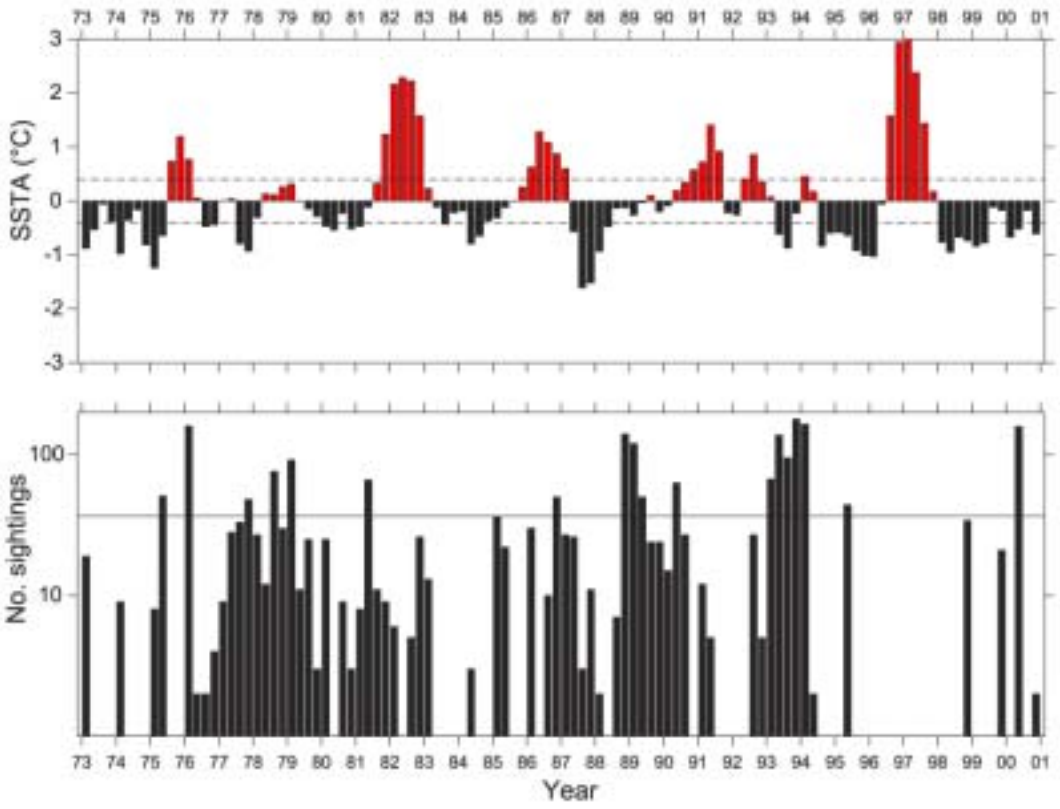

Figure 4.1: Time series for the period 1973–2000. Top: quarterly-averaged SST anomaly (SSTA) from the 5-month running mean of the CDRS monthly record (see p. 123). Bottom: quarterly number of sightings (in log scale) for the nine species of interest. The horizontal line indicates the average (36.5). Blank spaces are times during which no sightings were made.

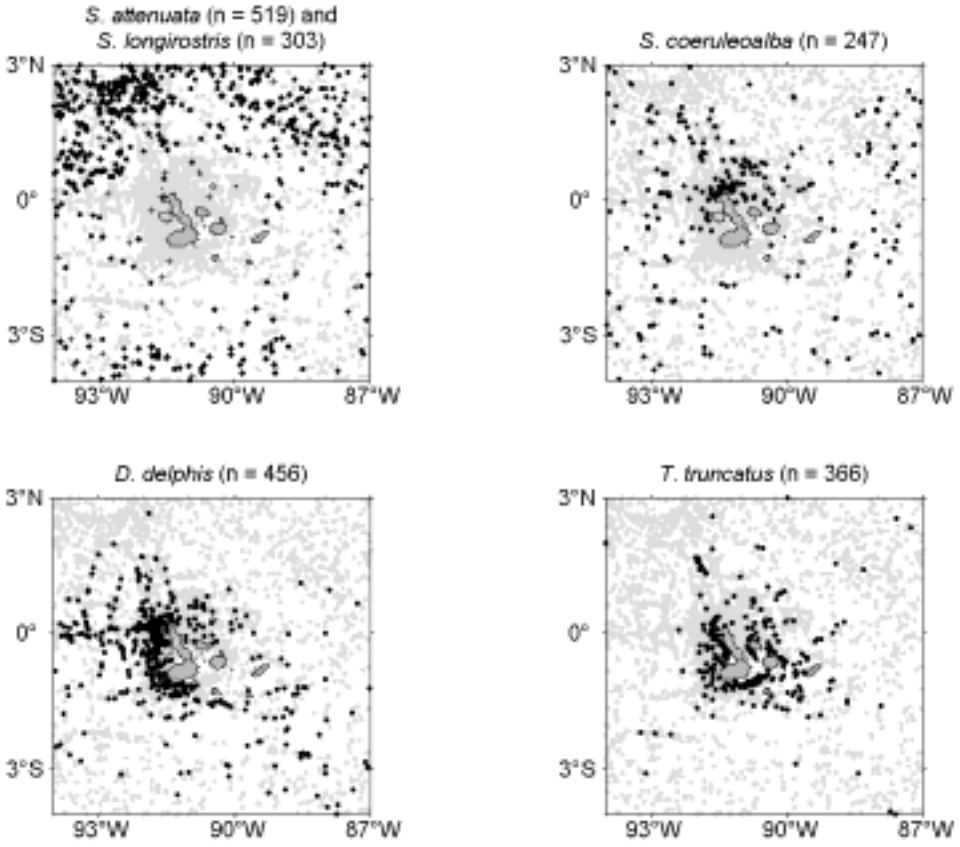

Figure 4.2: Cumulative sighting locations for *S. attenuata*, *S. longirostris* (plus symbols), *S. coeruleoalba*, *D. delphis*, and *T. truncatus*, for the period 1973–2000. Gray dots are the locations of all marine mammal sightings (identified and unidentified) in the study area (n = 4817).

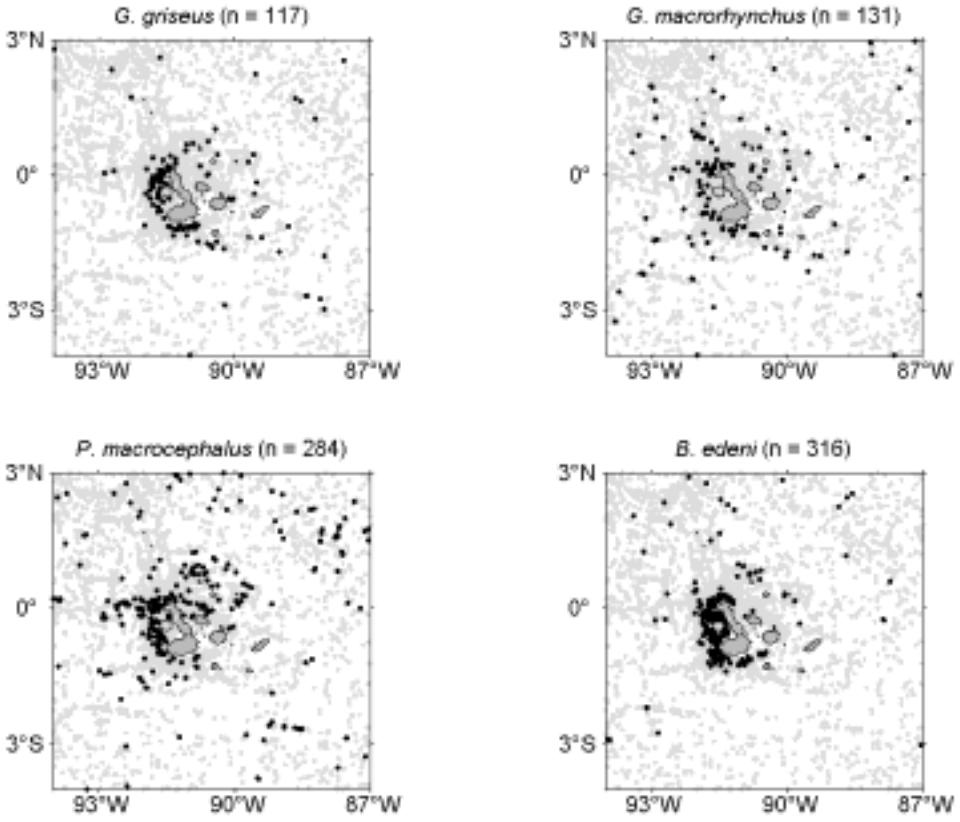

Figure 4.2: Continued. Cumulative sighting locations for *G. griseus*, *G. macrorhynchus*, *P. macrocephalus*, and *B. edeni*, for the period 1973–2000. Gray dots are the locations of all marine mammal sightings (identified and unidentified) in the study area (n = 4817).

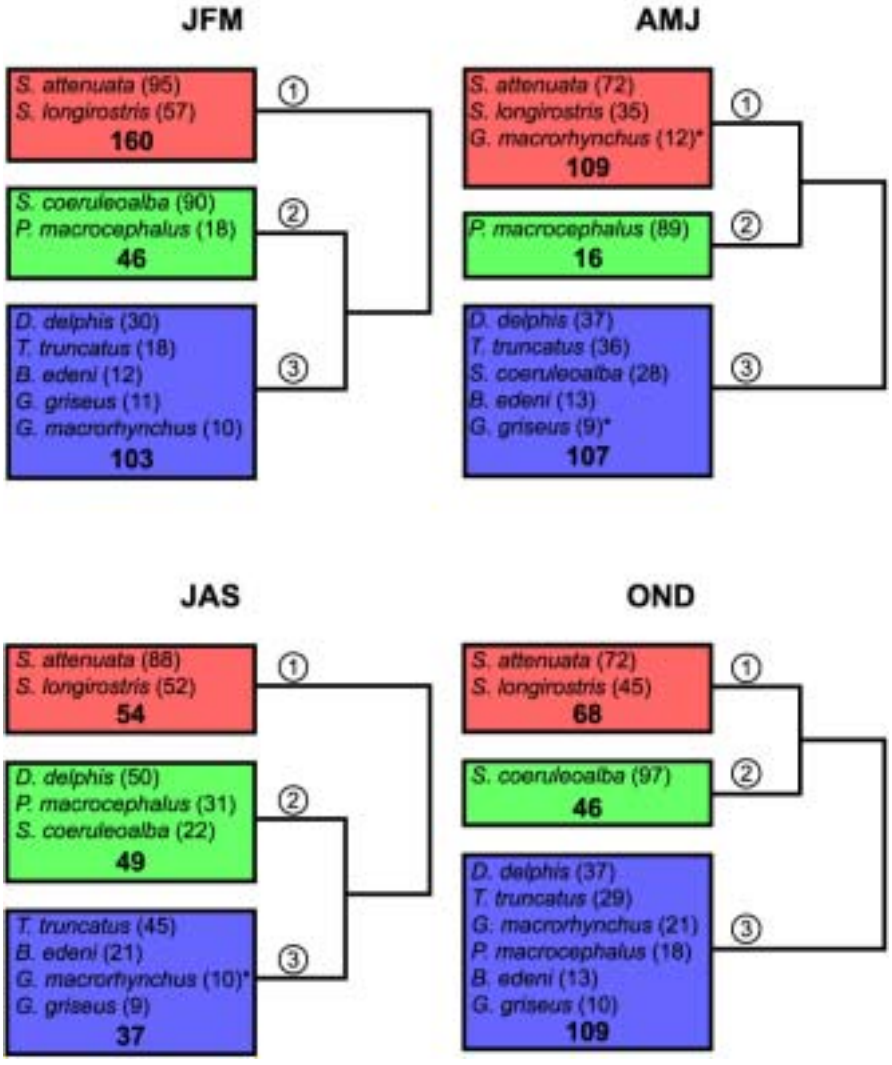

Figure 4.3: Schematic dendrograms of the three major groups of sample units extracted with cluster analysis for each season. The number of sample units within each group is shown in bold type. The species assemblage characteristic of each group from the indicator species analysis is listed, along with the indicator value for each species (in parenthesis). An asterisk next to a species name indicates that the indicator value for that species was statistically non-significant according to the Monte Carlo test.

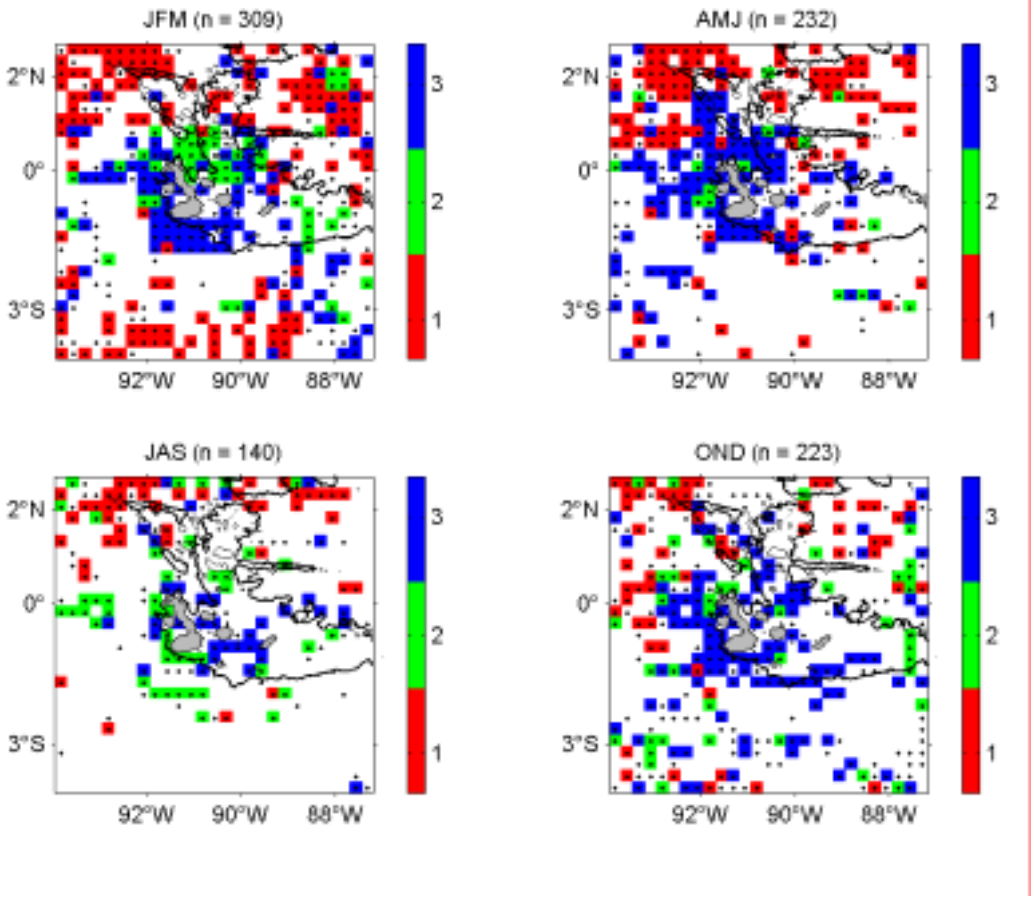

Figure 4.4: Spatial distribution of the three groups of sample units identified through cluster analysis for each season. The 2000-m depth contour is indicated. Black dots represent grid cells with with marine mammal sightings (including rare and unidentified species). The number of sample units (i.e., valid grid cells) is shown in parenthesis.

Table 4.1: Average within-group distance, chance-corrected within-group agreement (*A*), and *p*-value from MRPP analyses on the seasonal rank-transformed distance matrices. The number of sample units in each group is given in parenthesis.

	Average within-group distance			
Group	JFM	AMJ	JAS	OND
1	0.14 (160)	0.24 (109)	0.12 (54)	0.11 (68)
2	0.18 (46)	0.10 (16)	0.38 (49)	0.10 (46)
3	0.44 (103)	0.36 (107)	0.36 (37)	0.41 (109)
A	0.46	0.38	0.41	0.45
p	< 0.0001	< 0.0001	< 0.0001	< 0.0001

In terms of species composition (Fig. 4.3), group 1 was characterized by the presence of *S. attenuata* and *S. longirostris* in all seasons. *Stenella attenuata* had the highest indicator value (72–95%) for this group. *Globicephala macrorhynchus* was also included with group 1 in AMJ, but its indicator value was not significant (*p*-value = 0.173). The relatively small group 2 was characterized by one to three species, depending on season. *Stenella coeruleoalba* was the predominant indicator species for this group in JFM (90%) and OND (97%), although it was also present in JAS. *Physeter macrocephalus* was present in JFM, AMJ, and JAS, and it was the only species in the group in AMJ. *Delphinus delphis* was the most characteristic species of group 2 in JAS (50%). The assemblage typical of Group 3 included four

to six species. *Delphinus delphis* had the highest indicator value (30–37%) for this group in all seasons except for JAS, when it associated with group 2, as mentioned above. *Tursiops truncatus* had the second highest indicator values in JFM, AMJ, and OND (18–36%), and it was the characteristic species of group 3 in JAS (45%). Other species characteristic of this group in most seasons included *B. edeni*, *G. griseus*, and *G. macrorhynchus*.

The sample units in each group tended to occupy distinct zones. Group 1 occupied the offshore waters along the northern and to some extent southern sectors of the study area, especially in JFM (Fig. 4.4). Group 3 was associated with the periphery of the archipelago in JFM, AMJ, and OND, particularly with its western sector. During JAS, group 3 occupied the shallow central waters. The comparatively few sample units that made up group 2 were concentrated between northern Isabela, Santiago, Marchena, Pinta and Genovesa islands in JFM. During JAS, group 2 occupied the western and southern periphery of the archipelago. No clear pattern was evident in AMJ and OND, as sample units for this group were scattered throughout the study area.

4.4.3 Ordination

The two-dimensional solution obtained with the NMS procedure was rotated by 231° to maximize the loading of RAD onto the main axis of the ordination. The intent was to account for the spatial component in cetacean distributions associated with the presence of the archipelago, while removing the variation associated with this variable in the second axis. After rotation, the first axis captured 86% of the variance in the species data, while the second axis represented 4.2%, for a total of 90.2%. The arrangement of sample units, environmental variables, and average species locations in the ordination space is shown in Figure 4.5. Maps depicting the spatial distribution of sample unit scores

on axis 1 and axis 2 for each season are shown in Figure 4.6 and Figure 4.7, respectively.

The results of the principal component analysis on the environmental variables describing direct effects of physical forcing on the system are given in Table 4.2. The dominant component, PC1, was characterized by a deep (shallow) thermocline (Z20) and pycnocline (ZMBVF), a strong (weak) thermocline (ZTD), a high (low) pycnocline stability (MBVF), a shallow (deep) and thick (thin) OML (ZOML and ZOD, respectively), and warm (cold) SST. These conditions describe the main environmental gradient in the study area, from warm, stratified conditions offshore, to cold, upwelling conditions close to the islands. Since the second and third components had negligible correlations with the ordination axes (see below), they are not described here. The interested reader is referred to Appendix B.

After rotation, the point cloud was primarily aligned with axis 1 (Fig. 4.5). Scatter about axis 2 was greater on the negative side of axis 1, while there was very little scatter on the positive side. Average species scores were located on the negative side of axis 1 for seven species (*S. coeruleoalba*, *P. macrocephalus*, *G. macrorhynchus*, *B. edeni*, *D. delphis*, *G. griseus*, and *T. truncatus*), and on the positive side for two (*S. attenuata* and *S. longirostris*) (Fig. 4.5). On axis 2, the average scores were near zero for all species.

The spatial distribution of the ordination scores on axis 1 (Fig. 4.6) shows that the negative scores were found around the periphery of the archipelago in all seasons, whereas the positive scores were primarily associated with the northern sector of the study area (and also with the southern sector in JFM). Relatively few sample units had intermediate values. Scores were most negative in JAS and most positive in OND. Scores on axis 2 followed a cycle with negative values becoming more negative and positive values becoming more positive as the year progressed

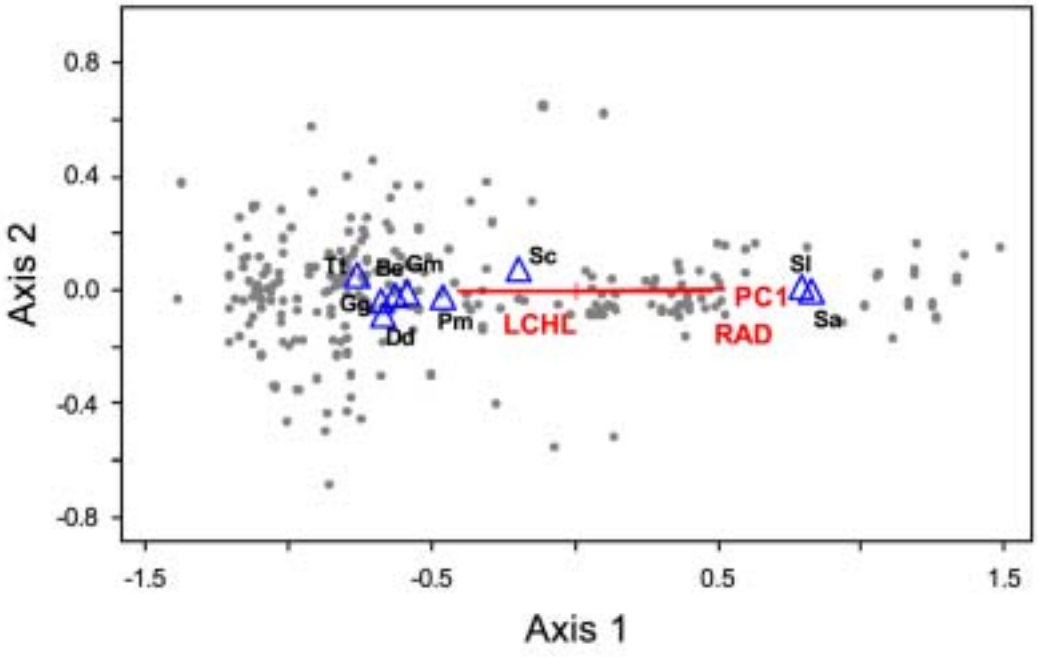

Figure 4.5: Biplot of NMS ordination (after 231° rotation). Gray dots represent sample units and open triangles are the average positions of the nine species of interest, calculated by weighted averaging. Vectors for environmental variables with $r^2 < 0.2$ in respect to both axes are not shown.

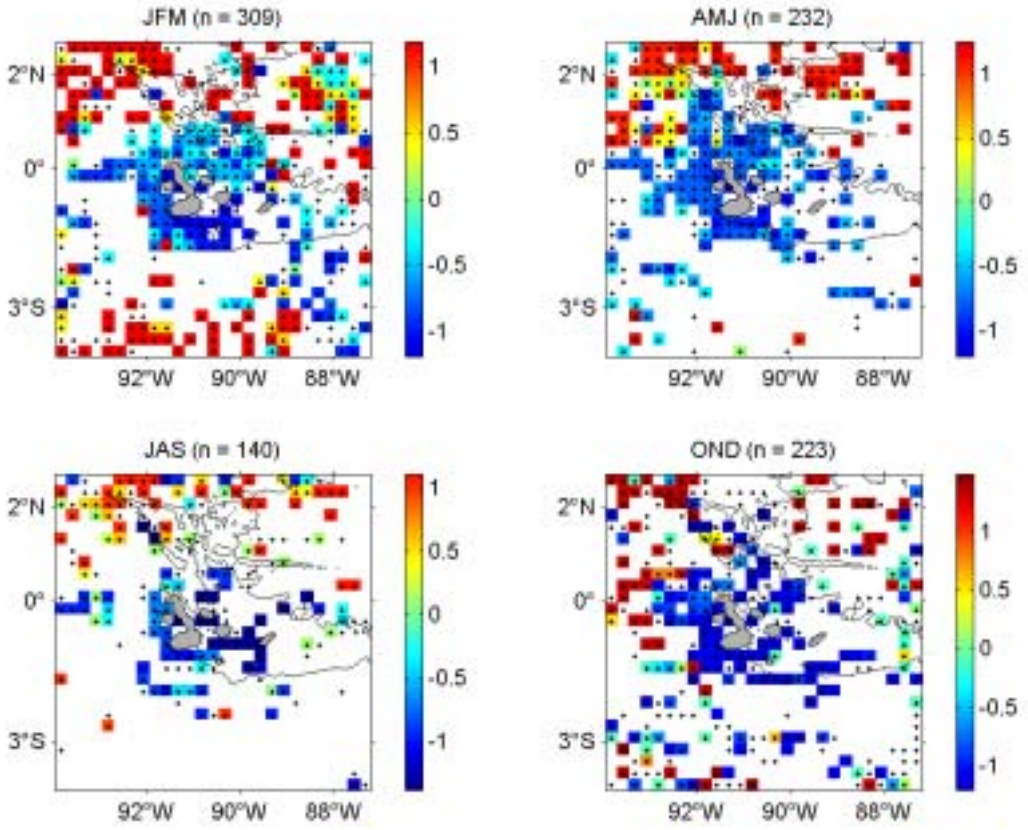

Figure 4.6: Spatial distribution of NMS scores on axis 1 (after 231° rotation) for each season. The 2000-m depth contour is indicated. Black dots represent grid cells with marine mammal sightings (including rare and unidentified species). The total number of sample units (i.e., valid grid cells) is shown in parenthesis.

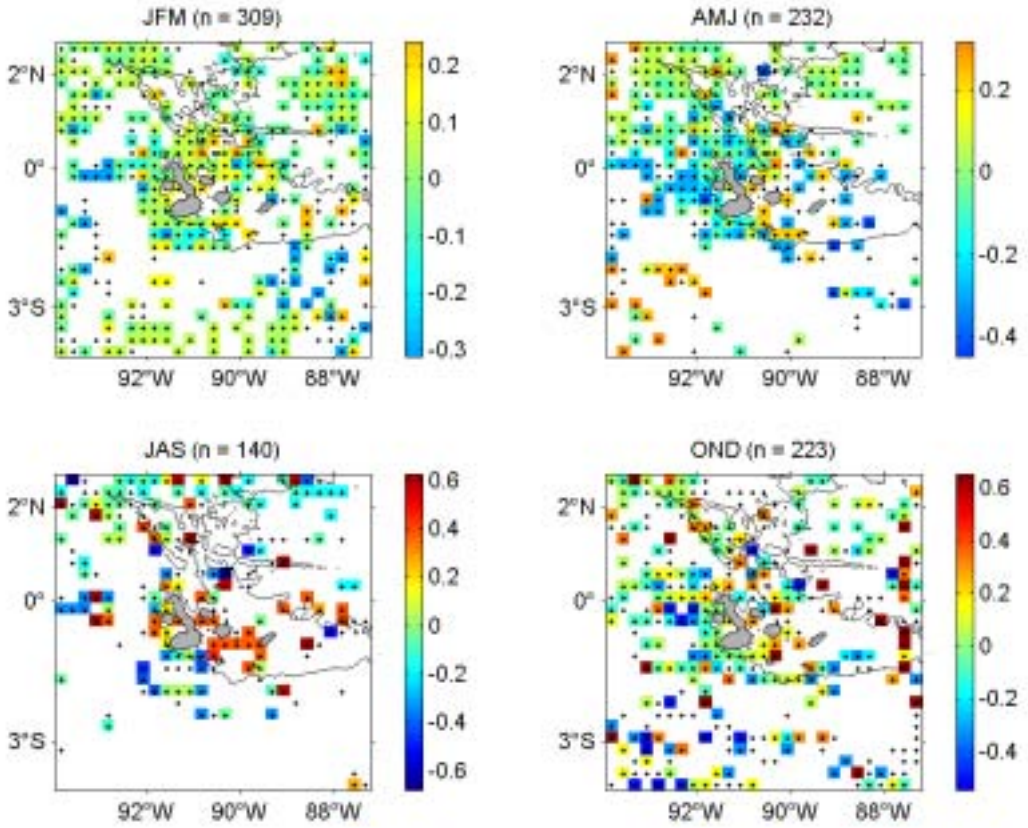

Figure 4.7: Spatial distribution of NMS scores on axis 2 (after 231° rotation) for each season. The 2000-m depth contour is indicated. Black dots represent grid cells with marine mammal sightings (including rare and unidentified species). The total number of sample units (i.e., valid grid cells) is shown in parenthesis.

Table 4.2: Loadings (eigenvectors) for the first three principal components (PC) of the seven variables describing direct effects of physical forcing in the water column and at the surface. Values greater than 0.3 are shown in bold to highlight the variables with the greatest contribution to each PC. The eigenvalues and the fraction of the variance represented by each PC are also indicated.

Variable	PC1	PC2	PC3
Z20	**-0.47**	0.07	**-0.31**
ZTD	**0.30**	**0.52**	0.20
MBVF	**-0.34**	**0.49**	0.15
ZMBVF	**-0.35**	**-0.51**	-0.24
ZOML	0.27	0.08	**-0.81**
ZOD	**-0.45**	-0.07	**0.35**
SST	**-0.42**	**0.45**	0.10
Eigenvalue	3.4	1.4	1.0
Variance fraction (%)	48.4	19.7	14.7

from JFM to JAS, and then returning in OND (Fig. 4.7). In JAS, spatially cohesive positive-negative contrasts were apparent between sample units in the central shallow waters and those to the north, south, and west. Contrasts between sample units were also evident in OND, but they were scattered and did not have a clear pattern.

Correlation coefficients (r) between scores on the ordination axes and synthetic abundances for each species are given in Table 4.3. Most species showed intermediate to high correlations with the first axis ($0.773 \leq |r| \leq 0.978$), with only two species (*S. coeruleoalba* and *P. macrocephalus*) showing a low degree of linear correlation ($|r| < 0.5$). Correlations with the second axis were moderate for

three species, *D. delphis* (r = -0.4), *S. coeruleoalba* (r = 0.35), and *T. truncatus* (r = 0.2), and they were low or neglible for the other six (Table 4.3).

Table 4.3: Pearson (r) and Kendall (tau) correlations of synthetic abundances with ordination axes (after 231° rotation) for the nine species of interest.

Axis	1			2		
	r	r^2	tau	r	r^2	tau
Stenella attenuata	0.978	0.957	0.778	-0.009	0.000	-0.011
Stenella longirostris	0.937	0.878	0.777	0.060	0.004	0.154
Stenella coeruleoalba	-0.221	0.049	-0.207	0.349	0.121	0.047
Delphinus delphis	-0.773	0.597	-0.644	-0.401	0.161	-0.206
Tursiops truncatus	-0.743	0.551	-0.686	0.210	0.044	0.070
Grampus griseus	-0.614	0.377	-0.570	-0.137	0.019	-0.036
Globicephala macrorhynchus	-0.536	0.287	-0.647	-0.028	0.001	-0.075
Physeter macrocephalus	-0.483	0.233	-0.452	-0.083	0.007	-0.052
Balaenoptera edeni	-0.588	0.346	-0.649	-0.041	0.002	-0.060

The synthetic abundances corresponding to each sample unit for each species are shown in the ordination space in Figure 4.8 as dots of different sizes. A few sample units with *scores* higher (lower) than ± 0.5 on axis 2 (which are beyond ± 2 standard deviations and are probably outliers to the ordination) stand out as having large abundances for only two species: *S. coeruleoalba* and *P. macrocephalus* (Fig. 4.8). The scatterplots on the sides of the main ordination space show the abundance along axis 1 and axis 2 separately. The fitted curves highlight the species responses to the compositional gradients (and, for most species, demonstrate the limitations of using the correlation coefficient for this purpose). The responses on axis 1 were linear with maximum abundance at the negative end of the gradient for *T. truncatus* and *G. griseus*. For *S. attenuata* and *S. longirostris* the response had a linear trend with abundance increasing toward the positive end, but with distinct humps along the gradient. *Globicephala macrorhynchus* and *B. edeni* showed a similar response, but with abundance increasing toward the negative side. Species that showed unimodal or more complex responses with maxima at intermediate locations along the gradient were *S. coeruleoalba*, *D. delphis*, and *P. macrocephalus*. On axis 2, both *S. attenuata* and *S. longirostris* had a unimodal response with maximum abundance at the middle of the gradient. *Delphinus delphis* and *T. truncatus* also showed distinct unimodal responses, but their maxima were on opposite sides of the axis. The response curve of *G. griseus* was rather flat and broad, while *G. macrorhynchus* and *B. edeni* had bimodal responses with minima near the middle of the gradient. Finally, the response curves for *S. coeruleoalba* and *P. macrocephalus* appeared to be driven by the outliers (to the ordination) at both ends of the gradient, and otherwise would have been unimodal with peaks near the middle (Fig. 4.8).

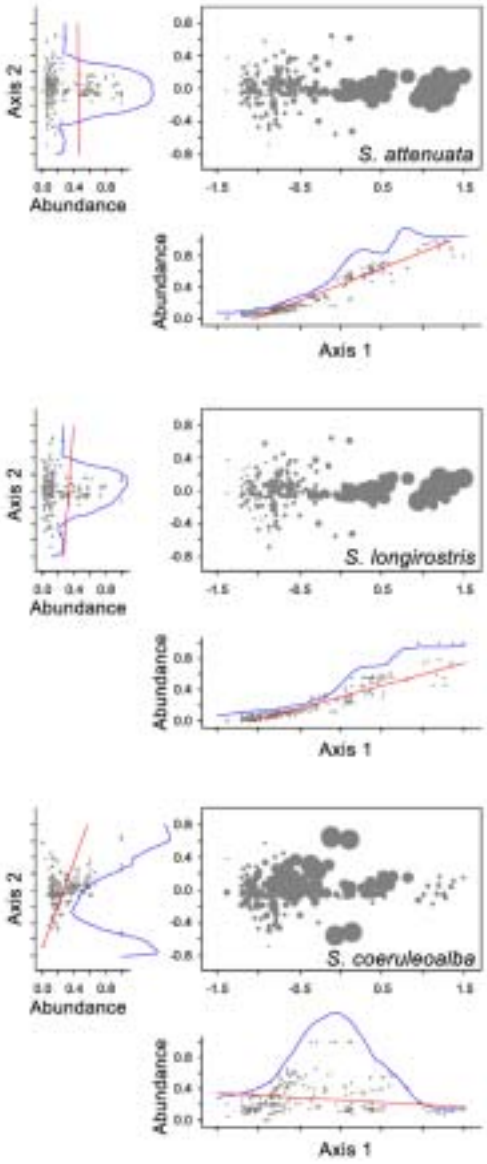

Figure 4.8: Synthetic abundance for *S.attenuata*, *S. longirostris*, and *S. coeruleoalba* overlaid on ordination. Size of dots is proportional to the abundance of the species. Side scatterplots show abundance *vs*. scores for axis 1 (below) and axis 2 (left). Blue curve is an envelope that includes points falling within two standard deviations of a running mean along the axis. Red line is the least-squares fit.

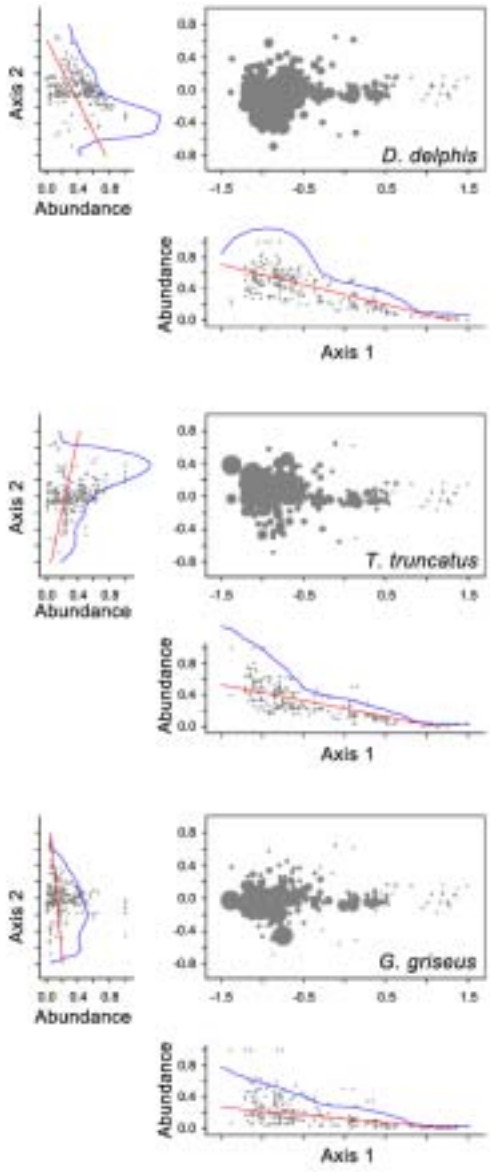

Figure 4.8: Continued. Synthetic abundance for *D. delphis*, *T. truncatus*, and *G. griseus* overlaid on ordination. Size of dots is proportional to the abundance of the species. Side scatterplots show abundance *vs*. scores for axis 1 (below) and axis 2 (left). Blue curve is an envelope that includes points falling within two standard deviations of a running mean along the axis. Red line is the least-squares fit.

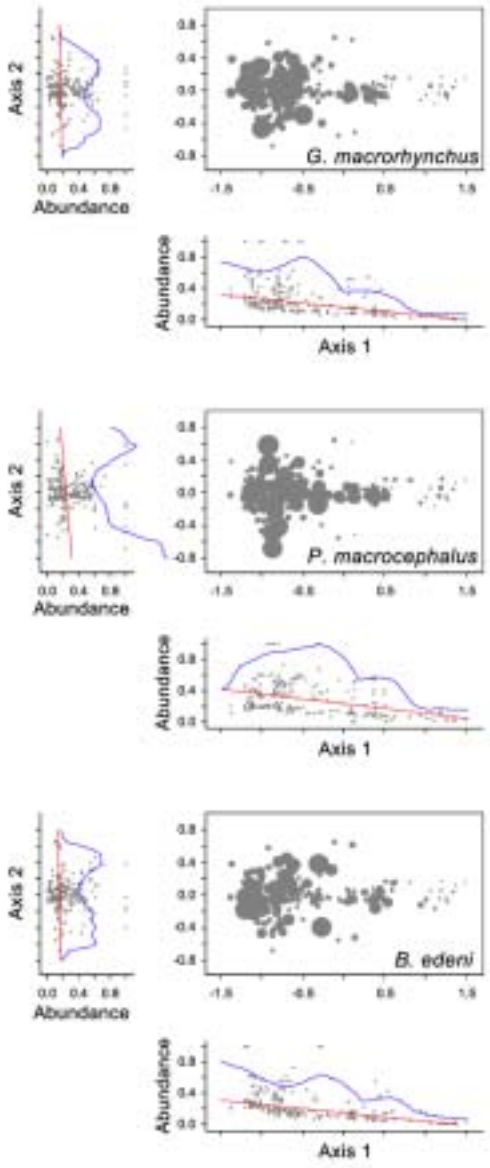

Figure 4.8: Continued. Synthetic abundance for *G. macrorhynchus*, *P. macrocephalus*, and *B. edeni* overlaid on ordination. Size of dots is proportional to the abundance of the species. Side scatterplots show abundance *vs*. scores for axis 1 (below) and axis 2 (left). Blue curve is an envelope that includes points falling within two standard deviations of a running mean along the axis. Red line is the least-squares fit.

Correlations among environmental variables and with each axis are listed in Table 4.4. Three of the five variables, LCHL, RAD, and PC1, had intermediate correlations with the scores on axis 1 (r = -0.52, 0.56, and 0.59, respectively). The percentage of the variance in axis 1 explained by these variables (i.e., the square of the correlation coefficient) ranged between 27.4 and 34.2%. PC2 and PC3 had negligible correlations with this axis 1, and all five variables had negligible correlations with axis 2. These correlations are evident in the biplot in Figure 4.5, which shows that the three environmental vectors (not just RAD) were almost completely aligned with axis 1 after the rotation. A fairly high degree of collinearity was evident among the dominant environmental variables (r = -0.78 for LCHL *vs*. PC1; r = -0.69 for LCHL *vs*. RAD; and r = 0.73 for PC1 *vs*. RAD) (Table 4.4).

Table 4.4: Pearson correlations among environmental variables and ordination axes (after 231° rotation).

	PC1	PC2	PC3	LCHL	RAD	Axis 1	Axis 2
PC1	1.00						
PC2	0.00	1.00					
PC3	0.00	0.00	1.00				
LCHL	-0.78	0.11	0.01	1.00			
RAD	0.73	-0.09	0.23	-0.69	1.00		
Axis 1	0.59	0.04	0.08	-0.52	0.56	1.00	
Axis 2	0.06	0.01	0.07	-0.03	-0.02	0.04	1.00

4.5 DISCUSSION

4.5.1 Sample unit groups and species assembalges as indicators of community types and habitat preferences

Although the groups extracted with cluster analysis had a number of similarities across seasons, direct comparisons are limited because the sample units that entered the analysis were different for each season (only 54 sample units were common to all four seasons). In particular, it is not possible to determine whether the observed seasonal differences in group size or in species composition are related to shifts in habitat use or community structure, or if they are due to differences in sampling effort. Nevertheless, it is possible to draw several generalizations about these groups and the species assemblages that were associated with them.

Groups 1 and 3 were fairly persistent in terms of size, distribution, and species composition. Group 1 occupied the warm, stratified habitat found north of the EF and was characterized by *S. attenutata* and *S. longirostris* (this group also occupied the seasonally warm waters along the southern sector of the study area in JFM). Group 3 occupied the periphery of the archipelago, particularly the western sector where the EUC upwells. The species assemblage associated with this group was characterized by *D. delphis*, which typifies upwelling-modified habitats (see Introduction), but it also included species that associate with nearshore habitats (*T. truncatus*, *B. edeni*, *G. griseus*, and *G. macrorhynchus*).

The comparatively fewer sample units that made up group 2 make it difficult draw ecological interpretations. Sample units were scattered throughout the study area in all seasons except JFM, when a discrete cluster occupied an area between northern Isabela, Santiago, Marchena, Pinta and Genovesa islands. This group was consistently characterized by *S. coeruleoalba* and/or *P. macrocephalus*. Even though the group did not occur in a habitat of known characteristics, the persistence of the indicator species suggests that the sample units meet specific

requirements or that the species composition is the result of interactions with the species in the other groups.

Other studies in the eastern tropical Pacific have remarked on the apparent lack of a preference for particular oceanographic conditions by *S. coeruleoalba*. The species tends to occur wherever *S. attenuata*, *S. longirostris*, and *D. delphis* are least abundant (Au and Perryman, 1985; Reilly, 1990; Reilly and Fiedler, 1994), implying some sort of segregation. There is further evidence that niche partitioning takes place between *S. coeruleoalba* and *D. delphis* in the Mediterranean and the northeast Atlantic, where *S. coeruleoalba* is a highly opportunistic feeder, taking cephalopods, crustaceans, and mesopelagic fishes, whereas *D. delphis* appears to be somewhat more piscivorous (Hassani et al., 1997; Sagarminaga and Cañadas, 1998; Das et al., 2000). It is also interesting to observe that *P. macrocephalus* tended to occur with *S. coeruleoalba* (or in its own group in AMJ). The scattered distribution of *S. coeruleoalba* and *P. macrocephalus* appears to occur throughout the eastern tropical Pacific (Polacheck, 1987), but has not been adequately explained because of the lack of consistent association with other species or with particular environmental conditions.

4.5.2 Community gradients in relation to environmental conditions

The maps of the ordination scores on axis 1 contrasted sample units clustered around the periphery of the archipelago with those found offshore, with little or no transition in between them. This suggests strong ecological differences among the two areas. Species abundances along axis 1 showed a clear compositional gradient, with *S. attenuata* and *S. longirostris* reaching their maximum abundance at the positive end; *S. coeruleoalba*, *P. macrocephalus* and *D. delphis* at intermediate locations; and *G. macrorhynchus*, *G. griseus*, and *B. edeni* at the negative end of the gradient (Fig. 4.8). This pattern represented 86% of the variance in the species data.

Rotation of the axes maximized the correlation of axis 1 with all three of the environmental variables which had any relationship with the ordination (PC1, LCHL, and RAD). These variables, which together describe a gradient from warm/ stratified/phytoplankton-poor conditions offshore to cold/upwelling/phytoplankton-rich conditions close to the islands, explained 27–35% of the variance contained in the compositional gradient on axis 1. Thus, the variety of environmental conditions found inside the study area appear to be responsible for the presence of communities of stratified, upwelling, and coastal habitats in close proximity to each other. In fact, the patterns of species abundance around the Galápagos mirror the response of eastern tropical Pacific cetaceans to large-scale thermocline topography and distance from land (e.g., Polacheck, 1987; Reilly, 1990; Fiedler and Reilly, 1994).

Although direct comparisons across seasons are limited because the sample units were not necessarily in the same locations, seasonal information was taken into account in the calculation of the ordination scores, as all 904 sample units were ranked and arranged together by the NMS procedure. The main observation is the shift toward more negative scores during JAS on axis 1 (Fig. 4.6), which implies that sample units become more favorable for those species whose abundance peaks in the negative region of the gradient (see Fig. 4.8). Thus, the shift is consistent with a community response to the expansion of the upwelling-modified habitat resulting from the intensification of wind-induced equatorial upwelling at this time of the year (see Chapter 3 and Appendix B).

Variability on axis 2 was most pronounced during JAS (Fig. 4.7). Comparison with the map showing the distribution of groups from cluster analysis for the same period (Fig. 4.4) indicates that most of the sample units with positive scores in the central shallow waters correspond with those in group 3, while several sample units with negative scores to the south, north, and west appear to correspond with those in group 2. These two groups were characterized by species

assemblages of nearshore and upwelling environments, respectively (see section 4.4.2). The response curves along axis 2 for the species with highest indicator value in these groups, *D. delphis* and *T. truncatus*, respectively (Fig. 4.8), show that their abundances peak at opposite sides of the gradient. Thus, axis 2 may suggest a separation between nearshore and upwelling-associated species, at least during JAS. Variability was also pronounced during OND, but the sample units were not organized in a recognizable pattern (Fig. 4.7). It should be stressed, however, that any interpretation of this axis is speculative, as it only described 4.2% of the variance in the species data (any pattern may have been weakened by the Beals transformation). Axis 2 was unrelated to environmental variability.

Because the compositional gradient along axis 1 appeared to be primarily driven by environmental conditions, it is possible to speculate on what would be the community response to strong El Niño-Southern Oscillation (ENSO) conditions. During El Niño events, conditions would be most similar (but more extreme) to those taking place at the peak of the warm season (March), when upwelling conditions are spatially restricted to the core of the topographic upwelling of the EUC, while stratified conditions are widespread. Thus, the environmental gradient would contract on the negative side and expand on the positive side. With the shrinking of favorable conditions for upwelling-adapted species, competition for space (i.e., food resources) in the vicinity of the islands would increase. Conversely, during La Niña, upwelling conditions are widespread while the stratified habitat shrinks. As discussed above for the changes observed during JAS, the upwelling-adapted species would expand their range with the expansion of the upwelling environment, while *S. attenuata* and *S. longirostris* would probably retreat to the north with the receding stratified waters. This picture is consistent with the regional responses described by Fiedler and Reilly (1994) to observed El Niño and La Niña events.

4.5.3 Implications for feeding ecology

Cluster and indicator species analysis demonstrated that most of the species in the study occupy distinct habitats that are persistent year-round (albeit with some degree of seasonal adjustment). Ordination further suggested strong ecological differences between waters around the periphery of the archipelago and those offshore. What is the basis for these differences? Addressing this question involves considering the way in which the species of interest use their habitats, particularly in regard to foraging strategies. Although the food and feeding habits of Galápagos cetaceans are largely unknown (with the exception of the sperm whale), insight can be gained from information available at the regional and global scale.

Stenella attenuata and *S. longirostris*, the two species that characterized the stratified environment, are known to feed mainly on mesopelagic organisms of the deep scattering layer at dawn and dusk, when they concentrate closer to the surface during their diel vertical migration (Perrin and Gilpatrick, 1994; Robertson and Chivers, 1997). The diet of *S. attenuata* is mainly composed of lanternfishes (family Myctophidae), enope squid (family Enoploteuthidae), and flying squid (family Ommastrephidae) (Roberston and Chivers, 1997). *Stenella longirostris* has a similar diet, but the size of the prey items and their depth distribution may be different (Perrin and Gilpatrick, 1994). These two dolphins are regularly found in polyspecific assemblages that include yellowfin tuna (*Thunnus albacares*), seabirds, and sharks (Au and Perryman, 1985; Au, 1991). As mentioned earlier, *S. coeruleoalba* is a highly opportunistic feeder, taking cephalopods (families Ommastrephidae and Histioteuthidae), crustaceans, and myctophids. It has been suggested that striped dolphins feed at great depths (200–700 m), on the basis of the luminescent organs often found on their prey (Perrin et al., 1994). The diet of *D. delphis*, the characteristic species of the upwelling environment, is primarily composed of epipelagic shoaling fishes (families Clupeidae and Engraulidae),

although it may also take cephalopods, myctophids, and bathylagids of the deep scattering layer (Evans, 1994; Young and Cockroft, 1994).

Grampus griseus, *G. macrorhynchus*, and *P. macrocephalus* feed primarily on cephalopods. However, *G. macrorhynchus* is also known to take fish (Bernard and Reilly, 1999), while *G. griseus* occasionally feeds on crustaceans (Kruse, 1999). Both species are presumed to be nocturnal feeders, and in the Galápagos they are regularly found in areas of steep slopes (although *G. macrorhynchus* appears to prefer deeper water). The diet of *P. macrocephalus* in Galápagos waters is primarily composed of histioteuthid squid (Smith and Whitehead, 2000). Animals typically forage at depths of 320–420 m (Papastavrou et al., 1989), both during daytime and nighttime (Smith and Whitehead, 1993). *Balaenoptera edeni* feeds on shoaling prey such as clupeids, engraulids, and euphausiids (Cummings, 1985), while *T. truncatus*, the most coastal species in this study, feeds on a wide variety of fishes and invertebrates, including demersal forms (Wells and Scott, 1999).

This information, together with knowledge of the local environmental conditions and other biological observations, can be of use in forming a general picture of trophic ecology in the different habitats indentified in this study. The warm, stratified habitat found along the northern sector of the study area (and seasonally along the south sector) overlays a thick and shallow OML. A distinct euphausiid assemblage (*Euphausia distinguenda*, *E. diomedeae*, *E. lamelligera*, *E. tenera*, and *Nematoscelis gracilis*) adapted to the oxygen-deficient conditions thrives in this habitat (Brinton, 1979). This assemblage is the dominant crustacean component of the deep scattering layer, while mesopelagic fishes (primarily myctophids) and cephalopods are the dominant nekton (e.g., Blackburn, 1968; Blackburn et al., 1970). Through trophic links among these groups, the deep scattering layer is believed to support the large populations of top predators like

yellowfin tuna (McGowan, 1971) and dolphins (Au and Perryman, 1985; Fiedler et al., 1998) found in this environment.

The upwelling habitat on the western side of the archipelago is created by the surfacing of the EUC. The waters of the EUC are well oxygenated (Anderson, 1977; Lukas, 1986), and are characterized by a different euphausiid assemblage (*E. eximia*, *E. paragibba*, and *Nyctiphanes simplex*) (Cornejo de González, 1977; Brinton, 1979). Observations of potential prey for cetaceans in this area include myctophids (*Myctophum nitidulum*), nail squid (*Onychoteuthis banksii*) (Palacios, 1999b), and Panamá lightfish (*Vinciguerria lucetia*) (García et al., 1993) among the mesopelagic organisms, and South American pilchard (*Sardinops sagax*), Pacific anchoveta (*Cetengraulis mysticetus*), and round herring (*Etrumeus teres*) (García et al., 1993; Grove and Lavenberg, 1997), among the epipelagic schooling fishes. The stomach contents of a Cuvier's beaked whale (*Ziphius cavirostris*), a deep-diving species collected in the upwelling habitat, contained beaks of several mesopelagic squid species (*Mastigoteuthys dentata*, *Histioteuthys heteropsis*, *Megalocranchia* sp., *Cranchia scabra*, *Ommastrephes bartrami*, *Liocranchia reinhardti*, and *Philidoteuthis* sp.), and the mesopelagic crustaceans *Gnathophausia ingens* and *Acanthephyra* sp. (Palacios, 1999b). Whitehead et al. (1989) have suggested that the strong flow of the EUC may transport and concentrate the slow-swimming histioteuthid squid that are the main prey of sperm whales in this area. The large ommastrephid *Dosidicus gigas* has also been collected in these waters (Palacios, 2000). Thus, its possible that other teuthivorous cetaceans like *G. macrorhynchus* and *G. griseus* also feed on several of the species just mentioned. Another marine mammal that feeds in the upwelling environment is the Galápagos fur seal (*Arctocephalus galapagoensis*). Its diet is composed of vertically migrating myctophids and bathylagids among the fishes (Dellinger and Trillmich, 1999), and *O. banksii* and ommastrephids among the squids (Clarke and Trillmich, 1980). *Delphinus delphis* is occasionally seen in daytime foraging aggregations with

Nazca boobies (*Sula granti*) and hammerhead sharks (*Sphyrna* sp.) (D.M. Palacios, personal observations), and given its food habits elsewhere, it probably preys upon *S. sagax* and the other shoaling fishes mentioned above. Au and Perryman (1985) have suggested that a shorter food chain in upwelling environments may be the basis for cetacean community differences with respect to stratified environments.

The EUC also plays a role in the productivity of the nearshore environment through branching and recirculation in the central part of the archipelago (Houvenaghel, 1978; also see Chapter 1). Two of the species in this study, *T. truncatus* and *B. edeni*, as well as the Galápagos sea lion (*Zalophus wollebaeki*) commonly occur there. Feeding frenzies involving some or all of these species, coastal seabirds (*Sula nebouxii*, *Pelecanus occidentalis*), and sharks are a common sight in these waters (D.M. Palacios, personal observations). Given that *S. sagax* is known to be the primary prey of *Z. wollebaeki* (Dellinger and Trillmich, 1999) and of the blue-footed booby (*S. nebouxii*) (Anderson, 1989), it is possible that the predators are converging on dense schools of this fish. Other schooling fishes that occur in high abundance in coastal waters are the black-striped and the white salema (*Xenocis jessiae* and *Xenichthys agassizi*, respectively; family Haemulidae), and the yellow-tailed and the Galápagos mullet (*Mugil rammelsbergii* and *M. galapagensis*, respectively) (Grove and Lavenberg, 1997). Large surface swarms of the euphausiid *N. simplex* have also been observed at a variety of nearshore locations, where they could be prey for *B. edeni* and other baleen whales (cf. Palacios, 1999a).

4.6 CAVEATS

Each of the different sources of sightings used in this study (see Appendix A) has its own set of biases due to the different protocols and platforms used to collect them. Combining these disparate data sets has the potential of compounding

the biases in an unknown way. However, this was necessary in order to obtain adequate coverage of the different environments occurring around the Galápagos (see the maps of distribution of sightings by sources in Fig. A4.1). The combined data set provided an opportunity to look at general patterns of species-species and species-environment relationships at a resolution rarely achieved in studies of cetacean ecology.

Although this study focused on the seasonal timescale, it is necessary to mention the possible effects of interannual (i.e., ENSO) variability in the sighting data, considering that, in the study area, seasonal and interannual variability are of the same order of magnitude (Fiedler, 1992; Delcroix, 1993). A time series of quarterly-averaged SST anomaly (SSTA) is shown for the same period of the marine mammal compilation in Figure 4.1. [SSTAs were computed from a monthly SST record collected by the Charles Darwin Research Station (CDRS) in Galápagos for the period 1965–2001. Monthly SSTAs were normalized by the standard deviation of SST, and a 5-month running mean was applied, from which the quarterly average was derived.] The dashed lines in the plot indicate the ± 0.4°C threshold that has been used to define El Niño and La Niña events in the study area (Trenberth, 1997). Trenberth (1997) found that under this definition, ENSO events occur about 55% of the time, while average conditions are less common. The continuous recurrence of warm and cold events suggests that long-lived animals like cetaceans should be adapted to them. With regard to unusually strong events, two El Niños (1982–1983 and 1997–1998) and one La Niña (1988–1989) took place during the period under consideration. However, only the 1982–1983 El Niño and the 1988–1989 La Niña are present in the sighting data set, because no survey effort took place between the third quarter of 1996 and the last quarter of 1998 (Fig. 4.1). Therefore, the effect of strong events on the data set are probably small.

Another important caveat is that the community analyses assume the contemporaneous presence of the different species in a sample unit (the Sørensen distance and the Beals smoothing computations are based on the patterns of co-occurrence). However, because the seasonal species matrices were constructed using cummulative sightings over a 28-yr period, species could have occurred in a sample unit at different times without ever being present together. For this reason, interpretation of the results is limited to the dominant patterns.

It should also be emphasized that the results presented here are primarily intended to give the broad outlines of community structure and its relationship to environmental variability. The relatively low percentage (27–35%) of the variance in community structure on axis 1 explained by the environmental variables may be due in part to the use of the coarse climatological data.

Finally, one particular set of variables not considered in this study which are known to influence cetacean distribution are those describing the physiography of the sea floor (i.e., depth and slope) (e.g., Hui, 1979; 1985; Baumgartner, 1997; Waring et al., 2001; Cañadas et al., 2002). These variables were not included in this study because it was felt that the spatial resolution imposed by the gridding scheme (~ 28 km) would smooth out the rapid changes in depth and other fine details of the steep topography around the archipelago. However, a preliminary examination of the distribution of the nine species with respect to these variables using a 3.7 km-resolution bathymetry data set indicated that *G. griseus* was strongly associated with the steepest underwater slopes around the volcanoes. This species is also known to have a close association with the steepest slopes of the northern Gulf of Mexico (Baumgartner, 1997).

4.7 CONCLUSION

Despite the caveats associated with the data sets, the community analyses provided a systematic characterization of the distribution patterns and

environmental associations of the nine cetaceans that commonly occur around the Galápagos (these were informally described in section 4.4.1 and Fig. 4.2). Seasonal change in community structure was only modest, in spite of the strong environmental variability in the region. This was attributed to the persistence of the upwelling of the EUC on the western side of the archipelago, which sustains a productive environment year-round.

Finally, available information on feeding habits and prey occurrence suggested that stratified, upwelling, and coastal environments are characterized by different types of trophic interactions which, in turn, are probably responsible for the type of cetacean assemblages found in them. Given the diversity of species in the upwelling habitat, further studies of cetacean distribution and abundance at finer scales have the potential of yielding useful information on interspecific interactions, niche specialization, and habitat partitioning in this complex environment.

4.8 ACKNOWLEDGEMENTS

Access to marine mammal sighting databases was kindly provided by T. Gerrodette (NMFS/SWFSC), I. Kerr (Ocean Alliance), and H. Whitehead (Dalhousie University). The environmental data sets were obtained online from the following sources. Monthly “Pathfinder + Erosion” SST climatologies from PO.DAAC/JPL/NASA (http://podaac.jpl.nasa.gov/order/order_sstemp.html#Product112). WOA98 temperature, salinity, and oxygen from NOAA’s National Oceanographic Data Center (http://www.nodc.noaa.gov/OC5/data_woa.html). SIMBIOS-NASDA-OCTS and SeaWiFS ocean color from the SeaWiFS project (code 970.2) and the GES DISC DAAC (code 902) at GSFC/ NASA, Greenbelt, MD 20771 (http://daac.gsfc.nasa.gov/data/dataset/OCTS/ and http://daac.gsfc.nasa.gov/data/dataset/SEAWIFS/). The “Smith and Sandwell”

global sea-floor topography v. 8.2 from the Institute of Geophysics and Planetary Physics at the Scripps Institution of Oceanography (http://topex.ucsd.edu/marine_topo/ mar_topo.html). The 37-yr (1965–2001) *in-situ* SST record from Academy Bay was graciously provided by S. Rea of the Monitoring Program at the CDRS. K.C. Palacios produced Figure 4.3. Funding for this study was provided by the Endowed Marine Mammal Program at Oregon State University. B. McCune provided useful clarifications on the techniques used. The manuscript was improved by careful reviews from C.B. Miller, B.R. Mate, P.T. Strub, and W.G. Pearcy.

4.9 REFERENCES

Anderson, J.J. 1977. Identification and tracing of water masses with an application near the Galápagos Islands. Ph.D. Thesis, University of Washington. 144 pp.

Anderson, D.J. 1989. Differential responses of boobies and other seabirds in the Galápagos to the 1986–87 El Niño-Southern Oscillation Event. Marine Ecology Progress Series 52(3):209–216.

Au, D.W. 1991. Polyspecific nature of tuna schools: shark, dolphin, and seasbird associates. Fishery Bulletin 89:343–354.

Au, D.K., and W.L. Perryman. 1985. Dolphin habitats in the eastern tropical Pacific. Fishery Bulletin 83(4):623–643.

Baumgartner, M.F. 1997. The distribution of Risso's dolphin (*Grampus griseus*) with respect to the physiography of the northern Gulf of Mexico. Marine Mammal Science 13(4):614–638.

Bernard H.J., and S.B. Reilly. 1999. Pilot whales *Globicephala* Lesson, 1828. Pages 245–280 *in* Ridgway, S.H., and R. Harrison, eds. Handbook of Marine Mammals, Volume 6, The Second Book of Dolphins and Porpoises. Academic Press, London.

Berzin, A.A. 1978. Whale distribution in tropical eastern Pacific waters. Report of the International Whaling Commission 28:173–177.

Blackburn, M. 1968. Micronekton of the eastern tropical Pacific Ocean: family composition, distribution, abundance, and relations to tuna. Fishery Bulletin 67(1):71–115.

Blackburn, M., R.M. Laurs, R.W. Owen, and B. Zeitschel. 1970. Seasonal and aereal changes in standing stocks of phytoplankton, zooplankton and micronekton in the eastern tropical Pacific. Marine Biology 7:14–31.

Brinton, E. 1979. Parameters relating to the distributions of planktonic organisms, especially Euphausiids in the eastern tropical Pacific. Progress in Oceanography 8:125–189.

Cañadas, A., R. Sagarminaga, and S. García-Tiscar. 2002. Cetacean distribution related with depth and slope in the Mediterranean waters off southern Spain. Deep-Sea Research I 49:2053–2073.

Casey, K.S., and P. Cornillon. 1999. A comparison of satellite and *in situ*-based sea surface temperature climatologies. Journal of Climate 12(6):1848–1863.

Clarke M.R., and F. Trillmich. 1980. Cephalopods in the diets of fur seals of the Galápagos Islands. Journal of Zoology (London) 190:211–215.

Conkright, M., S. Levitus, T. O'Brien, T. Boyer, J. Antonov, and C. Stephens. 1998. World Ocean Atlas 1998 CD-ROM Data Set Documentation, Technical Report 15, NODC Internal Report, Silver Spring, MD, 16 pp.

Cornejo de González, M. 1977. Distribución de los eufaúsidos al oeste de las islas Galápagos, durante el crucero “Eastward” E-5L-76 (29 de Octubre al 12 de Noviembre , 1976). Boletín ERFEN 1(2):21–24.

Cummings, W.C. 1985. Bryde’s whale *Balaenoptera edeni* Anderson, 1878. Pages 137–154 *in* Ridgway, S.H., and R.J. Harrison, eds. Handbook of Marine Mammals, Volume 3, The Sirenians and Baleen Whales. Academic Press, London.

Das, K., G. Lepoint, V. Loizeau, V. Debacker, P. Dauby, and J.M. Bouquegneau. 2000. Tuna and dolphin associations in the North-east Atlantic: evidence of different ecological niches from stable isotope and heavy metal measurements. Marine Pollution Bulletin 40(2):102–109.

Delcroix, T. 1993. Seasonal and interannual variability of sea surface temperatures in the tropical Pacific, 1969–1991. Deep-Sea Research I 40(11-12):2217–2228.

Dellinger, T., and F. Trillmich. 1999. Fish prey of the sympatric Galápagos fur seals and sea lions: seasonal variation and niche separation. Canadian Journal of Zoology 77(8):1204–1216.

Dessier, A., and J.R. Donguy. 1985. Planktonic copepods and environmental properties of the eastern equatorial Pacific: seasonal and spatial variations. Deep-Sea Research 32:1117–1133.

Dufrêne, M., and P. Legendre. 1997. Species assemblages and indicator species: the need for a flexible asymmetrical approach. Ecological Monographs 67:345–366.

Evans, W.E. 1994. Common dolphin, white-bellied porpoise *Delphinus delphis* Linnaeus, 1758. Pages 191–224 *in* Ridgway, S.H., and R. Harrison, eds. Handbook of Marine Mammals, Volume 5, The First Book of Dolphins. Academic Press, London.

Ewald, J. 2002. A probabilistic approach to estimating species pools from large compositional matrices. Journal of Vegetation Science 13:191–198.

Fager, E.W. 1957. Determination and analysis of recurrent groups. Ecology 38(4):586–595.

Feldman, G.C. 1986. Patterns of phytoplankton production around the Galápagos Islands. Pages 77–106 *in* Bowman, M.J., C.M. Yentsch, and W.T. Peterson, eds. Tidal mixing and plankton dynamics. Lecture Notes on Coastal and Estuarine Studies 17, Springer-Verlag, Berlin.

Feldman, G., D. Clark, and D. Halpern. 1984. Satellite color observations of the phytoplankton distribution in the eastern equatorial Pacific during the 1982–1983 El Niño. Science 226(4678):1069–1071.

Fiedler, P.C. 1992. Seasonal climatologies and variability of eastern tropical Pacific surface waters. NOAA Technical Report NMFS 109:1–65.

Fiedler, P.C. 2002. The annual cycle and biological effects of the Costa Rica Dome. Deep-Sea Research I 49:321–338.

Fiedler, P.C., and S.B. Reilly. 1994. Interannual variability of dolphin habitats in the eastern tropical Pacific. II: Effects on abundances estimated from tuna vessel sightings, 1975–1990. Fishery Bulletin 92:451–463.

Fiedler, P.C., J. Barlow, and T. Gerrodette. 1998. Dolphin prey abundance determined from acoustic backscatter data in eastern Pacific surveys. Fishery Bulletin 96:237–247.

García, M.L., G. Larrea, C. Aguirre, and A. Vasquez. 1993. Zooplankton biomass, zooplankton and ichthyoplankton abundances around the Galápagos Islands in 1983–1984. Revista de Ciencias del Mar y Limnologia 3(1):89–114.

Gaskin, D.E. 1968. Distribution of Delphinidae (Cetacea) in relation to sea surface temperatures off eastern and southern New Zealand. New Zealand Journal of Marine and Freshwater Research 2:527–534.

Goold, J.C. 1998. Acoustic assessment of populations of common dolphin off the west Wales coast, with perspectives from satellite infrared imagery. Journal of the Marine Biological Association of the United Kingdom 78:1353–1364.

Grove, J.S. and R.J. Lavenberg. 1997. The fishes of the Galápagos Islands. Stanford University Press, Stanford, California. 936 pp.

Hassani, S., L. Antoine, and V. Ridoux. 1997. Diets of albacore, *Thunnus alalunga*, and dolphins, *Delphis delphis* and *Stenella coeruleoalba*, caught in the Northeast Atlantic drift-net fishery: a progress report. Journal of Northwest Atlantic Fishery Science 22:119–123.

Houvenaghel, G.T. 1978. Oceanographic conditions in the Galápagos Archipelago and their relationships with life on the islands. Pages 181–200 *in* Boje, R., and M. Tomczak, eds. Upwelling Ecosystems. Springer-Verlag, Berlin.

Hui, C.A. 1979. Undersea topography and the distribution of dolphins of the genus *Delphinus* in the Southern California Bight. Journal of Mammalogy 60(3):521–527.

Hui, C.A. 1985. Undersea topography and the comparative distributions of two pelagic cetaceans. Fishery Bulletin 83(3):472–475.

Kinzey, D., T. Gerrodette, A. Dizon, W. Perryman, P. Olson, and S. Rankin. 2001. Marine mammal data collected during a survey in the eastern tropical Pacific Ocean aboard the NOAA ships *McArthur* and *David Starr Jordan*, July 28–December 9, 2000. NOAA-TM-NMFS-SWFSC-303. 100 pp.

Kruse S., D.K. Caldwell, and M.C. Caldwell. 1999. Risso's dolphin *Grampus griseus* (G. Cuvier, 1812). Pages 183–212 *in* Ridgway, S.H., and R. Harrison, eds. Handbook of Marine Mammals, Volume 6, The Second Book of Dolphins and Porpoises. Academic Press, London.

Lee, T. 1993. Summary of cetacean survey data collected between the years of 1974 and 1985. NOAA Technical Memorandum NMFS-SWFSC 181:1–184.

Lee, T. 1994. Report on cetacean aerial survey data collected between the years of 1974 and 1982. NOAA Techical Memorandum NMFS-SWFSC 195:1–62.

Legendre, P., and L. Legendre. 1998. Numerical ecology. Second English edition. Developments in Environmental Modelling 20. Elsevier. Amsterdam. 853 pp.

Longhurst, A. 1967. Vertical distribution of zooplankton in relation to the eastern Pacific oxygen minimum. Deep-Sea Research 14:51–63.

Longhurst, A. 1998. Ecological geography of the sea. Academic Press, San Diego. 398 pp.

Lukas, R. 1986. The termination of the Equatorial Undercurrent in the eastern Pacific. Progress in Oceanography 16:63–90.

Lyrholm, T., I. Kerr, L. Galley, and R. Payne. 1992. Report of the "Expedición *Siben*," Ecuador 1988/89. Final Report submitted by the Whale Conservation Institute to the Charles Darwin Research Station and the Galápagos National Park Service, Puerto Ayora, Islas Galápagos, Ecuador. 38 pp.

McCune, B. 1994. Improving community analysis with the Beals smoothing function. Écoscience 1(1):82–86.

McCune, B., and M.J. Mefford. 1999. PC-ORD. Multivariate analysis of ecological data, version 4. MjM Software Design, Gleneden Beach, OR, USA. 237 pp.

McCune, B., and J.B. Grace. 2002. Analysis of ecological communities. MjM Software Design, Gleneden Beach, Oregon, USA. 300 pp.

McGowan, J.A. 1971. Oceanic biogeography of the Pacific. Pages 3–74 *in* Funnell, B.M., and W.R. Riedel, eds. The Micropalaeontology of the Oceans. Cambridge University Press, Cambridge.

Mielke, P.W., Jr. 1984. Meteorological applications of permutation techniques based on distance functions. Pages 813–830 in P.R. Krishnaiah and P.K. Sen, eds., Handbook of Statistics, Vol. 4. Elsevier Science Publishers.

Mielke, P.W., Jr., and K.J. Berry. 2001. Permutation methods: A distance function approach. Springer Series in Statistics. 334 pp.

Mullins, H.T., J.B. Thompson, K. McDougall, and T.L. Vercoutere. 1985. Oxygen-minimum zone edge effects: evidence from the central California coastal upwelling system. Geology 13:491–494.

Olson, D.B. 2002. Biophysical dynamics of ocean fronts. Pages 187–218 in Robinson, A.R., J.J. McCarthy, and B.J. Rothschild, eds. The Sea, Ideas and

Observations on Progress in the Study of the Seas, Vol. 12, Biological-Physical Interactions in the Sea. John Wiley & Sons, New York.

Palacios, D.M. 1999a. Blue whale (*Balaenoptera musculus*) occurrence off the Galápagos Islands, 1978–1995. Journal of Cetacean Research and Management 1(1):41–51.

Palacios, D.M. 1999b. Marine mammal research in the Galápagos Islands: the 1993–94 *Odyssey* Expedition. Final report submitted to Galápagos National Park Service and Charles Darwin Research Station. Puerto Ayora, Is. Galápagos, Ecuador, 10 November 1999. 6pp, 4 tables, 18 figures, and 3 appendices.

Palacios, D.M. 2000. *GalCet2K*: A line-transect survey for cetaceans across an environmental gradient off the Galápagos Islands, 5–19 April 2000. Final report submitted to: Galápagos National Park Service, Charles Darwin Research Station, Capitanía de Puerto Ayora, and Dirección General de Intereses Marítimos de la Armada Nacional. Puerto Ayora, Is. Galápagos, Ecuador, 17 July 2000. 9 pp.

Palacios, D.M. 2002. Factors influencing the island-mass effect of the Galápagos Islands. Geophysical Research Letters 29(23), 2134, doi: 10.1029/2002GL016232.

Palacios, D.M., and S. Salazar. 2002. Cetáceos. Pages 291–304 *in* Danulat, E., and G.J. Edgar, eds. Reserva Marina de Galápagos, Línea Base de la Biodiversidad. Fundación Charles Darwin/Servicio Parque Nacional Galápagos, Santa Cruz, Galápagos, Ecuador.

Papastavrou, V., S.C. Smith, and H. Whitehead. 1989. Diving behaviour of the sperm whale, *Physeter macrocephalus*, off the Galápagos Islands. Canadian Journal of Zoology 67:839–846.

Perrin, W.F., and J.W. Gilpatrick Jr. 1994. Spinner dolphin, *Stenella longirostris* (Gray, 1828). Pages 99–128 *in* Ridgway, S.H., and R. Harrison, eds. Handbook of Marine Mammals, Volume 5, The First Book of Dolphins. Academic Press, London.

Perrin, W.F., J.M. Coe, and J.R. Zweifel. 1976. Growth and reproduction of the spotted porpoise, Stenella attenuata, in the offshore eastern tropical Pacific. Fishery Bulletin 74(2):229–269.

Perrin, W.F., C.E. Wilson, and F.I. Archer III. 1994. Striped dolphin *Stenella coeruleoalba* (Meyen, 1833). Pages 129–159 *in* Ridgway, S.H., and R. Harrison, eds. Handbook of Marine Mammals, Volume 5, The First Book of Dolphins. Academic Press, London.

Polacheck, T. 1987. Relative abundance, distribution and inter-specific relationship of cetacean schools in the eastern tropical Pacific. Marine Mammal Science 3(1):54–77.

Reilly, S.B. 1990. Seasonal changes in distribution and habitat differences among dolphins in the eastern tropical Pacific. Marine Ecology Progress Series 66:1–11.

Reilly, S.B., and V.G. Thayer. 1990. Blue whale (*Balaenoptera musculus*) distribution in the eastern tropical Pacific. Marine Mammal Science 6(4):265–277.

Reilly, S.B., and P.C. Fiedler. 1994. Interannual variability of dolphin habitats in the eastern tropical Pacific. I: Research vessel surveys, 1986–1990.

Robertson, K.M., and S.J. Chivers. 1997. Prey occurrence in pantropical spotted dolphins, *Stenella attenuata*, from the eastern tropical Pacific. Fishery Bulletin 95:334–348.

Sagarminaga, R., and A. Cañadas. 1998. A comparative study on the distribution and behaviour of the common dolphin (*Delphinus delphis*) and the striped dolphin (*Stenella coeruleoalba*) along the south-eastern coast of Spain. Pages 175–181 *in* Evans, P.G.H., and E.C.M. Parsons, eds. European Research on Cetaceans 12, Proceedings of the twelfth annual conference of the European Cetacean Society, Monaco, 20–24 January 1998.

Selzer, L.A., and P.M. Payne. 1988. The distribution of white-sided (*Lagenorhynchus acutus*) and common dolphins (*Delphinus delphis*) vs.

environmental features of the continental shelf of the northeastern United States. Marine Mammal Science 4(2):141–153.

Smith, S.C., and H. Whitehead. 1993. Variations in the feeding success and behaviour of Galápagos sperm whales (*Physeter macrocephalus*) as they relate to oceanographic conditions. Canadian Journal of Zoology 71:1991–1996.

Smith, S.C., and H. Whitehead. 2000. The diet of Galápagos sperm whales *Physeter macrocephalus* as indicated by fecal sample analysis. Marine Mammal Science 16(2): 315–325.

Smith, S.D. and H. Whitehead. 1999. Distribution of dolphins in Galápagos waters. Marine Mammal Science 15(2):550–555.

Smith, R.C., P. Dustan, D. Au, K.S. Baker and E. Dunlap, 1986. Distribution of cetaceans and sea-surface chlorophyll concentrations in the California Current. Marine Biology 91:385–402.

Snell, H.M., P.A. Stone, and H.L. Snell. 1995. Geographical characteristics of the Galápagos Islands. Noticias de Galápagos 55:18–24.

Sournia, A. 1994. Pelagic biogeography and fronts. Progress in Oceanography 34:109–120.

Trenberth, K.E. 1997. The definition of El Niño. Bulletin of the American Meteorological Society 78:2771–2777.

van der Spoel, S. 1994. The basis for boundaries in pelagic biogeography. Progress in Oceanography 34:109–120.

Volkov, A.F., and I.F. Moroz. 1977. Oceanological conditions of the distribution of Cetacea in the eastern tropical part of the Pacific Ocean. Report of the International Whaling Commission 27:186–188.

Wade, P.R., and T. Gerrodette. 1993. Estimates of cetacean abundance and distribution in the eastern tropical Pacific. Report of the International Whaling Commission 43:477–493.

Waring, G.T., T. Hamazaki, D. Sheehan, G. Wood, and S. Baker. 2001.Characterization of beaked whale (Ziphiidae) and sperm whale (*Physeter macrocephalus*) summer habitat in shelf-edge and deeper waters off the northeast U.S. Marine Mammal Science 17(4):703–717.

Wells R.S., and M.D. Scott. 1999. Bottlenose dolphin *Tursiops truncatus* (Montagu, 1821). Pages 137–182 *in* Ridgway, S.H., and R. Harrison, eds. Handbook of Marine Mammals, Volume 6, The Second Book of Dolphins and Porpoises. Academic Press, London.

Whitehead, H., V. Papastavrou, and S.C. Smith. 1989. Feeding success of sperm whales and sea-surface temperature off the Galápagos Islands. Marine Ecology Progress Series 53:201–203.

Whittaker, R.H. 1972. Evolution and measurements of species diversity. Taxon 21:213–251.

Wishner, K.F., C.J. Ashjian, C. Gelfman, M.M. Gowing, L. Kann, L.A. Levin, L.S. Mullineaux, and J. Saltzman. 1995. Pelagic and benthic ecology of the lower interface of the eastern tropical Pacific oxygen minimum zone. Deep-Sea Research I 42(1):93–115.

Young, D.D., and V.G. Cockcroft. 1994. Diet of common dolphins (*Delphinus delphis*) off the south-east coast of southern Africa: opportunism or specialization? Journal of Zoology (London) 234(1):41–53.

4.10 APPENDICES

4.10.1 Appendix A: Compilation of the marine mammal database

Sighting records of marine mammals for the area defined in the Methods (section 4.3.1) were compiled from four principal sources. These were: (1) a historical database of cetacean sightings collected by scientific observers aboard

US tuna vessels during fishing trips to the eastern tropical Pacific for the period 1973–1990, available from the Southwest Fisheries Science Center (SWFSC) of the National Marine Fisheries Service (NMFS) (La Jolla, CA, USA); (2) a historical database of sightings collected during regional marine mammal surveys by the SWFSC throughout the eastern tropical Pacific between 1974 and 2000 (Lee, 1993; 1994; Wade and Gerrodette, 1993; Kinzey et al., 2001); (3) cetacean sightings collected opportunistically by scientists from Dalhousie University (Dalhousie, NS, Canada), during sperm whale research trips in Galápagos waters in 1985, 1987, 1989, 1991, 1992 and 1995 (Smith and Whitehead, 1999); and (4) sightings collected during three marine mammal studies in the Galápagos by the Ocean Alliance (OA) (Lincoln, MA, USA) in 1988–1989, 1993–1994 and 2000 (Lyrholm et al., 1992; Palacios, 1999b; 2000). The author participated in the 1993–1994 and 2000 studies, as part of a collaboration between OA and the Marine Mammal Program at Oregon State University (OSU) (Newport, OR, USA).

The number of records in the study area available from each source was as follows: tuna vessel trips, 1323; SWFSC research vessel surveys, 610; SWFSC aerial surveys, 36; Dalhousie University trips, 479; and OA/OSU studies, 1969. The total of number of sighting records was 4417, belonging to 23 identified marine mammal species (21 cetaceans and two otariid pinnipeds endemic to the Galápagos) (Table A4.1) and to eight unidentified categories (i.e., sightings that could only be identified to the family level or higher) (Table A4.2). The compiled database spanned the 28-yr period 1973–2000, although no sightings were available for the years 1996 and 1997. Each record in the database contained fields for source, date, time, latitude, longitude, species identification (or unidentified sighting category), and group size.

The final numbers for certain species in Table A4.1 are the result of combining taxonomically related sighting categories. This pooling was based on regional knowledge of the distribution of the species involved, following the

practice in Wade and Gerrodette (1993). For example, sightings of short-beaked common dolphins represent sightings positively identified as such plus sightings of *Delphinus* sp. (unidentified common dolphin species). The only other species of common dolphin in the eastern Pacific, the long-beaked common dolphin (*D. capensis*), is associated with neritic habitats in the California and Perú Currents, and thus could not be reasonably expected to occur in the study area. Similarly, sightings of short-finned pilot whales (*Globicephala macrorhynchus*) were grouped together with sightings of *Globicephala* sp.; sightings of dwarf sperm whales (*Kogia sima*) were grouped with sightings of *Kogia* sp.; and sightings of Bryde's whales were combined with sightings only identified as "Bryde's or sei whale". Sei whales (*Balaenoptera borealis*) are very similar in appearance to Bryde's whales, but they have a more subtropical distribution and therefore it is unlikely that they occur in the study area.

Although the number of records in the database was 4417, mixed schools of two or more species occurred in 400 of these sightings. Because this study uses the sighting location of each species whether seen in monospecific or mixed-species schools, the numbers listed in Tables A4.1 and A4.2 add up to 4817 sightings.

In terms of temporal and geographic coverage of each source, the two SWFSC databases provided long-term coverage, but because of the regional scale of their operations, only a few days were spent inside the study area in a typical year. Also, these operations covered mostly the offshore waters of the study area. The local studies, on the other hand, consisted of multiple trips around the archipelago, providing coverage for a few months in the case of the Dalhousie data and up to one continuous year for the OA/OSU 1993–1994 data. These trips were typically closer to the islands than the tuna and SWFSC research vessel operations. Sighting locations by source are presented in Figure A4.1.

The protocols under which the sightings were collected differed in other fundamental ways. Some were collected under methods specifically designed to

survey marine mammal populations (Lee, 1993; 1994; Wade and Gerrodette, 1993; Palacios, 2000; Kinzey et al., 2001), while others were collected incidentally to fishing (tuna vessel trips) or other research operations (Lyrholm et al., 1992; Palacios, 1999b; Smith and Whitehead, 1999). The platforms from which the sightings were made also differed widely, ranging from large research and tuna vessels to sailing vessels to survey aircraft. For these reasons, it is not possible to provide a unified measure of search effort, which could be used to compute an index of marine mammal abundance. However, this study is not concerned with determining population size or population changes through time. Rather, its primary objectives are to investigate community structure and environmental associations, provided that coverage of the study area by the operations described above was adequate. Therefore, and given that under fair sighting conditions at least some marine mammals will normally be seen on any given day at sea, one can use the cumulative locations for all sightings (including the ones that went unidentified) as a general indication of coverage. Weather and other visibility-related conditions in the Galápagos region are excellent during the first part of the year (sea states 0–3 in the Beaufort scale) and fair during the second part, when SE trade winds tend to create whitecaps (Beaufort 2–4). The cumulative locations for all sightings by season are shown in Figure A4.2.

Table A4.1: Marine mammal species identified in the study area from sightings collected during 1973–2000. Mixed-species sightings are counted once for each species involved.

Scientific name	Common name	No. sightings
Stenella attenuata	Pantropical spotted dolphin	519
Stenella longirostris	Spinner dolphin	303
Stenella coeruleoalba	Striped dolphin	247
Steno bredanensis	Rough-toothed dolphin	5
Delphinus delphis	Short-beaked common dolphin	456
Tursiops truncatus	Bottlenose dolphin	366
Grampus griseus	Risso's dolphin	117
Lagenodelphis hosei	Fraser's dolphin	10
Peponocephala electra	Melon-headed whale	4
Feresa attenuata	Pygmy killer whale	2
Pseudorca crassidens	False killer whale	12
Globicephala macrorhynchus	Short-finned pilot whale	131
Orcinus orca	Killer whale	38
Physeter macrocephalus	Sperm whale	284
Kogia sima	Dwarf sperm whale	10
Mesoplodon spp.	*Mesoplodon* species	11
Ziphius cavirostris	Cuvier's beaked whale	22
Balaenoptera acutorostrata	Minke whale	4
Balaenoptera edeni	Bryde's whale	316
Balaenoptera musculus	Blue whale	18
Megaptera novaeangliae	Humpback whale	4
Arctocephalus galapagoensis	Galápagos fur seal	104
Zalophus wollebaeki	Galápagos sea lion	61

Table A4.2: Unidentified sighting categories (family level or higher).

Category	No. sightings
Ziphiid whale	40
Unidentified rorqual	199
Unidentified dolphin	1148
Unidentified small whale	75
Unidentified large whale	101
Unidentified whale	144
Unidentified cetacean	33
Unidentified otariid	33

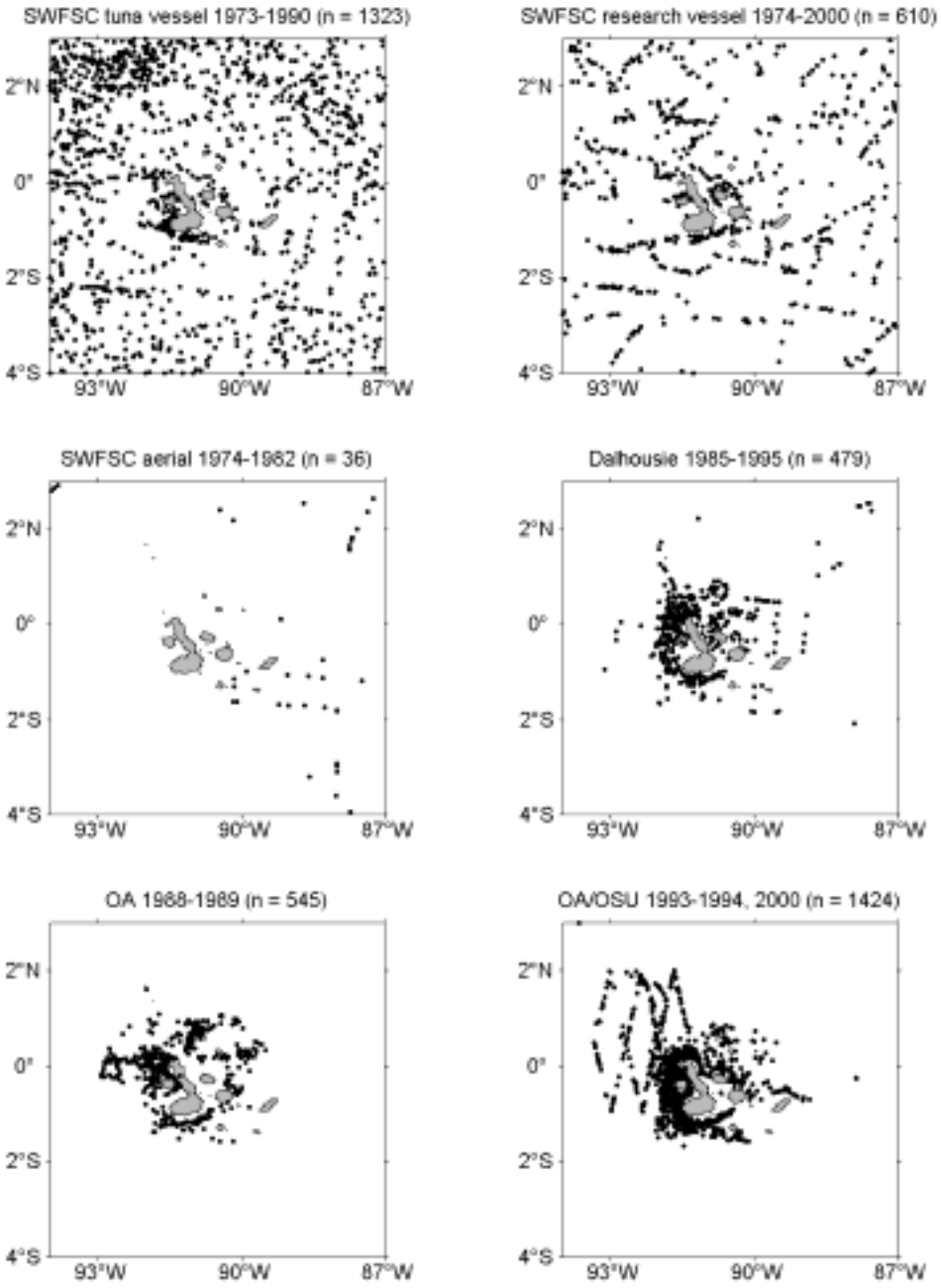

Figure A4.1: Marine mammal sighting locations (identified and unidentified) in the study area, by source, for the period 1973–2000.

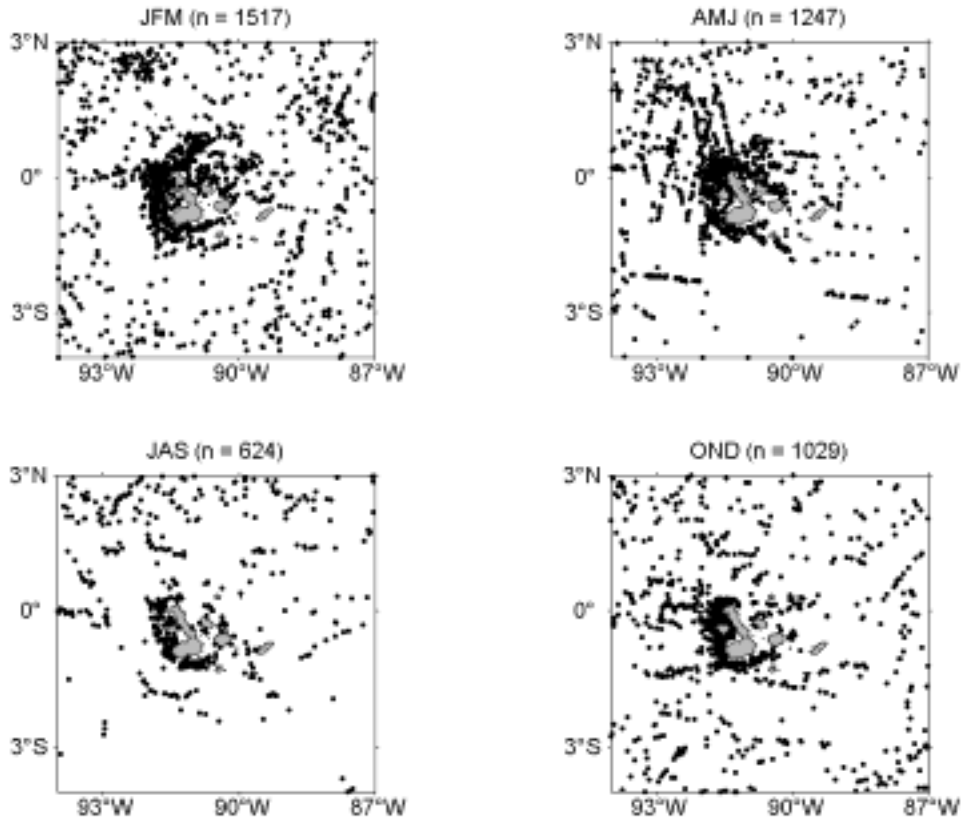

Figure A4.2: Cumulative locations of all marine mammal sightings (identified and unidentified) in the study area, by season, for the period 1973–2000.

4.10.2 Appendix B: Description of the seasonal climatologies

4.10.2.1 Data products and variable extraction

Global, gridded data sets were obtained, subset to the study area, and, where necessary, processed to derive the eight environmental variables of interest at seasonal timescales. Climatological monthly fields of satellite-derived SST were extracted from the "Pathfinder + Erosion" product, which was computed from the 13-yr base period 1985–1997 of Advanced Very High Radiometer (AVHRR) measurements (Casey and Cornillon 1999). Similarly, monthly climatologies of near-surface chl were obtained from satellite-derived ocean color measurements for the 5-yr base period 1996–2001 of combined data from the Ocean Color and Temperature Scanner (OCTS) and the Sea-viewing Wide-Field-of-view Sensor (SeaWiFS), as described in Chapter 3. Seasonal fields were produced from the monthly climatologies. Chl was log-transformed (LCHL) to account for the log-normal distribution of this variable. The original resolution of the SST and LCHL data sets was 9.28 km.

Seasonal climatologies of 1-degree resolution water-column properties were obtained from the World Ocean Atlas 1998 (WOA98) (Conkright et al., 1998). At each grid cell, 1-m vertical resolution profiles of temperature, salinity, and dissolved oxygen were extracted from the standard depth levels by cubic-spline interpolation. The following six variables were derived from these data: (1) depth of the thermocline (i.e., the depth of the 20°C isotherm, or Z20); (2) thermocline strength (i.e., the vertical distance between the 20°C and 15°C isotherms, or ZTD); (3) maximum Brunt-Väisälä frequency (i.e., the maximum resistance to turbulent mixing in the pycnocline, in cycles h^{-1}, or MBVF, also known as the maximum buoyancy frequency); (4) depth of the MBVF (or ZMBVF, also called the depth of the pycnocline); (5) depth of the OML (i.e., the depth at which dissolved oxygen concentrations were < 1 ml l^{-1}, or ZOML); and (6) thickness of the OML (i.e., the vertical distance between the upper and lower boundaries of the OML, or ZOD).

The eight variables were re-gridded from their original resolution to a common resolution of 0.25 degrees for compatibility with the sighting grid. For variables with a coarser resolution than the sighting grid, the value of a coarse cell was assigned to all of the 0.25-degree cells whose center fell inside the coarse cell. For variables with a finer resolution, the average of all cells inside a 0.25-degree cell was assigned to it.

4.10.2.2 Sea-surface and water-column variables: Seasonal patterns

Seasonal fields of SST and LCHL are presented in Figure B4.1. The dominant seasonal cycle is evident in these fields (see also Chapter 3), with high SST and low chl in JFM, and low SST and high chl in JAS. Also evident is the persistence of the area with lowest SST and highest chl on the western side of the archipelago in all seasons, which marks the location where the EUC upwells.

As mentioned in section 4.3.3.3, a principal component analysis was perfomed on the seven variables thought to describe the direct effects of physical forcing on the system (i.e., Z20, ZTD, MBVF, ZMBVF, ZOML, ZOD, and SST). The results were reported in section 4.4.3 for grid cells with valid data in the corresponding species matrices, with emphasis on the first component, since that component was the only one relevant to the ordination results. A description of the first three components is provided here based on analysis of the full data sets.

Table 1 lists the loadings for the first three principal components (PC). Together, they explained 83% of the variance in the original data sets. Figure B4.2 shows the site scores and their seasonal evolution for each PC. The first PC (41%) described the effects of the EUC around the archipelago (principally a shallow thermocline, weak pycnocline stratification, a thin OML, and low SST), which are most intense in JAS (see also Chapter 2). The OML is thin in this area because the EUC has a high-oxygen core (Anderson, 1977; Lukas, 1986), which effectively erodes the top of the OML directly beneath it. The second PC (26%) depicted a

NE-SW pattern principally driven by a strong, shallow pycnocline (resulting from heavy precipitation in the Panamá Bight) and high SST. This pattern is strongest in JFM. Finally, the third PC (16%) represented an W-E gradient, with a shallow, thick OML, and a weak thermocline on the eastern sector. This pattern was also strongest in JFM, and is probably associated with the W-E shoaling of the thermocline in the eastern tropical Pacific (Fiedler, 1992), and the thickening of the oxygen minimum layer off the coast of South America.

Table B4.1: Loadings (eigenvectors) for the first three principal components (PC) of the seven variables describing direct effects of physical forcing in the water column and at the surface. Values greater than 0.3 are shown in bold to highlight the variables with the greatest contribution to each PC. The eigenvalues and the fraction of the variance represented by each PC are also indicated.

Variable	PC1	PC2	PC3
Z20	**-0.52**	0.13	-0.23
ZTD	0.27	**0.37**	**0.47**
MBVF	**-0.37**	**0.47**	0.02
ZMBVF	-0.27	**-0.50**	**-0.37**
ZOML	0.23	**0.39**	**-0.65**
ZOD	**-0.44**	-0.24	**0.40**
SST	**-0.45**	**0.41**	0.02
Eigenvalue	2.9	1.8	1.0
Variance fraction (%)	41.9	25.9	15.5

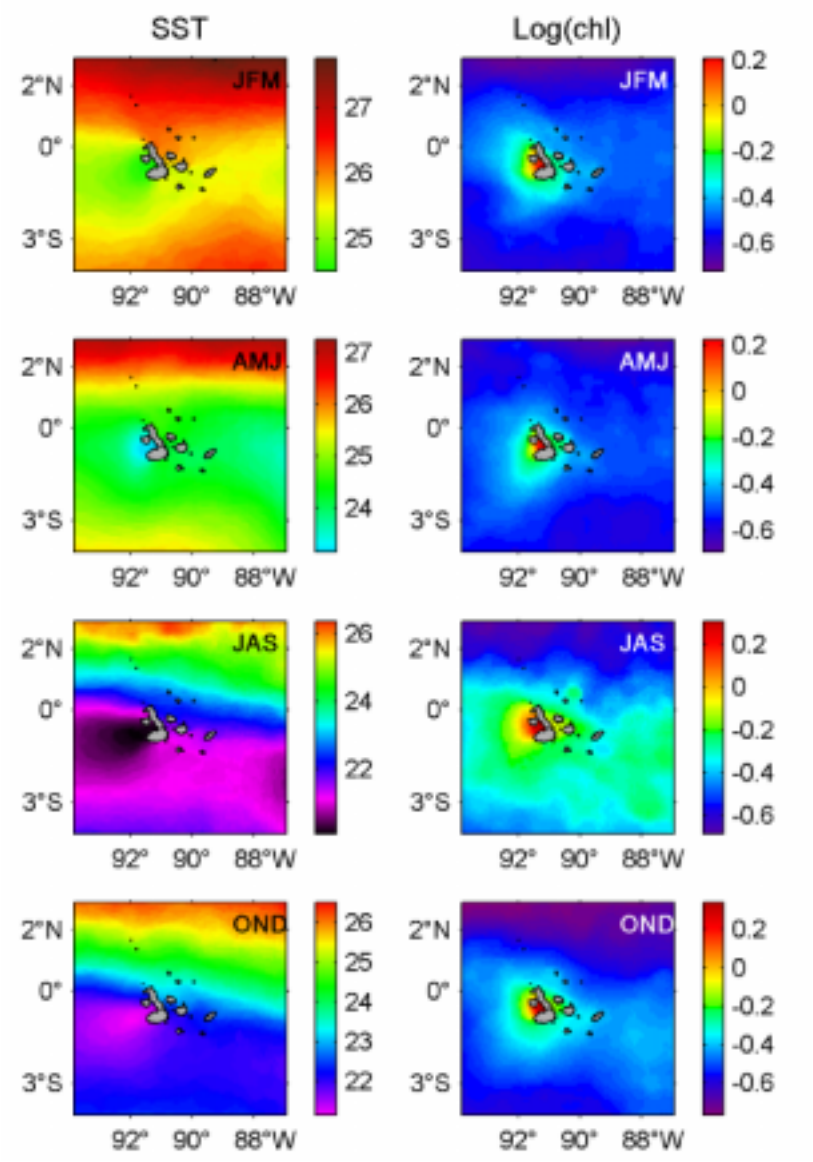

Figure B4.1: Seasonal climatologies of sea-surface temperature (SST) (°C) and log-transformed phytoplankton concentration (chl) (mg m^{-3}) for the study area.

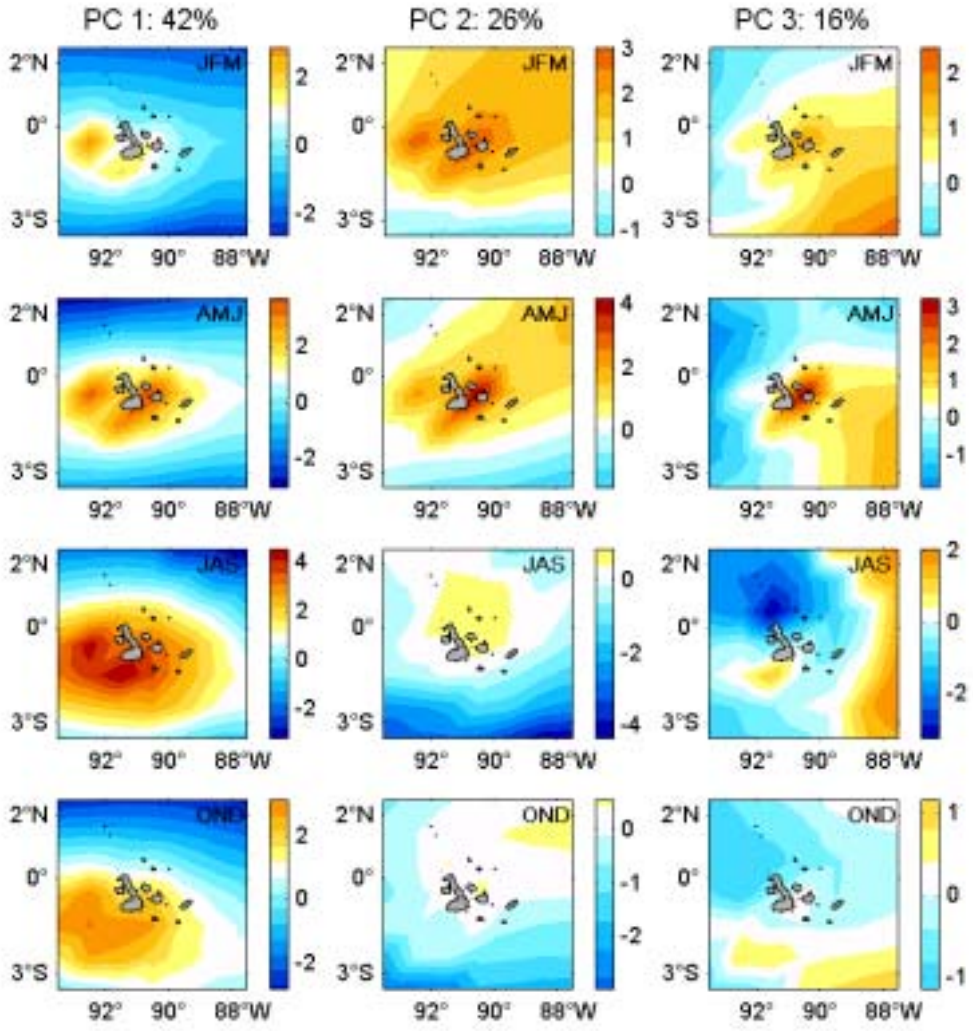

Figure B4.2: Seasonal evolution of the first three principal components (PC) of Z20, ZTD, MBVF, ZMBVF, ZOML, ZOD, and SST. The fraction of variance explained by each component is given.

4.10.3 Appendix C: Further details of the community analyses

4.10.3.1 Species diversity

Diversity measures provide concise summaries about the community and the properties of the data set. A measure of heterogeneity (see below), in particular, gives an indication of the degree of difficulty faced by ordination methods with a given data set (e.g., McCune and Grace, 2002). Common measures include Whittaker's (1972) three levels of diversity: alpha, beta, and gamma. Alpha diversity is the average number of species per sample unit (also known as species richness). Beta diversity is a measure of the amount of compositional heterogeneity in the data, which was estimated here as the ratio of the total number of species to the average number of species (gamma over alpha). Gamma diversity refers to the diversity of the study area, which is simply the total number of species across sample units (Whittaker, 1972). Three other widely used indices: Pielou's evenness, Shannon's entropy, and Simpson's diversity, are also included (Legendre and Legendre, 1998, McCune and Grace, 2002).

All these six diversity measures are reported for matrices containing the nine species of interest in Table C4.1 and for matrices containing all identified species in Table C4.2 for comparison. Also included in these tables are coefficients of variation for sample unit totals and for species totals, as well as average Sørensen distances among sample units in the distance matrices.

Table C4.1: Diversity measures and summary statistics for presence-absence matrices after removing rare species. SU is the number of sample units for each season. Pielou's evenness (*E*), Shannon's entropy (*H*), and Simpson's diversity (*D*) are also shown, along with the coefficient of variation (%) for row (CV_{su}) and column (CV_{sp}) totals. *d* is the average Sørensen distance among sample units in the distance matrices.

Season	SU	alpha	beta	gamma	*E*	*H*	*D*	CV_{su}	CV_{sp}	*d*
JFM	309	1.9	4.7	9	0.56	0.50	0.32	55.9	67.3	0.80
AMJ	232	1.8	5.0	9	0.50	0.44	0.28	57.4	55.4	0.83
JAS	140	1.6	5.6	9	0.39	0.35	0.23	58.9	52.2	0.86
OND	223	1.6	5.6	9	0.42	0.36	0.24	57.6	44.0	0.87

Table C4.2: Diversity measures and summary statistics for presence-absence matrices containing all identified species. SU is the number of sample units for each season. Pielou's evenness (*E*), Shannon's entropy (*H*), and Simpson's diversity (*D*) are also shown, along with the coefficient of variation (%) for row (CV_{su}) and column (CV_{sp}) totals. *d* is the average Sørensen distance among sample units in the distance matrices.

Season	SU	alpha	beta	gamma	*E*	*H*	*D*	CV_{su}	CV_{sp}	*d*
JFM	312	2.0	9.5	19	0.58	0.54	0.34	63.1	127.5	0.80
AMJ	237	1.9	10.0	19	0.55	0.51	0.32	64.4	111.5	0.84
JAS	151	1.7	12.4	21	0.38	0.37	0.23	71.1	115.9	0.89
OND	234	1.8	12.2	22	0.47	0.43	0.27	66.7	111.1	0.88

4.10.3.2 Distance among sample units in species space

The first step in the analyses was to obtain a matrix of distances among all sample units for each season (for the NMS ordination, a single distance matrix was obtained from the combined seasonal species matrices). Given a presence-absence species matrix **X** with *m* rows (i.e., sample units) and *n* columns (i.e., species)**,** the distance *D* between two sample units *i* and *h* was computed using the one-complement of Sørensen's coefficient of similarity (Legendre and Legendre, 1998; McCune and Grace, 2002) as:

$$D_{i,h} = \frac{\sum_{j=1}^{n} \left| x_{ij} - x_{hj} \right|}{\sum_{j=1}^{n} x_{ij} + \sum_{j=1}^{n} x_{hj}} \quad \text{for} \quad j = 1, \ldots, n \qquad (1)$$

The resulting distances were then arranged into a $m \times m$ matrix Δ, with elements δ_{ij}. *D* is referred to throughout this manuscript as the "Sørensen distance".

4.10.3.3 The Beals smoothing function

Prior to ordination, the data for each species in the presence-absence matrices were transformed with the Beals smoothing function, which yields quantitative values representing the "favorability" of each sample unit for each species (regardless of whether the species was present in the sample unit), using the proportions of joint occurrences of the species of interest and the species that were actually in the sample unit (McCune, 1994). The main purpose of this transformation is to relieve the "zero truncation problem" (i.e., the lack of information about habitat quality outside of the observed range of a species because its abundance is zero), which is most severe in heterogeneous community data sets with a large number of zeros in the data matrix (McCune, 1994; Ewald, 2002). The

method also smoothes out differences due to varying sampling effort (McCune, 1994).

For a given presence-absence species matrix **X**, McCune (1994) defines the Beals smoothing function as:

$$b_{ij} = \frac{1}{S_i} \sum_k \left(\frac{M_{jk}}{N_k} \right) \text{ for all } k \text{ with } x_{ik} \neq 0 \qquad (2)$$

where b_{ij} is the adjusted value in the transformed data matrix **B** that replaces the original value in **X**, S_i is the number of species in sample unit i, M_{jk} is the number of sample units with both species j and k, and N_k is the number of sample units with species k.

The transformation was applied to improve the stability of the solution from the NMS ordination on the presence-absence data. Diagnostic analyses of the data indicated that although the matrix was about 81% sparse, all nine species were present in at least 8% of the sample units (i.e., there were no "rare species" remaining). Also, there were no outliers beyond ± 2 standard deviations in the distribution of Sørensen distances. However, a frequency histogram of the average Sørensen distance to each sample unit revealed that there were two "populations" with little or no overlap, as shown in Figure C4.1. A considerable number of sample units had low average Sørensen distances (< 0.71) and appeared grouped together at the low end of the histogram, while the remainder were spread more widely over the rest of the distance range. Examination of the spatial pattern of these distances (Fig. C4.2) indicated that the low-distance population corresponded with the group of sample units found in the northern sector of the study area (and also in the southern sector in JFM) that was characterized almost exclusively by the presence of *S. attenuata* and *S. longirostris* (see section 4.4.2). The NMS procedure interpreted the low-distance population as outliers competing with the main

population for a stable solution. In this case, the effect of the Beals transformation was to enhance the main compositional gradient. After smoothing, the Sørensen distances were more normally distributed (Figs. C4.1 and C4.3) and a low-stress, stable solution was reached. (see section 4.10.3.4)

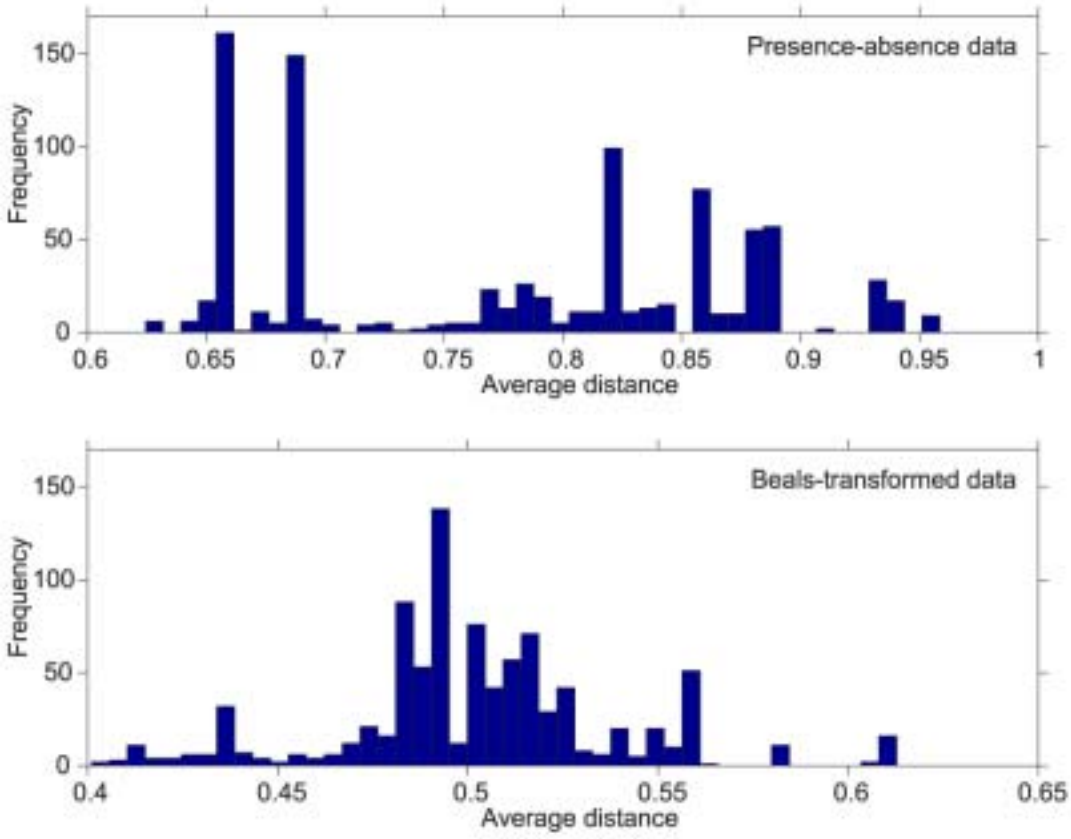

Figure C4.1: Frequency distribution of average Sørensen distances to each sample unit (m = 904). Top: calculated from the presence-absence data. Bottom: calculated from the Beals-transformed data.

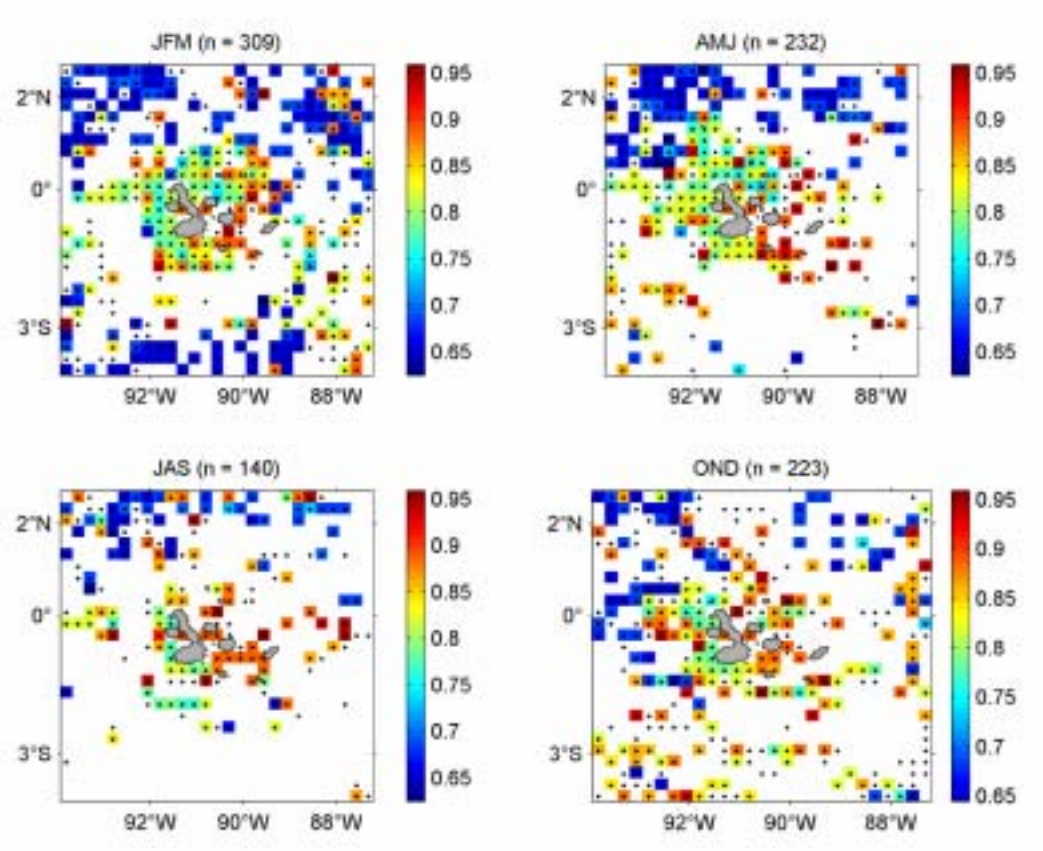

Figure C4.2: Spatial distribution of average Sørensen distance to each sample unit for each season in the presence-absence data set.

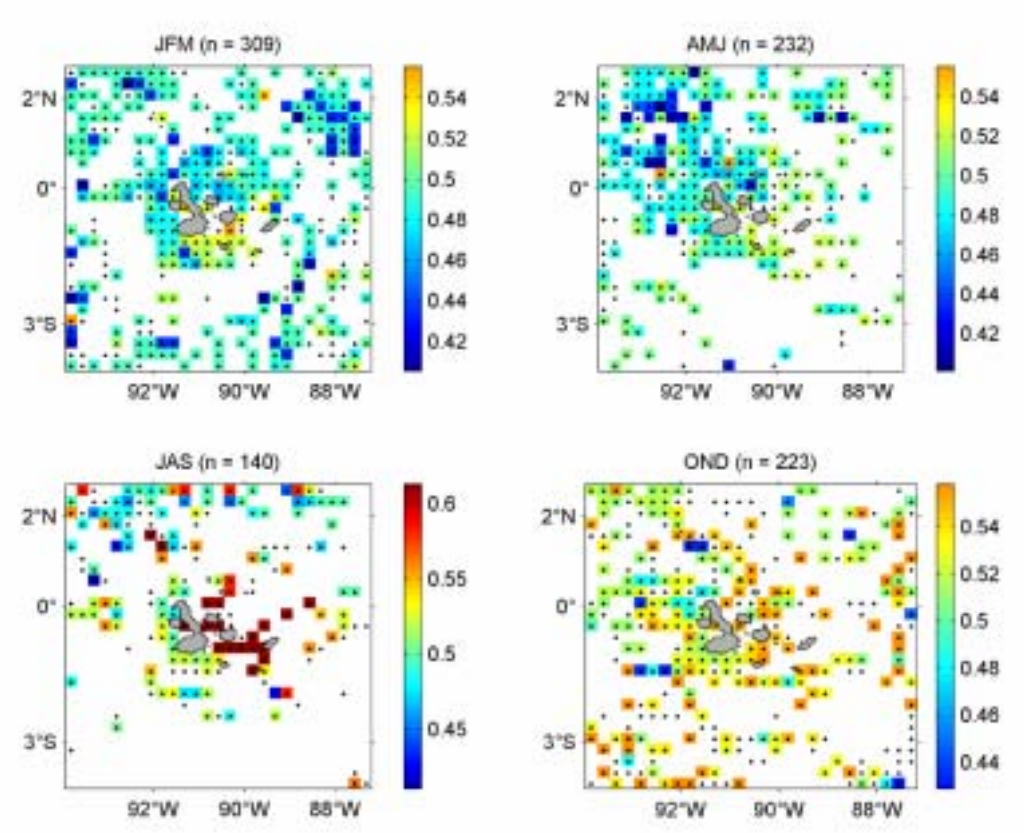

Figure C4.3: Spatial distribution of average Sørensen distance to each sample unit for each season after the Beals transformation.

4.10.3.4 Setup and intermediate steps of the NMS ordination

Unlike other ordination methods, NMS is not based on eigenanalysis, and it has no particular underlying model (either linear or unimodal). Its objective is to arrange dissimilar objects far apart and similar objects close to one another in a small and specified number of dimensions (i.e., number of axes). This preservation of ordering relationships among objects (sample units in this case) is accomplished by maximizing the rank-order correlation between distance in the full-dimensional space and distance in the ordination space. NMS operates as an iterative search for the best positions, which are assessed with "stress", an objective function that measures the lack-of-fit between the two kinds of distance. Improvements are accomplished by gradual changes to the configuration in a direction that progressively minimizes stress, using the method of steepest descent (an optimization algorithm) (Legendre and Legendre, 1998; McCune and Grace, 2002).

The search for the best solution was conducted in two stages, using the software package PC-ORD version 4.25 (McCune and Mefford, 1999). First, the sample units were configured at random and the program was allowed to run, starting with a six-dimensional solution and stepping down to a one-dimensional solution. The initial step length (i.e., the rate of movement toward minimum stress) was set at 0.2. At each step, 400 iterations of the calculations were performed. The stability criterion, defined as the standard deviation in stress over the preceding 15 iterations and used as a cut-off value to stop the iterative process if is a stable solution is reached before the predetermined number of iterations, was set at 0.00001. Forty runs with the real data and 50 runs with the randomized data were used as the basis for a Monte Carlo test of significance at each dimensionality, which tested the probability that a similar final stress could not have been obtained by chance. Selection of the final number of dimensions was done by examining a scree plot of stress values as a function of number of axes, choosing for the best solution the dimensionality where the change in stress became small. The final

solution was obtained in the second stage, by rerunning an NMS once, with the configuration of the chosen solution as the starting configuration. The number of iterations and the stability criterion were as with the preliminary runs.

The results from the initial unconstrained NMS run, which cascaded down from six to one dimensions, were assessed graphically with a scree plot of final stress *vs*. the number of dimensions (Fig. C4.4). The best ordination was obtained by selecting the number of dimensions after which additional dimensions provided only small reductions in stress; in this case at two dimensions. The Monte Carlo test of significance indicated a better than random solution for this dimensionality (p-value = 0.0196) (Table C4.1 and Fig. C4.4). The final two-dimensional solution was also assessed graphically using plots of stress, instability, step length, and magnitude of the gradient vector *vs*. iteration (see) (Fig. C4.5). From these plots it was evident that the stress curve stabilized at a low level after about 40 iterations and that the procedure ended with a periodic but low level of instability (Fig. C4.5). Since the final stress was low (12.4) and the final instability was about 10^{-3}, the ordination result was judged acceptable.

Table C4.3: Stress in relation to dimensionality (i.e., number of axes) from the initial unconstrained NMS runs for real and randomized data.

	Stress in real data (40 runs)			Stress in randomized data (Monte Carlo test, 50 runs)			
Axes	Minimum	Mean	Maximum	Minimum	Mean	Maximum	p
1	16.2	47.9	54.2	52.2	54.8	57.7	0.0196
2	10.7	12.4	17.6	28.8	31.0	42.0	0.0196
3	8.6	9.3	13.4	20.0	20.3	20.6	0.0196
4	7.5	8.1	9.9	27.7	27.7	27.7	0.0196
5	6.9	7.7	10.3	24.2	24.2	24.2	0.0196
6	6.3	9.2	23.3	21.8	21.8	21.8	0.0196

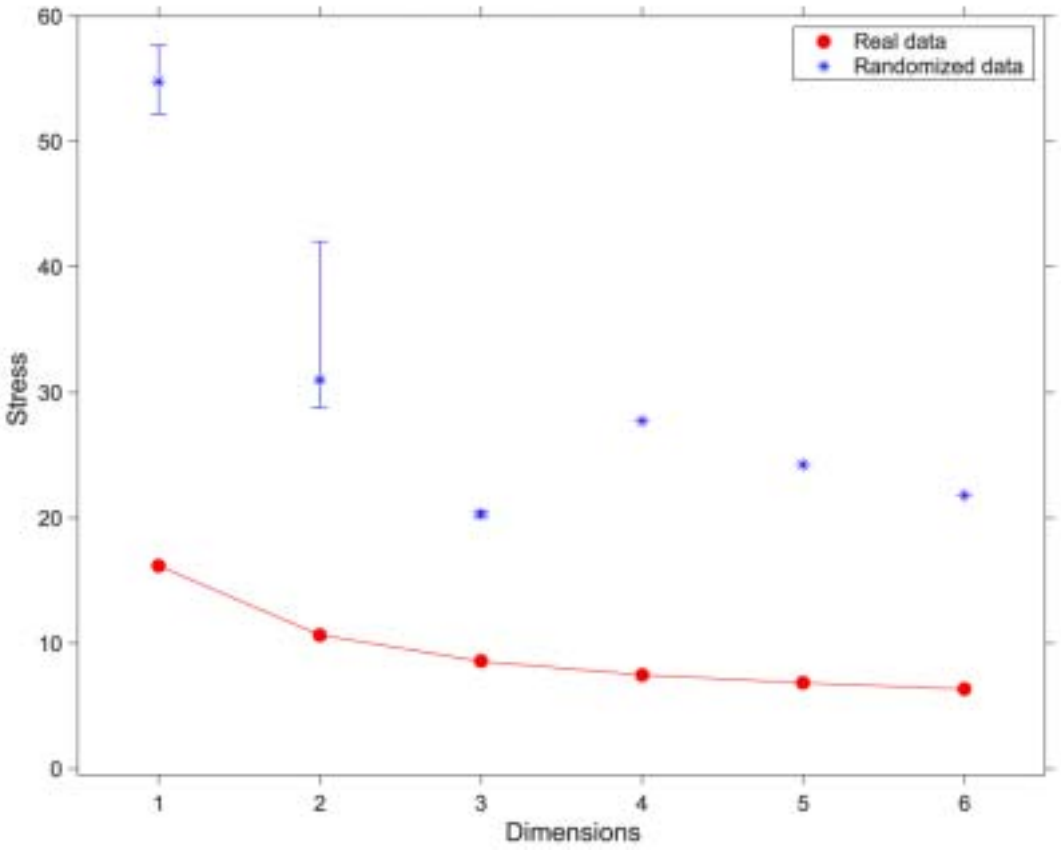

Figure C4.4: Scree plot of stress *vs*. dimensions from the initial unconstrained NMS runs for real and randomized data. Red dots are the minimum stress in the real data. Blue stars are the mean stress in the randomized data, while bars indicate the minimum and maximum (see Table C4.1).

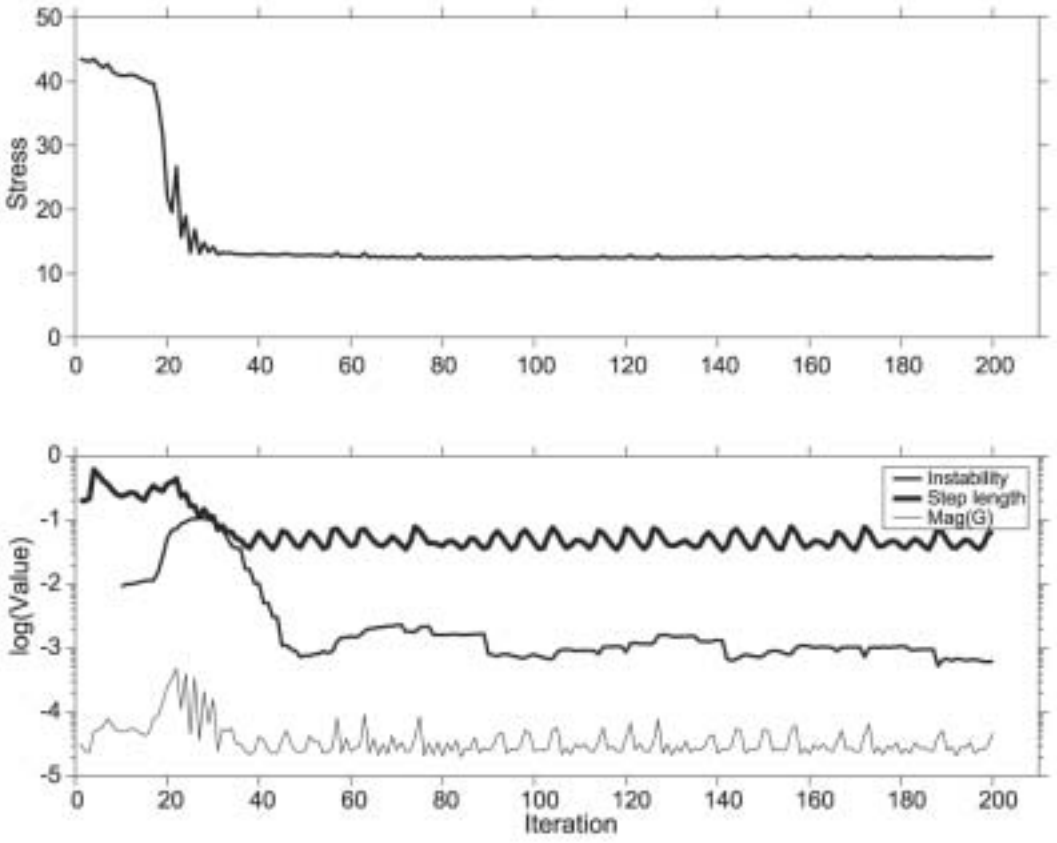

Figure C4.5: Stability of the final two-dimensional NMS solution. Top: stress *vs*. iteration. Bottom: instability, step length, and magnitude of the gradient vector *vs*. iteration. Only the first 200 iterations are shown.

5 GENERAL CONCLUSION

The areal extent and seasonal variability of the different environments around the Galápagos Islands was illustrated by the satellite fields. Emphasis was placed on describing the ecological processes associated with the island-mass effect (IME) of this archipelago, which is fueled by the topographic upwelling of the Equatorial Undercurrent (EUC) combined with a local input of iron. The year-round persistence of the Galápagos IME underscores its importance as an "oasis" for marine biota, exploited by all trophic levels from primary producers to apex predators. This biological response exemplifies Margalef's (1978) model of upwelling as a deformation of the local ecological fields. Variability in the depth, strength, and nutrient content of the EUC upstream probably have a large impact on the extent of the upwelling ecosystem (cf. Barber and Smith, 1981; Steger et al., 1998). However, the supply of iron from a local source is probably crucial for the development of this habitat. Therefore, a question that should be addressed by future studies is which is the source of iron: hydrothermal fluxes or resuspension of iron-rich sediments? The possibility that secondary IMEs develop in the lee of the tallest volcanoes on Isla Isabela should also be explored.

Finally, the patterns of cetacean distribution indicated strong habitat differences that probably have trophic preferences as the underlying cause. However, the local trophic ecology is largely unknown, and efforts should be placed on a comprehensive description of the stocks and the roles of mesopelagic and epipelagic zooplankton (crustacean and gelatinous) and nekton (squid and fishes).

BIBLIOGRAPHY

Abbott, D.P. 1966. Factors influencing the zoogeographic affinities of the Galápagos inshore marine fauna. Pages 108–122 *in* Bowman, R.I.,ed. The Galápagos: Proceedings of the Symposia of the Galápagos International Scientific Project. University of California Press, Berkeley.

Anderson, J.J. 1977. Identification and tracing of water masses with an application near the Galápagos Islands. Ph.D. Thesis, University of Washington. 144 pp.

Anderson, D.J. 1989. Differential responses of boobies and other seabirds in the Galápagos to the 1986–87 El Niño-Southern Oscillation Event. Marine Ecology Progress Series 52(3):209–216.

Arcos, F. 1981. A dense patch of *Acartia levequei* (Copepoda, Calanoida) in upwelled Equatorial Undercurrent water around the Galapagos Islands. Pages 427–432 *in* Richards, F.A., ed., Coastal Upwelling. Estuarine Sciences 1, American Geophysical Union, Washington, D.C.

Arístegui, J., P. Tett, A. Hernández-Guerra, G. Basterretxea, M.F Montero, K. Wild, P. Sangrá, S. Hernández-León, M. Cantón, J.A. García-Braun, M. Pacheco, and E.D. Barton. 1997. The influence of island-generated eddies on chlorophyll distribution: a study of mesoscale variation around Gran Canaria. Deep-Sea Research I 44(1):71–96.

Au, D.W. 1991. Polyspecific nature of tuna schools: shark, dolphin, and seasbird associates. Fishery Bulletin 89:343–354.

Au, D.K., and W.L. Perryman. 1985. Dolphin habitats in the eastern tropical Pacific. Fishery Bulletin 83(4):623–643.

Barber, R.T., and R.L. Smith. 1981. Coastal upwelling ecosystems. Pages 31–68 *in* Longhurst, A.R., ed. Analysis of Marine Ecosystems. Academic Press, London.

Barber, R.T., and F.P. Chavez. 1983. Biological consequences of El Niño. Science 222:1203–1210.

Barton, E.D., G. Basterretxea, P. Flament, E.G. Mitchelson-Jacob, B. Jones, J. Arístegui, and F. Herrera. 2000. Lee region of Gran Canaria. Journal of Geophysical Research 105:17173–17193.

Baumgartner, M.F. 1997. The distribution of Risso's dolphin (*Grampus griseus*) with respect to the physiography of the northern Gulf of Mexico. Marine Mammal Science 13(4):614–638.

Baumgartner, M.F., K.D. Mullin, L. Nelson, and T.D. Leming. 2001. Cetacean habitats in the northern Gulf of Mexico. Fishery Bulletin 99:219–239.

Beals, E.W. 1984. Bray-Curtis ordination: an effective strategy for analysis of multivariate ecological data. Advances in Ecological Research 14:1–55.

Bensted-Smith, R. 1998. The special law for Galápagos. Noticias de Galápagos 59:6.

Bernard H.J., and S.B. Reilly. 1999. Pilot whales *Globicephala* Lesson, 1828. Pages 245–280 *in* Ridgway, S.H., and R. Harrison, eds. Handbook of Marine Mammals, Volume 6, The Second Book of Dolphins and Porpoises. Academic Press, London.

Berzin, A.A. 1978. Whale distribution in tropical eastern Pacific waters. Report of the International Whaling Commission 28:173–177.

Blackburn, M. 1968. Micronekton of the eastern tropical Pacific Ocean: family composition, distribution, abundance, and relations to tuna. Fishery Bulletin 67(1):71–115.

Blackburn, M., M.R. Laurs, R.W. Owen, and B. Zeitschel. 1970. Seasonal and aereal changes in standing stocks of phytoplankton, zooplankton and micronekton in the eastern tropical Pacific. Marine Biology 7:14–31.

Boersma, P.D. 1978. Breeding patterns of Galapagos penguins as an indicator of oceanographic conditions. Science 200:1481–1483.

Brinton, E. 1979. Parameters relating to the distributions of planktonic organisms, especially Euphausiids in the eastern tropical Pacific. Progress in Oceanography 8:125–189.

Bucciarelli, E., S. Blain, and P. Tréguer. 2001. Iron and manganese in the wake of the Kerguelen Islands (Southern Ocean). Marine Chemistry 73:21–36.

Cañadas, A., R. Sagarminaga, and S. García-Tiscar. 2002. Cetacean distribution related with depth and slope in the Mediterranean waters off southern Spain. Deep-Sea Research I 49:2053–2073.

Casey, K.S., and P. Cornillon. 1999. A comparison of satellite and *in situ*-based sea surface temperature climatologies. Journal of Climate 12(6):1848–1863.

Cattell, R.B. 1966. The data box: its ordering of total resources in terms of possible relational systems. Pages 67–128 *in* Cattell, R.B., ed. Handbook of Multivariate Experimental Psychology. Rand McNally & Co. Chicago.

Chavez, F.P. 1989. Size distribution of phytoplankton in the central and eastern tropical Pacific. Global Biogeochemical Cycles 3:27–35.

Chavez, F.P., and R.C. Brusca. 1991. The Galápagos Islands and their relation to oceanographic processes in the tropical Pacific. Pages 9–33 *in* James, M.J., ed. Galápagos Marine Invertebrates. Taxonomy, Biogeography, and Evolution in Darwin's Islands. Topics in Geobiology, Vol. 8. Plenum Press, New York and London.

Chelton, D.B., F.J. Wentz, C.L. Gentemann, R.A. de Szoeke, and M.G. Schlax. 2000a. Satellite microwave SST observations of transequatorial tropical instability waves. Geophysical Research Letters 27(9):1239–1242.

Chelton, D.B., M.H. Freilich, and S.K. Esbensen. 2000b. Satellite observations of the wind jets off the Pacific coast of Central America, Part I: Case studies and statistical characteristics. Monthly Weather Review 128:1993–2018.

Cipollini, P., D. Cromwell, P.G. Challenor, and S. Raffaglio. 2001. Rossby waves detected in ocean colour data. Geophysical Research Letters 28:323–326.

Clarke M.R., and F. Trillmich. 1980. Cephalopods in the diets of fur seals of the Galápagos Islands. Journal of Zoology (London) 190:211–215.

Coale, K.H. (Ed.). 1998. The Galápagos iron experiments: A tribute to John Martin. Deep-Sea Research II 45:915–1150.

Coale, K.H., S.E. Fitzwater, R.M. Gordon, K.S. Johnson, and R.T. Barber. 1996a. Control of community growth and export production by upwelled iron in the equatorial Pacific. Nature 379:621–624.

Coale, K.H., K.S. Johnson, S.E. Fitzwater, R.M. Gordon, S. Tanner, F.P. Chavez, L. Ferioli, C. Sakamoto, P. Rogers, F. Millero, P. Steinberg, P. Nightingale, D. Cooper, W.P. Cochlan, M.R. Landry, J. Constantinou, G. Rollwagen, A. Trasvina, and R. Kudela. 1996b. A massive phytoplankton bloom induced by an ecosystem-scale iron fertilization experiment in the equatorial Pacific Ocean. Nature 383:495–501.

Conkright, M., S. Levitus, T. O'Brien, T. Boyer, J. Antonov, and C. Stephens. 1998. World Ocean Atlas 1998 CD-ROM Data Set Documentation. Technical Report 15. NODC Internal Report, Silver Spring, MD, 16 pp.

Cornejo de González, M. 1977. Distribución de los eufaúsidos al oeste de las islas Galápagos, durante el crucero “Eastward” E-5L-76 (29 de Octubre al 12 de Noviembre , 1976). Boletín ERFEN 1(2):21–24.

Coutis, P.F., and J.H. Middleton. 1999. Flow-topography interaction in the vicinity of an isolated, deep ocean island. Deep-Sea Research I 46:1633–1652.

Cromwell, T., and E.B. Bennett. 1959. Surface drift charts for the eastern tropical Pacific Ocean. Inter-American Tropical Tuna Commission Bulletin 3(5):217–237.

Cummings, W.C. 1985. Bryde’s whale *Balaenoptera edeni* Anderson, 1878. Pages 137–154 *in* Ridgway, S.H., and R.J. Harrison, eds. Handbook of Marine

Mammals, Volume 3, The Sirenians and Baleen Whales. Academic Press, London.

Dandonneau, Y., and L. Charpy. 1985. An empirical approach to the island mass effect in the south tropical Pacific based on sea surface chlorophyll concentrations. Deep-Sea Research 32:707–721.

Das, K., G. Lepoint, V. Loizeau, V. Debacker, P. Dauby, and J.M. Bouquegneau. 2000. Tuna and dolphin associations in the North-east Atlantic: evidence of different ecological niches from stable isotope and heavy metal measurements. Marine Pollution Bulletin 40(2):102–109.

Davis, R.W., J.G. Ortega-Ortíz, C.A. Ribic, W.E. Evans, D.C. Biggs, P.H. Ressler, R.B. Caddy, R.R. Leben, K.D. Mullin, and B. Würsig. 2002. Cetacean habitat in the northern oceanic Gulf of Mexico. Deep-Sea Research I 49:121–142.

Delcroix, T. 1993. Seasonal and interannual variability of sea surface temperatures in the tropical Pacific, 1969–1991. Deep-Sea Research I 40(11/12):2217–2228.

Dellinger, T., and F. Trillmich. 1999. Fish prey of the sympatric Galápagos fur seals and sea lions: seasonal variation and niche separation. Canadian Journal of Zoology 77(8):1204–1216.

Dessier, A., and J.R. Donguy. 1985. Planktonic copepods and environmental properties of the eastern equatorial Pacific: seasonal and spatial variations. Deep-Sea Research 32:1117–1133.

Doty, M.S., and M. Oguri. 1956. The island mass effect. Journal du Conseil International pour l'Exploration de la Mer 22:33–37.

Dufrêne, M., and P. Legendre. 1997. Species assemblages and indicator species: the need for a flexible asymmetrical approach. Ecological Monographs 67:345–366.

Emery, W.J., and R.E. Thomson. 1997. Data analysis methods in physical oceanography. Pergamon, Exeter, UK.

Evans, W.E. 1994. Common dolphin, white-bellied porpoise *Delphinus delphis* Linnaeus, 1758. Pages 191–224 *in* Ridgway, S.H., and R. Harrison, eds. Handbook of Marine Mammals, Volume 5, The First Book of Dolphins. Academic Press, London.

Ewald, J. 2002. A probabilistic approach to estimating species pools from large compositional matrices. Journal of Vegetation Science 13:191–198.

Fager, E.W. 1957. Determination and analysis of recurrent groups. Ecology 38(4):586–595.

Feldman, G.C. 1986. Patterns of phytoplankton production around the Galápagos Islands. Pages 77–106 *in* Bowman, M.J., C.M. Yentsch, and W.T. Peterson, eds. Tidal mixing and plankton dynamics. Lecture Notes on Coastal and Estuarine Studies 17, Springer-Verlag, Berlin.

Feldman, G., D. Clark, and D. Halpern. 1984. Satellite color observations of the phytoplankton distribution in the eastern equatorial Pacific during the 1982–1983 El Niño. Science 226(4678):1069–1071.

Fiedler, P.C. 1992. Seasonal climatologies and variability of eastern tropical Pacific surface waters. NOAA Technical Report NMFS 109:1–65.

Fiedler, P.C. 2002. The annual cycle and biological effects of the Costa Rica Dome. Deep-Sea Research I 49:321–338.

Fiedler, P.C., and S.B. Reilly. 1994. Interannual variability of dolphin habitats in the eastern tropical Pacific. II: Effects on abundances estimated from tuna vessel sightings, 1975–1990. Fishery Bulletin 92:451–463.

Fiedler, P.C., J. Barlow, and T. Gerrodette. 1998. Dolphin prey abundance determined from acoustic backscatter data in eastern Pacific surveys. Fishery Bulletin 96:237–247.

Friedrichs, M.A.M., and E.E. Hofmann. 2001. Physical control of biological processes in the central equatorial Pacific Ocean. Deep-Sea Research I 48:1023–1069.

García, M.L., G. Larrea, C. Aguirre, and A. Vasquez. 1993. Zooplankton biomass, zooplankton and ichthyoplankton abundances around the Galápagos Islands in 1983–1984. Revista de Ciencias del Mar y Limnologia 3(1):89–114.

Gargett, A.E. 1997. The optimal stability "window": a mechanism underlying decadal fluctuations in North Pacific salmon stocks? Fisheries Oceanography 6(2):109–117.

Gaskin, D.E. 1968. Distribution of Delphinidae (Cetacea) in relation to sea surface temperatures off eastern and southern New Zealand. New Zealand Journal of Marine and Freshwater Research 2:527–534.

Gaskin, D.E. 1976. The evolution, zoogeography and ecology of Cetacea. Oceanography and Marine Biology Annual Review 14:247–346.

Glynn, P.W., G.M. Wellington, and J.W. Wells. 1983. Corals and coral reefs of the Galápagos Islands. University of California Press, Berkeley. 330 pp.

Goold, J.C. 1998. Acoustic assessment of populations of common dolphin off the west Wales coast, with perspectives from satellite infrared imagery. Journal of the Marine Biological Association of the United Kingdom 78:1353–1364.

Gordon, R.M., K.H. Coale, and K.S. Johnson. 1997. Iron distributions in the equatorial Pacific: implications for new production. Limnology and Oceanography 42:419–431.

Gordon, R.M., K.S. Johnson, and K.H. Coale. 1998. The behaviour of iron and other trace elements during the IronEx-I and PlumEx experiments in the equatorial Pacific. Deep-Sea Research II 45:995–1041.

Grove, J.S. and R.J. Lavenberg. 1997. The fishes of the Galápagos Islands. Stanford University Press, Stanford, California. 936 pp.

Harris, M.P. 1969. Breeding seasons of sea-birds in the Galápagos Islands. Journal of Zoology, London 159:145–165.

Hassani, S., L. Antoine, and V. Ridoux. 1997. Diets of albacore, *Thunnus alalunga*, and dolphins, *Delphis delphis* and *Stenella coeruleoalba*, caught in the Northeast Atlantic drift-net fishery: a progress report. Journal of Northwest Atlantic Fishery Science 22:119–123.

Hayes, S.P. 1985. Sea level and near surface temperature variability at the Galápagos Islands, 1979–83. Pages 49–81 *in* Robinson, G., and E.M. del Pino, eds. El Niño in the Galápagos Islands: The 1982–1983 Event. Publication of the Charles Darwin Research Foundation for the Galápagos Islands, Quito, Ecuador.

Hayes, S.P., L.J. Magnum, R.T. Barber, A. Huyer, and R.L. Smith. 1986. Hydrographic variability west of the Galápagos Islands during the 1982–83 El Niño. Progress in Oceanography 17:137–162.

Heywood, K.J., E.D. Barton, and J.H. Simpson. 1990. The effects of flow disturbance by an oceanic island. Journal of Marine Research 48:55–73.

Heywood, K.J., D.P. Stevens, and G.R. Bigg. 1996. Eddy formation behind the tropical island of Aldabra. Deep-Sea Research I 43:555–578.

Hernández-León, S., C. Almeida, M. Gómez, S. Torres, I. Montero, and A. Portillo-Hannefeld. 2001. Zooplankton biomass and indices of feeding and metabolism in island-generated eddies around Gran Canaria. Journal of Marine Systems 30:51–66.

Hoge, F.E., C.W. Wright, R.N. Swift, J.K. Yungel, R.E. Berry, and R. Mitchell. 1998. Airborne bio-optics survey of the Galápagos Islands margins. Deep-Sea Research II 45:1083–1092.

Houvenaghel, G.T. 1978. Oceanographic conditions in the Galápagos Archipelago and their relationships with life on the islands. Pages 181–200 *in* Boje, R., and M. Tomczak, eds. Upwelling ecosystems. Springer-Verlag, Berlin.

Houvenaghel, G.T. 1984. Oceanographic setting of the Galápagos Islands. Pages 43–54 *in* Perry, R., ed. Key Environments, Galápagos. Pergamon Press, Oxford.

Hui, C.A. 1979. Undersea topography and the distribution of dolphins of the genus *Delphinus* in the Southern California Bight. Journal of Mammalogy 60(3):521–527.

Hui, C.A. 1985. Undersea topography and the comparative distributions of two pelagic cetaceans. Fishery Bulletin 83(3):472–475.

Hutchinson, G.E. 1961. The paradox of the plankton. American Naturalist 95:137–147.

Jackson, M.H. 1993. Galápagos, a natural history. University of Calgary Press, Calgary, Alberta, Canada. 315 pp.

Jimenez, R. 1981. Composition and distribution of phytoplankton in the upwelling system of the Galapagos Islands. Pages 327–338 *in* Richards, F.A., ed., Coastal Upwelling. Estuarine Sciences 1, American Geophysical Union, Washington, D.C.

Johnson, G.C, B.M. Sloyan, W.S. Kessler, and K.E. McTaggart. 2002. Direct measurements of upper ocean currents and water properties across the tropical Pacific during the 1990's. Progress in Oceanography 52(1):31–61.

Johnson, K.S., F.P. Chavez, and G.E. Friedrich. 1999. Continental-shelf sediment as a primary source of iron for coastal phytoplankton. Nature 398:697–700.

Katona, S., and H. Whitehead. 1988. Are Cetacea ecologically important? Oceanography and Marine Biology Annual Review 26:553–568.

Kelly, K.A. 1988. Comment on "Empirical Orthogonal Function Analysis of Advanced Very High Resolution Radiometer Surface Temperature Patterns in Santa Barbara Channel" by G.S.E. Lagerloef and R.L. Bernstein. Journal of Geophysical Research 93:15753–15754.

Kessler, W.S. 2002. Mean three-dimensional circulation in the northeast tropical Pacific. Journal of Physical Oceanography 32:2457–2471.

Kinzey, D., T. Gerrodette, A. Dizon, W. Perryman, P. Olson, and S. Rankin. 2001. Marine mammal data collected during a survey in the eastern tropical Pacific Ocean aboard the NOAA ships *McArthur* and *David Starr Jordan*, July 28–December 9, 2000. NOAA-TM-NMFS-SWFSC-303. 100 pp.

Kogelschatz, J., L. Solorzano, R. Barber, and P. Mendoza. 1985. Oceanographic conditions in the Galápagos Islands during the 1982/1983 El Niño. Pages 91–123 *in* Robinson, G., and E.M. del Pino, eds. El Niño in the Galápagos Islands: The 1982–1983 Event. Publication of the Charles Darwin Research Foundation for the Galápagos Islands, Quito, Ecuador.

Kruse S., D.K. Caldwell, and M.C. Caldwell. 1999. Risso's dolphin *Grampus griseus* (G. Cuvier, 1812). Pages 183–212 *in* Ridgway, S.H., and R. Harrison, eds. Handbook of Marine Mammals, Volume 6, The Second Book of Dolphins and Porpoises. Academic Press, London.

Lagerloef, G.S.E., and R.L. Bernstein. 1988. Empirical Orthogonal Function analysis of Advanced Very High Resolution Radiometer surface temperature patterns in Santa Barbara Channel. Journal of Geophysical Research 93(C6):6863–6873.

Legeckis, R. 1988. Upwelling off the Gulfs of Panamá and Papagayo in the tropical Pacific during March 1985. Journal of Geophysical Research 93(C12):15485–15489.

Lee, T. 1993. Summary of cetacean survey data collected between the years of 1974 and 1985. NOAA Technical Memorandum NMFS-SWFSC 181:1–184.

Lee, T. 1994. Report on cetacean aerial survey data collected between the years of 1974 and 1982. NOAA Techical Memorandum NMFS-SWFSC 195:1–62.

Legendre, P., and L. Legendre. 1998. Numerical ecology. Second English edition. Developments in Environmental Modelling 20. Elsevier. Amsterdam. 853 pp.

Longhurst, A. 1967. Vertical distribution of zooplankton in relation to the eastern Pacific oxygen minimum. Deep-Sea Research 14:51–63.

Longhurst, A. 1998. Ecological geography of the sea. Academic Press, San Diego. 398 pp.

Lukas, R. 1986. The termination of the Equatorial Undercurrent in the eastern Pacific. Progress in Oceanography 16:63–90.

Lyrholm, T., I. Kerr, L. Galley, and R. Payne. 1992. Report of the "Expedición *Siben*," Ecuador 1988/89. Final Report submitted by the Whale Conservation Institute to the Charles Darwin Research Station and the Galápagos National Park Service, Puerto Ayora, Islas Galápagos, Ecuador. 38 pp.

Margalef, R. 1958. Information theory in ecology. General Systems 3:36–71.

Margalef, R. 1968. Perspectives in ecological theory. University of Chicago Press, Chicago. 111 pp.

Margalef, R. 1978. What is an upwelling ecosystem? Pages 12–14 *in* Boje, R., and M. Tomczak, eds. Upwelling Ecosystems. Springer-Verlag, Berlin.

Martin, J.H., K.H. Coale, K.S. Johnson, S.E. Fitzwater, R.M. Gordon, S.J. Tanner, C.N. Hunter, V.A. Elrod, J.L. Nowicki, T.L. Coley, R.T. Barber, S. Lindley, A.J. Watson, K. Van Scoy, C.S. Law, M.I. Liddicoat, R. Ling, T. Stanton, J. Stockel, C. Collins, A. Anderson, R. Bidigare, M. Ondrusek, M. Latasa, F.J. Millero, K. Lee, W. Yao, J.Z. Zhang, G. Friederich, C. Sakamoto, F. Chavez, K. Buck, Z. Kolber, R. Greene, P. Falkowski, S.W. Chisholm, F. Hoge, R. Swift, J. Yungel, S. Turner, P. Nightingale, A. Hatton, P. Liss, and N.W. Tindale. 1994. Testing the iron hypothesis in ecosystems of the equatorial Pacific Ocean. Nature 371:123–129.

MathSoft, Inc. 1999. S-PLUS 2000 Guide to Statistics, Volume 1. Data Analysis Products Division, MathSoft, Seattle, WA. 638 pp.

McCune, B. 1994. Improving community analysis with the Beals smoothing function. Écoscience 1(1):82–86.

McCune, B., and M.J. Mefford. 1999. PC-ORD. Multivariate analysis of ecological data, version 4. MjM Software Design, Gleneden Beach, OR, USA. 237 pp.

McCune, B., and J.B. Grace. 2002. Analysis of ecological communities. MjM Software Design, Gleneden Beach, Oregon, USA. 300 pp.

McGowan, J.A. 1971. Oceanic biogeography of the Pacific. Pages 3–74 *in* Funnell, B.M., and W.R. Riedel, eds. The Micropalaeontology of the Oceans. Cambridge University Press, Cambridge.

McPhaden, M.J. 1999. Genesis and evolution of the 1997–98 El Niño. Science 283:950–954.

McPhaden, M.J., A.J.Busalacchi, R. Cheney, J.-R. Donguy, K.S. Gage, D. Halpern, M. Ji, P. Julian, G. Meyers, G.T. Mitchum, P.P. Niiler, J. Picaut, R.W. Reynolds, N. Smith, and K. Takeuchi. 1998. The Tropical Ocean Global Atmosphere observing system: A decade of progress. Journal of Geophysical Research 103(C7):14169–14240.

Mielke, P.W., Jr. 1984. Meteorological applications of permutation techniques based on distance functions. Pages 813–830 *in* Krishnaiah, P.R., and P.K. Sen, eds. Handbook of Statistics, Vol. 4. Elsevier Science Publishers.

Mielke, P.W., Jr., and K.J. Berry. 2001. Permutation methods: A distance function approach. Springer Series in Statistics. 334 pp.

Mouginis-Mark, P.J., S.K. Rowland, and H. Garbeil. 1996. Slopes of western Galapagos volcanoes from airborne interferometric radar. Geophysical Research Letters 23:3767–3770.

Mullins, H.T., J.B. Thompson, K. McDougall, and T.L. Vercoutere. 1985. Oxygen-minimum zone edge effects: evidence from the central California coastal upwelling system. Geology 13:491–494.

Murray, J.W., E. Johnson, and C. Garside. 1995. A U.S. JGOFS Process Study in the equatorial Pacific (EqPac): Introduction. Deep Sea Research II 42(2–3):275–293.

Murray, J.W., R. Le Borgne, and Y. Dandonneau. 1997. JGOFS studies in the equatorial Pacific. Deep Sea Research II 44(9–10):1759–1763.

Olson, D.B. 2002. Biophysical dynamics of ocean fronts. Pages 187–218 in Robinson, A.R., J.J. McCarthy, and B.J. Rothschild, eds. The Sea, Ideas and Observations on Progress in the Study of the Seas, Vol. 12, Biological-Physical Interactions in the Sea. John Wiley & Sons, New York.

Paden, C.A., M.R. Abbott, and C.D. Winant. 1991. Tidal and atmospheric forcing of the upper ocean in the Gulf of California 1. Sea surface temperature variability. Journal of Geophysical Research 96(C10):18337–18359.

Pak, H., and J.R.V. Zaneveld. 1973. The Cromwell Current on the east side of the Galápagos Islands. Journal of Geophysical Research 78(33):7845–7859.

Pakhomov, E.A., P.W. Froneman, I.J. Ansorge, J.R.E. Lutjeharms. 2000. Temporal variability in the physico-biological environment of the Prince Edward Islands (Southern Ocean). Journal of Marine Systems 26:75–95.

Palacios, D.M. 1999a. Blue whale (*Balaenoptera musculus*) occurrence off the Galápagos Islands, 1978–1995. Journal of Cetacean Research and Management 1(1):41–51.

Palacios, D.M. 1999b. Marine mammal research in the Galápagos Islands: the 1993–94 *Odyssey* Expedition. Final report submitted to Galápagos National Park Service and Charles Darwin Research Station. Puerto Ayora, Is. Galápagos, Ecuador, 10 November 1999. 6pp, 4 tables, 18 figures, and 3 appendices.

Palacios, D.M. 2000. *GalCet2K*: A line-transect survey for cetaceans across an environmental gradient off the Galápagos Islands, 5–19 April 2000. Final report submitted to: Galápagos National Park Service, Charles Darwin Research Station, Capitanía de Puerto Ayora, and Dirección General de Intereses

Marítimos de la Armada Nacional. Puerto Ayora, Is. Galápagos, Ecuador, 17 July 2000. 9 pp.

Palacios, D.M. 2002. Factors influencing the island-mass effect of the Galápagos Islands. Geophysical Research Letters 29(23), 2134, doi: 10.1029/2002GL016232.

Palacios, D.M., and S. Salazar. 2002. Cetáceos. Pages 291–304 *in* Danulat, E., and G.J. Edgar, eds. Reserva Marina de Galápagos, Línea Base de la Biodiversidad. Fundación Charles Darwin/Servicio Parque Nacional Galápagos, Santa Cruz, Galápagos, Ecuador.

Palka, D. 1995. Influences on spatial patterns of Gulf of Maine harbor porpoises. Pages 69–75 *in* Bix, A.S., L. Wallace, and Ø. Ulltang, eds. Whales, seals, fish and man. Elsevier, Amsterdam.

Palmer, C.E., and R.L. Pyle. 1966. The climatological setting of the Galápagos. Pages 93–99 *in* Bowman, R.I., ed. The Galápagos: Proceedings of the Symposia of the Galápagos International Scientific Project. University of California Press, Berkeley.

Papastavrou, V., S.C. Smith, and H. Whitehead. 1989. Diving behaviour of the sperm whale, *Physeter macrocephalus*, off the Galápagos Islands. Canadian Journal of Zoology 67:839–846.

Perissinotto, R., J.R.E. Lutjeharms, and R.C. van Ballegooyen. 2000. Biological-physical interactions and pelagic productivity at the Prince Edward Islands, Southern Ocean. Journal of Marine Systems 24:327–341.

Perrin, W.F., and J.W. Gilpatrick, Jr. 1994. Spinner dolphin, *Stenella longirostris* (Gray, 1828). Pages 99–128 *in* Ridgway, S.H., and R. Harrison, eds. Handbook of Marine Mammals, Volume 5, The First Book of Dolphins. Academic Press, London.

Perrin, W.F., J.M. Coe, and J.R. Zweifel. 1976. Growth and reproduction of the spotted porpoise, Stenella attenuata, in the offshore eastern tropical Pacific. Fishery Bulletin 74(2):229–269.

Perrin, W.F., C.E. Wilson, and F.I. Archer III. 1994. Striped dolphin *Stenella coeruleoalba* (Meyen, 1833). Pages 129–159 *in* Ridgway, S.H., and R. Harrison, eds. Handbook of Marine Mammals, Volume 5, The First Book of Dolphins. Academic Press, London.

Philander, S.G.H., D. Gu, D. Halpern, G. Lambert, N.-C. Lau, T. Li, and R.C. Pacanowski. 1996. Why the ITCZ is mostly north of the equator. Journal of Climate 9:2958–2972.

Pielou, E.C. 1975. Ecological diversity. John Wiley & Sons, New York. 165 pp.

Podestá, G.P., and P.W. Glynn. 1997. Sea surface temperature variability in Panamá and Galápagos: Extreme temperatures causing coral bleaching. Journal of Geophysical Research 102(C7):15749–15759.

Polacheck, T. 1987. Relative abundance, distribution and inter-specific relationship of cetacean schools in the eastern tropical Pacific. Marine Mammal Science 3(1):54–77.

Ramsey, F.L., and D.W. Schafer. 1997. The statistical sleuth, a course in methods of data analysis. Duxbury Press, Belmont, CA. 742 pp.

Reilly, S.B. 1990. Seasonal changes in distribution and habitat differences among dolphins in the eastern tropical Pacific. Marine Ecology Progress Series 66:1–11.

Reilly, S.B., and V.G. Thayer. 1990. Blue whale (*Balaenoptera musculus*) distribution in the eastern tropical Pacific. Marine Mammal Science 6(4):265–277.

Reilly, S.B., and P.C. Fiedler. 1994. Interannual variability of dolphin habitats in the eastern tropical Pacific. I: Research vessel surveys, 1986–1990.

Ripa, P., and S.P. Hayes. 1981. Evidence of equatorial trapped waves at the Galápagos Islands. Journal of Geophysical Research 86(C7):6509–6516.

Robinson, G., and E.M. del Pino, eds. 1985. El Niño in the Galápagos Islands: the 1982–83 Event. Publication of the Charles Darwin Foundation for the Galápagos Islands (Contribution No. 388). Quito, Ecuador. 534 pp.

Robertson, K.M., and S.J. Chivers. 1997. Prey occurrence in pantropical spotted dolphins, *Stenella attenuata*, from the eastern tropical Pacific. Fishery Bulletin 95:334–348.

Rodríguez, J.M., E.D Barton, L. Eve, and S. Hernández-León. 2001. Mesozoolpankton and ichthyoplankton distribution around Gran Cabaria, and oceanic island in the NE Atlantic. Deep-Sea Research I 48:2161–2183.

Sagarminaga, R., and A. Cañadas. 1998. A comparative study on the distribution and behaviour of the common dolphin (*Delphinus delphis*) and the striped dolphin (*Stenella coeruleoalba*) along the south-eastern coast of Spain. Pages 175–181 *in* Evans, P.G.H., and E.C.M. Parsons, eds. European Research on Cetaceans 12, Proceedings of the Twelfth Annual Conference of the European Cetacean Society, Monaco, 20–24 January 1998.

Sakamoto, C.M., F.J. Millero, W. Yao, G.E. Friederich, and F.P. Chavez. 1998. Surface seawater distributions of inorganic carbon and nutrients around the Galápagos Islands: results from the PlumEx experiment using automated chemical mapping. Deep-Sea Research II 45:1055–1071.

Sander, F. 1981. A preliminary assessment of the main causative mechanisms of the "Island Mass Effect" of Barbados. Marine Biology 64:199–205.

Selzer, L.A., and P.M. Payne. 1988. The distribution of white-sided (*Lagenorhynchus acutus*) and common dolphins (*Delphinus delphis*) vs. environmental features of the continental shelf of the northeastern United States. Marine Mammal Science 4(2):141–153.

Signorini, S.R., C.R. McClain, and Y. Dandonneau. 1999. Mixing and phytoplankton bloom in the wake of the Marquesas Islands. Geophysical Research Letters 26:3121–3124.

Smith, S.C., and H. Whitehead. 1993. Variations in the feeding success and behaviour of Galápagos sperm whales (*Physeter macrocephalus*) as they relate to oceanographic conditions. Canadian Journal of Zoology 71:1991–1996.

Smith, S.C., and H. Whitehead. 2000. The diet of Galápagos sperm whales *Physeter macrocephalus* as indicated by fecal sample analysis. Marine Mammal Science 16(2): 315–325.

Smith, S.D. and H. Whitehead. 1999. Distribution of dolphins in Galápagos waters. Marine Mammal Science 15(2):550–555.

Smith, W.H.F., and D.T. Sandwell. 1997. Global seafloor topography from satellite altimetry and ship depth soundings. Science 277:1957–1962.

Smith, R.C., P. Dustan, D. Au, K.S. Baker and E. Dunlap, 1986. Distribution of cetaceans and sea-surface chlorophyll concentrations in the California Current. Marine Biology 91:385–402.

Snell, H.M., P.A. Stone, P.A., and H.L. Snell. 1995. Geographical characteristics of the Galápagos Islands. Noticias de Galápagos 55:18–24.

Sournia, A. 1994. Pelagic biogeography and fronts. Progress in Oceanography 34:109–120.

Steger, J.M., C.A. Collins, and P.C. Chu. 1998. Circulation in the Archipiélago de Colón (Galápagos Islands), November, 1993. Deep-Sea Research II 45(6):1093–1114.

Stevenson, M. 1970. Circulation in the Panama Bight. Journal of Geophysical Research 75(3):659–672.

Strub, P.T., J.M. Mesías, V. Montecino, J. Rutllant, and S. Salinas. 1998. Coastal ocean circulation off western South America. Pages 273–313 *in* Robinson, A.R., and K.H. Brink, eds. The Sea, Ideas and Observations on Progress in the Study of the Seas, Vol. 11, Global Coastal Ocean Regional Studies and Syntheses. John Wiley & Sons, Inc., New York.

Tomczak, M., and J.S. Godfrey. 1994. Regional oceanography: an introduction. Pergamon, London. 422 pp.

Trenberth, K.E. 1997. The definition of El Niño. Bulletin of the American Meteorological Society 78:2771–2777.

Valenti, G., C. McClain, G. Feldman, G., and R. Bustamante. 1999. SeaWiFS captures El Niño/La Niña transition. Backscatter 10(2):31–33.

van der Spoel, S. 1994. The basis for boundaries in pelagic biogeography. Progress in Oceanography 34:109–120.

Volkov, A.F., and I.F. Moroz. 1977. Oceanological conditions of the distribution of Cetacea in the eastern tropical part of the Pacific Ocean. Report of the International Whaling Commission 27:186–188.

Wade, P.R., and T. Gerrodette. 1993. Estimates of cetacean abundance and distribution in the eastern tropical Pacific. Report of the International Whaling Commission 43:477–493.

Wang, B., and Y. Wang. 1999. Dynamics of the ITCZ–Equatorial Cold Tongue complex and causes of the latitudinal climate asymmetry. Journal of Climate 12:1830–1847.

Waring, G.T., T. Hamazaki, D. Sheehan, G. Wood, and S. Baker. 2001.Characterization of beaked whale (Ziphiidae) and sperm whale (*Physeter macrocephalus*) summer habitat in shelf-edge and deeper waters off the northeast U.S. Marine Mammal Science 17(4):703–717.

Weidman, P.D., D.L. Mickler, B. Dayyani, and G.H. Born. 1999. Analysis of Legeckis eddies in the near-equatorial Pacific. Journal of Geophysical Research 104(C4):7865–7887.

Wellington, G.M., A.E. Strong, and G. Merlen. 2001. Sea surface temperature variation in the Galápagos Archipelago: A comparison between AVHRR night-time satellite data and in-situ instrumentation (1982-1998). Bulletin of Marine Science 69:27–42.

Wells R.S., and M.D. Scott. 1999. Bottlenose dolphin *Tursiops truncatus* (Montagu, 1821). Pages 137–182 *in* Ridgway, S.H., and R. Harrison, eds. Handbook of Marine Mammals, Volume 6, The Second Book of Dolphins and Porpoises. Academic Press, London.

Whitehead, H., V. Papastavrou, and S.C. Smith. 1989. Feeding success of sperm whales and sea-surface temperature off the Galápagos Islands. Marine Ecology Progress Series 53:201–203.

Whittaker, R.H. 1972. Evolution and measurements of species diversity. Taxon 21:213–251.

Wishner, K.F., C.J. Ashjian, C. Gelfman, M.M. Gowing, L. Kann, L.A. Levin, L.S. Mullineaux, and J. Saltzman. 1995. Pelagic and benthic ecology of the lower interface of the eastern tropical Pacific oxygen minimum zone. Deep-Sea Research I 42(1):93–115.

Wooster, W.S. 1959. Oceanographic observations in the Panama Bight, "Askoy" Expedition, 1941. Bulletin of the American Museum of Natural History 118:113–152.

Wooster, W.S., and J.W. Hedgpeth. 1966. The oceanographic setting of the Galápagos. Pages 100–107 *in* Bowman, R.I., ed. The Galápagos: Proceedings of the Symposia of the Galápagos International Scientific Project. University of California Press, Berkeley.

Wyrtki, K. 1967. Circulation and water masses in the eastern equatorial Pacific Ocean. International Journal of Oceanology and Limnology 1(2):117–147.

Young, D.D., and V.G. Cockcroft. 1994. Diet of common dolphins (*Delphinus delphis*) off the south-east coast of southern Africa: opportunism or specialization? Journal of Zoology (London) 234(1):41–53.

Yu, X., and M.J. McPhaden. 1999. Seasonal variability in the equatorial Pacific. Journal of Physical Oceanography 29:925–947.

Zaneveld, J.R.V., H. Pak, and W.S. Plank. 1973. Optical and hydrographic observations of the Cromwell Current between 92°00'W and the Galápagos Islands. Journal of Geophysical Research 78(15):2708–2714.